NASA CONTRACTOR REPORT

NASA CR-1533

NASA CR-1533

HIGH-VELOCITY EXPLOSIVELY DRIVEN GUNS

by J. D. Watson

Prepared by
PHYSICS INTERNATIONAL COMPANY
San Leandro, Calif.
for Ames Research Center

NATIONAL AERONAUTICS AND SPACE ADMINISTRATION • WASHINGTON, D. C. • JUNE 1970

NASA CR-1533

HIGH-VELOCITY EXPLOSIVELY DRIVEN GUNS

By J. D. Watson

Issued by Originator as Report No. PIFR-113

Prepared under Contract No. NAS 2-4903 by
PHYSICS INTERNATIONAL COMPANY
San Leandro, Calif.

for Ames Research Center

NATIONAL AERONAUTICS AND SPACE ADMINISTRATION

For sale by the Clearinghouse for Federal Scientific and Technical Information
Springfield, Virginia 22151 – CFSTI price $3.00

ABSTRACT

This report describes the research conducted during the period May 1968 through May 1969 to develop an explosively driven gun that would accelerate models of known mass to high velocities. A two-stage gun has been used to launch intact 2-g models to 12.2 km/sec in several experiments. A single-stage gun has also been developed to accelerate 2-g models to 12 km/sec, although it has a lower velocity limit and the peak projectile base pressures generated are considerably higher than those produced in the two-stage device.

The performance limits of the one- and two-stage guns are discussed. In the two-stage gun, the design problems associated with the first stage have been resolved; however, unfavorable operation of the second stage has prevented higher velocities from being achieved. In particular, the second-stage explosive lens was operated in an asymmetric mode for ease of fabrication and instrumentation. The asymmetric collapse of the barrel to form the second-stage piston appeared not to be complete and the anticipated performance was not achieved. It is postulated that in future experiments the second stage would be operated in a symmetric mode. The symmetric collapse process has been studied in greater detail, and it is felt this mode is more suited to collapsing the barrel to form the second-stage piston. Velocities of 13 to 20 km/sec should be possible with this second-stage design.

In support of the experimental work this report includes sections on current explosive driver design criteria, a discussion of gasdynamic cycles for achieving high velocities, and a calculational method to predict explosive gun performance.

ACKNOWLEDGMENTS

The author wishes to express thanks to the staff of the Shock Dynamics Department for their contributions to this program. Particular acknowledgment is given to Mr. E. T. Moore, Jr. for his advice and supervision of the program, to Dr. S. P. Gill for his calculations of phased and jetting drivers, and to Mr. Steve Hancock for his work on the GANG-POD computer program.

CONTENTS

ILLUSTRATIONS

ILLUSTRATIONS (cont.)

ILLUSTRATIONS (cont.)

ILLUSTRATIONS (cont.)

ILLUSTRATIONS (cont.)

SECTION I

INTRODUCTION

This report covers the progress made in the past year toward developing an explosively driven gun that would launch models of known mass to 20 km/sec. The primary purpose of this effort was to extend the range of velocities obtainable for laboratory simulation of meteoroid impact. At present nearly all impact testing is carried out with conventional two-stage light-gas guns operating from 2 to 10 km/sec. Those who design future spacecraft will require a knowledge of impact phenomena occurring at velocities two or three times higher than those presently attainable in the laboratory.

A secondary purpose of this effort is to be able to launch reentry configurations to 20 km/sec in order to provide laboratory simulation of planetary reentry phenomena in which radiative heat transfer dominates the flow field. These and other applications of such a high-velocity gun have been considered in developing the explosively driven gun described in this report.

In 1967 a two-stage, explosively driven launcher was used to accelerate a 0.170-g projectile to 12.2 km/sec. However, the projectile was damaged because of a mismatch between the first and second stage of the gun (Reference 1). In the present program the mismatch between stages has been corrected and the problem of projectile integrity has been satisfactorily resolved. The mass of the projectile has been increased to 2 g and several models have been accelerated intact to 12.2 km/sec.

The explosive driver used as the first stage of the two-stage system provides proper conditions for augmentation by the second

stage. The second-stage explosive lens was made in an asymmetric geometry (Reference 1), but was not entirely satisfactory in forming the second-stage piston. The unfavorable operation of the second stage in this year's program prevented the attainment of even higher velocities.

In addition to reporting the progress of this year's effort, this report discusses some of the current principles used in the design of explosive drivers. Representative calculations and experiments which illustrate some of these design criteria are presented in Section II. This is followed in Section III by a discussion of several possible gasdynamic cycles for obtaining high velocities. A method of calculating launcher performance is given in Section IV. Section V summarizes the single- and two-stage launcher experiments that led to launching an intact 2-g model to 12.2 km/sec.

SECTION II

CURRENT DESIGN CRITERIA FOR EXPLOSIVE DRIVERS

This section presents experimental and theoretical results that contribute to the knowledge of explosive driver design. These investigations include both linear and phased explosive drivers. For example the two-stage gun discussed in this report uses a linear driver as the first stage and a phased driver (the explosive lens) as the second stage.

A. RADIAL EXPANSION AND COLLAPSE OF THE PRESSURE TUBE

The ideal operation of a linear explosive driver is shown in Figure 1. The progressive collapse of the pressure tube behind the detonation wave drives a strong shock into the helium driver gas. Over the range of temperatures and pressures in which most explosive drivers operate, the helium can be considered a perfect gamma-law gas where γ is the ratio of specific heats of the gas. The pressure, P_2, in the gas behind the shock is related to the initial gas density, ρ_1, and the detonation velocity of the explosive, D, by the equation

$$\left(P_2 = \rho_1\right) \frac{\gamma+1}{2} D^2 \qquad (1)$$

The shocked-gas pressures typically reach several thousand atmospheres, causing the thin-wall pressure tube to expand radially. The primary method of controlling this expansion is to surround the explosive with a thick-wall steel tube that will inertially contain the pressures for the desired period. The result is that the inner pressure tube will expand at a much slower rate which is controlled by the inertia of the thick-wall outer tube.

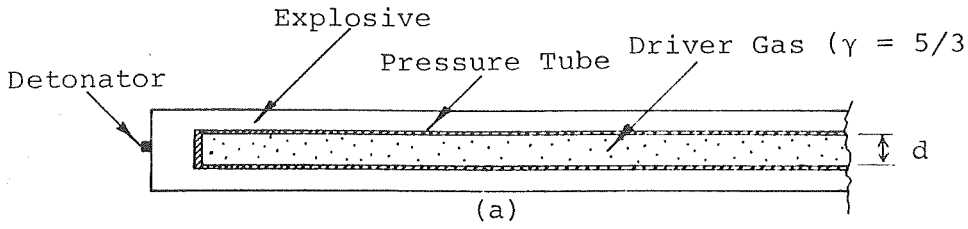

Time $\bar{t} = 0$, Before Initiation of the Explosive

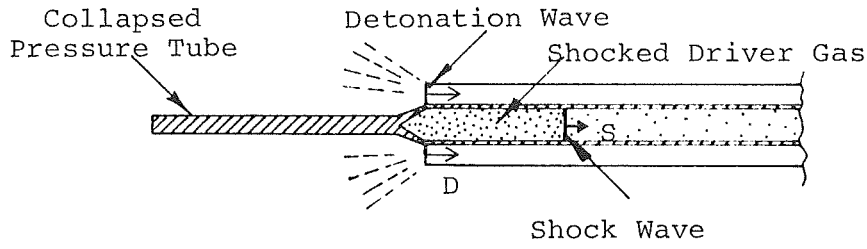

Time $\bar{t} = \bar{t}_1$, After Initiation of the Explosive

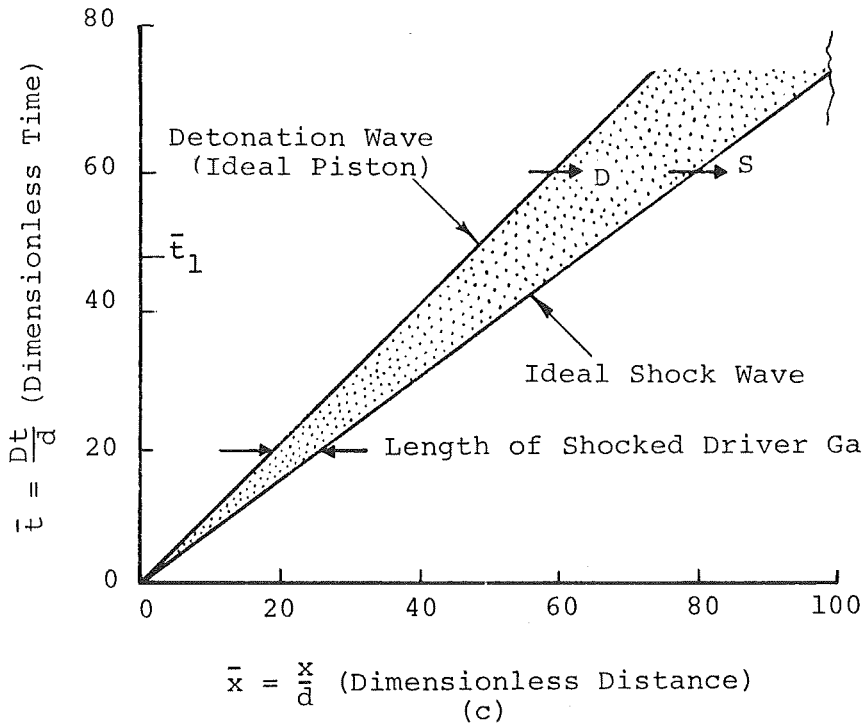

Position-Time History of Shock and Detonation Wave

FIGURE 1. IDEAL OPERATION OF THE LINEAR EXPLOSIVE DRIVER

As an example, calculations using a one-dimensional Lagrangian computer program (POD) are shown in Figure 2 for a driver with a thin and thick wall outer tube. The radius-time plots of expansion are expressed in dimensionless coordinates

$$\bar{r} = \frac{r}{r_o} - 1$$

and

$$\bar{t} = \frac{tD}{r_o}$$

where r_o is the initial internal radius of the pressure tube and D is the detonation velocity of the driver explosive. For purposes of the calculation the gas pressure inside the pressure tube is constrained to be constant. This type of calculation accounts for the strength of both the inner and outer tube as well as the wave dynamics of the steel and explosive.

Experiments were carried out under another contract (Reference 2) in which 600-kV flash X rays were taken of an explosive driver in operation. These X rays were used together with measured shock and detonation wave trajectories to obtain expansion histories of the pressure tube. The experimentally measured expansion histories were compared with calculations such as described above. Two cases are considered. In the first calculation the pressure on the inside of the pressure tube is held constant, and in the second calculation the pressure is allowed to vary isentropically as $r^{-2\gamma}$. The observed data (Figure 3) appear to follow the constant pressure solution over the entire range of measured data, suggesting that the expansion does not reduce the driver pressure as much as would be expected. The increased volume of gas caused by expansion appears to be compensated by an adjustment in the length of the column of shocked gas.

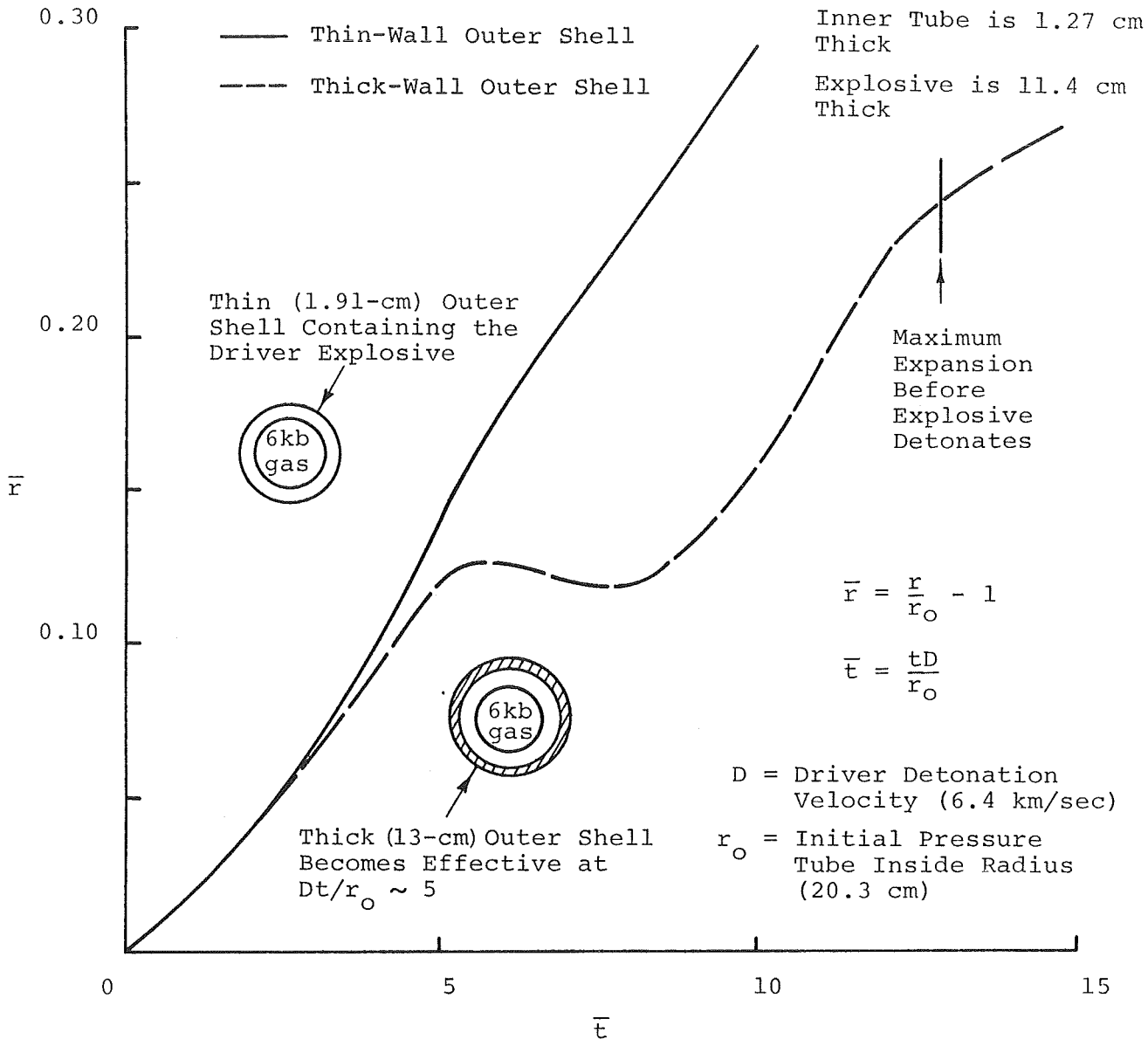

FIGURE 2. RADIAL EXPANSION HISTORIES OF THE INNER TUBE FOR EXPLOSIVE DRIVER DESIGNS (COMPUTER SOLUTIONS FOR TAMPED AND UNTAMPED DRIVERS WITH CONSTANT INTERNAL PRESSURE OF 6 kbar)

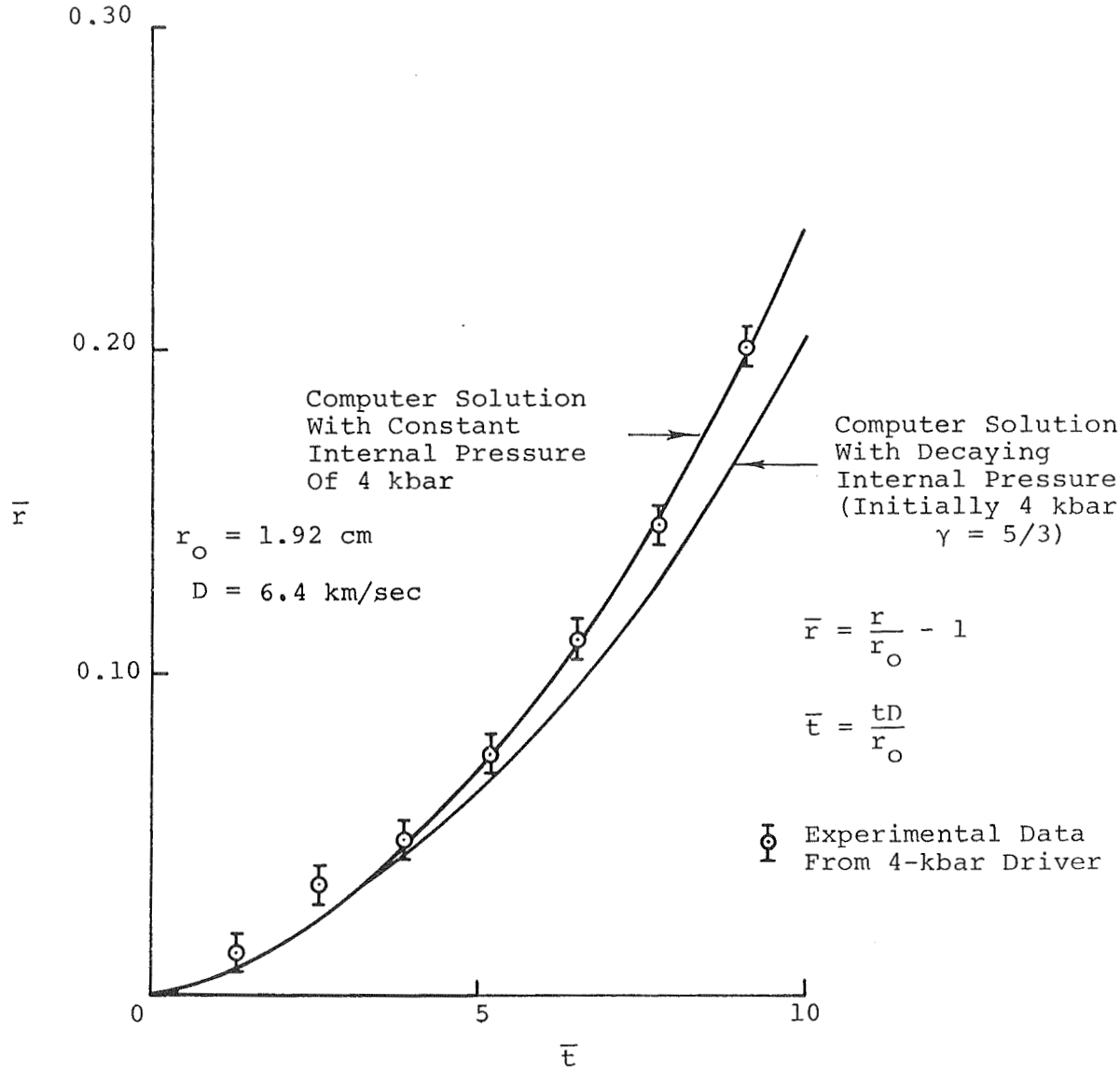

FIGURE 3. RADIAL EXPANSION HISTORIES FOR AN EXPLOSIVE DRIVER (OBSERVED AND CALCULATED SOLUTIONS FOR A 4-kbar UNTAMPED DRIVER)

This type of calculation is used in driver design to optimize the thickness of the pressure tube wall, the explosive layer, and the outer tube so that expansion of the pressure tube is held below a certain arbitrary limit (usually 30% to preclude its dynamic rupture during driver operation).

In determining the size of the pressure tube, the thickness of the explosive layer, and the size of the outer tube, consideration must also be given to the collapse process. Care must be taken to provide enough explosive energy to overcome the strength of the pressure tube and to collapse it against the driver gas pressure while allowing for losses by Taylor rarefaction in the explosive products and expansion of the outer tube. The method used in this aspect of driver design is essentially that described for calculating expansion. A one-dimensional Lagrangian computer program (POD) is employed to calculate the combined expansion and collapse histories. In the design case the pressure tube is allowed to expand to its maximum value as described above. At the appropriate time the explosive equation of state is changed from an inert liquid description to a volume-burned explosive products description. The expansion and collapse history of the pressure tube calculated in this manner is shown for a typical design case in Figure 4. Care must also be taken to prevent the pressure tube from collapsing too quickly. If the collapse angle is too steep, a significant jet can be formed (Reference 3).

The actual collapse process is a two-dimensional phenomenon. The conditions in the explosive products are relieved in the axial direction by the Taylor rarefaction, and the axial gradients in the gas in the pressure tube may be substantial. In addition, there may be jetting of the collapsing pressure tube or leakage of boundary-layer gas. Therefore the one-dimensional calculation method described

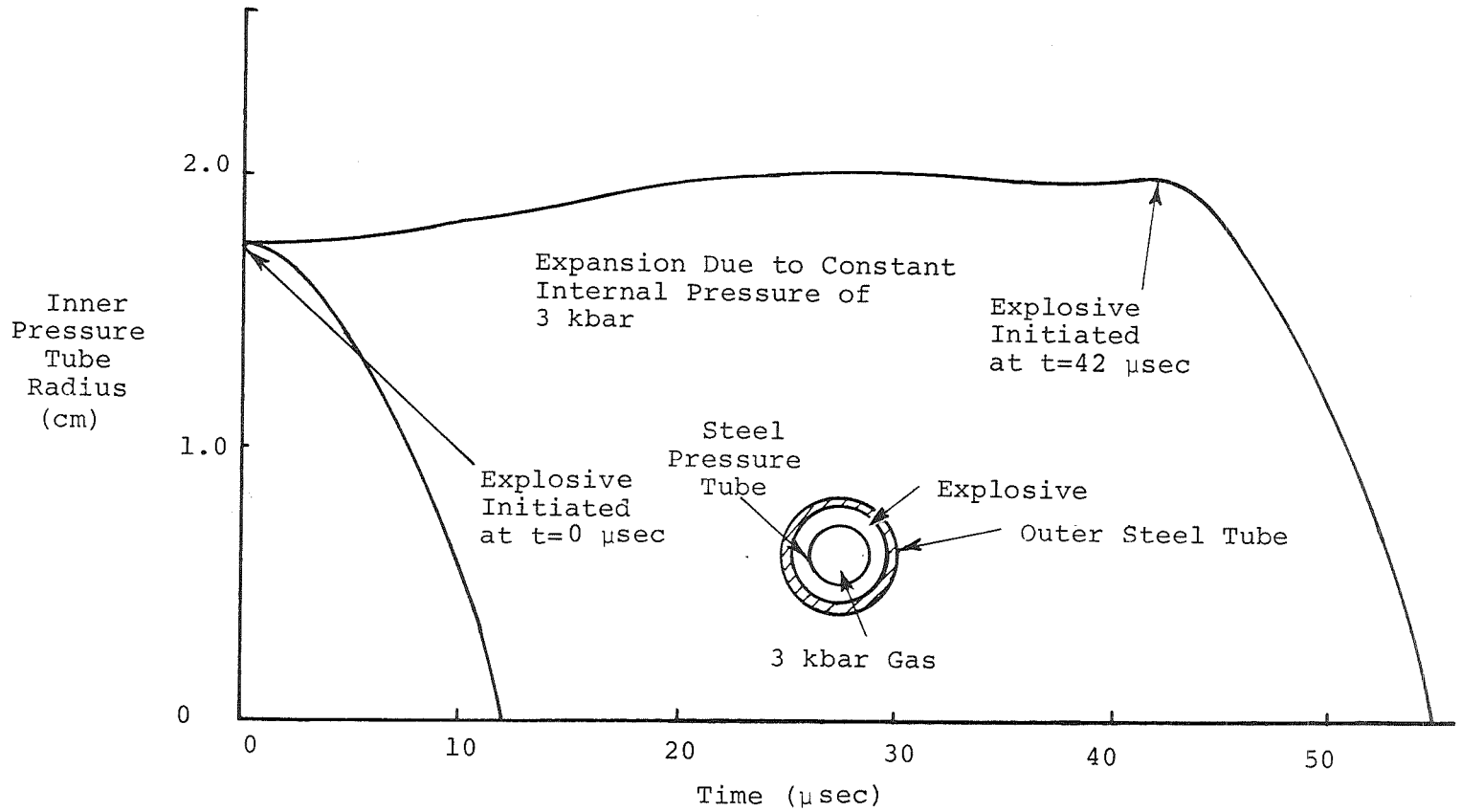

FIGURE 4. CALCULATED EXPANSION AND COLLAPSE HISTORIES FOR a 3-kbar DRIVER USING ONE-DIMENSIONAL LAGRANGIAN PROGRAM (POD)

described above is not exact. It does, however, provide a figure of merit for comparing various driver designs. For instance, the collapse calculation of a new driver design may be compared with the calculations carried out for a proved driver design. A comparison of the calculations will often suggest if conditions for significant jetting or incomplete tube collapse are present in the new driver design.

B. VARIABLE PISTON VELOCITY DRIVERS

The highest detonation velocity obtainable in an explosive is 9.1 km/sec. To accelerate projectiles to 20 km/sec it will be necessary to increase the effective detonation velocity by about a factor of two. This can be accomplished by phasing the detonation wave. A phased detonation wave is one whose point of contact with the plate or tube it is to collapse travels at a phase velocity, V, greater than the detonation velocity, D. An explosive lens developed during the past two years' effort (Reference 1) has been used to phase a detonation in a programmed manner. The most common mode of operation of the explosive lens is to provide a uniformly accelerating phased detonation wave that can be used to collapse the barrel and form an accelerating second-stage piston for an explosively driven gun. The operation of this lens system is shown schematically in Figure 5. After the lens is initiated, a detonation wave front proceeds along the steel tube at a velocity equal to the detonation velocity in the slow explosive. However, the higher detonation velocity of the fast explosive combined with the changing contour of the interface between the fast and slow explosives produces a continuously tilting wave front (phased detonation wave) in the slow explosive. As a result, the piston formed by the collapse of the steel pressure tube begins to accelerate.

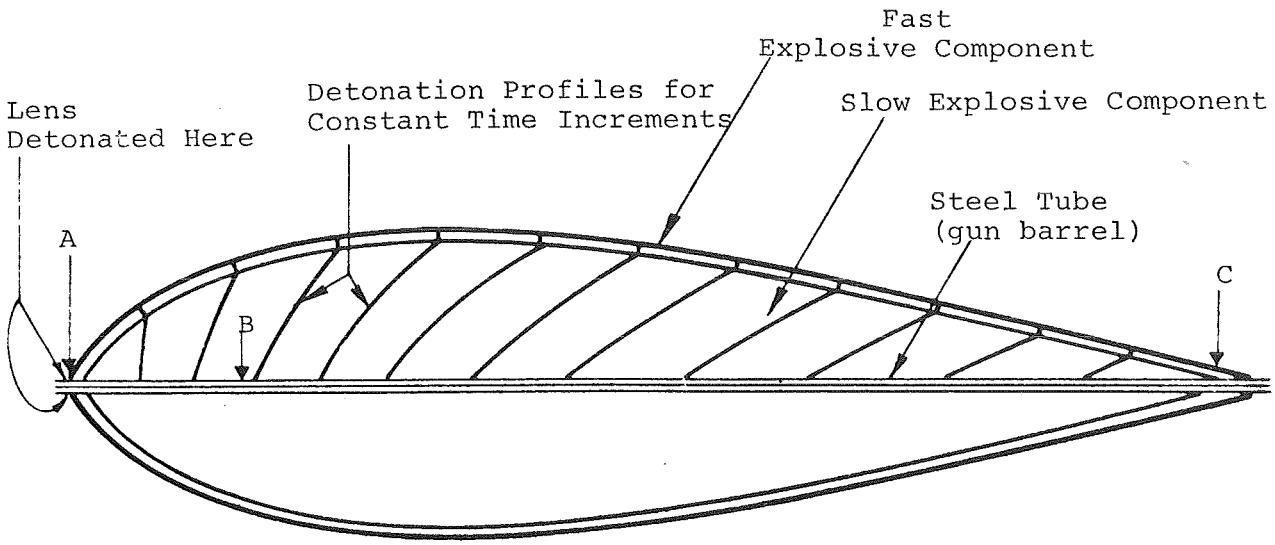

Note: Detonation velocity along the outside of the tube is constant from A to B and increases uniformly from B to C.

a. Initial Configuration

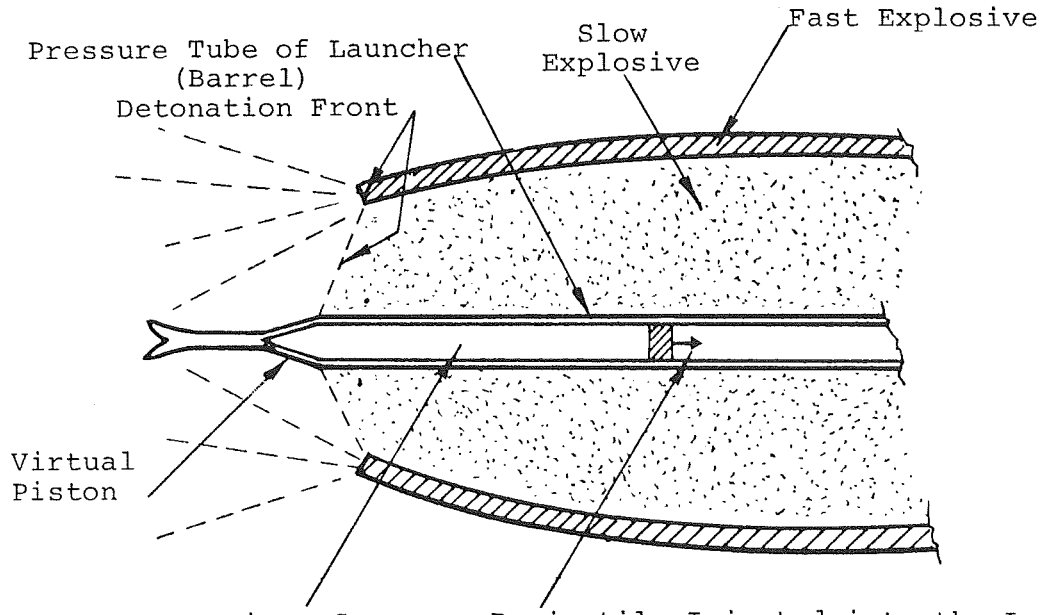

b. Lens in Operation

FIGURE 5. OPERATION OF AN EXPLOSIVE LENSING SYSTEM

The accurate and precisely controllable operation of the lens has been experimentally demonstrated (Reference 1); however, the upper limits of the lens phase velocity have not yet been investigated. In particular, the energy density of the explosive is fixed and the maximum inward velocity which the explosive can impart to the tube must therefore be limited. As the phase velocity of the explosive is increased, the conical piston region (in the case of the collapsing barrel) elongates. For very high phase velocities, the collapse cone can become unrealistically long. Therefore, it is the fixed energy density of the explosive that will ultimately limit the phased piston velocities that can be achieved.

A calculation has been carried out which indicates that phase velocities of two to three times the detonation velocity of the explosive will not result in prohibitively long collapse cones (Reference 4). Although the details of this calculation are much too involved to present here, the assumptions, methods, and results of the approach will be given.

In the calculation a phased detonation interacts with a metal plate (Figure 6). The explosive is assumed infinite so there are no boundary conditions and the state of the detonation products is constant at Chapman-Jouguet conditions except where affected by the accelerating metal plate. The flow, in the frame of reference of the detonation wave, is assumed steady.

Phased detonations differ from unphased detonations in that the disturbance first caused in the detonation products by the accelerating plate is a reflected shock rather than a rarefaction (Figure 6). The pressure behind this reflected shock is subsequently reduced by rarefactions generated by the accelerating plate. If the initial shock is weak enough, the increase in entropy across the shock can be neglected and the flow field calculated by means of a

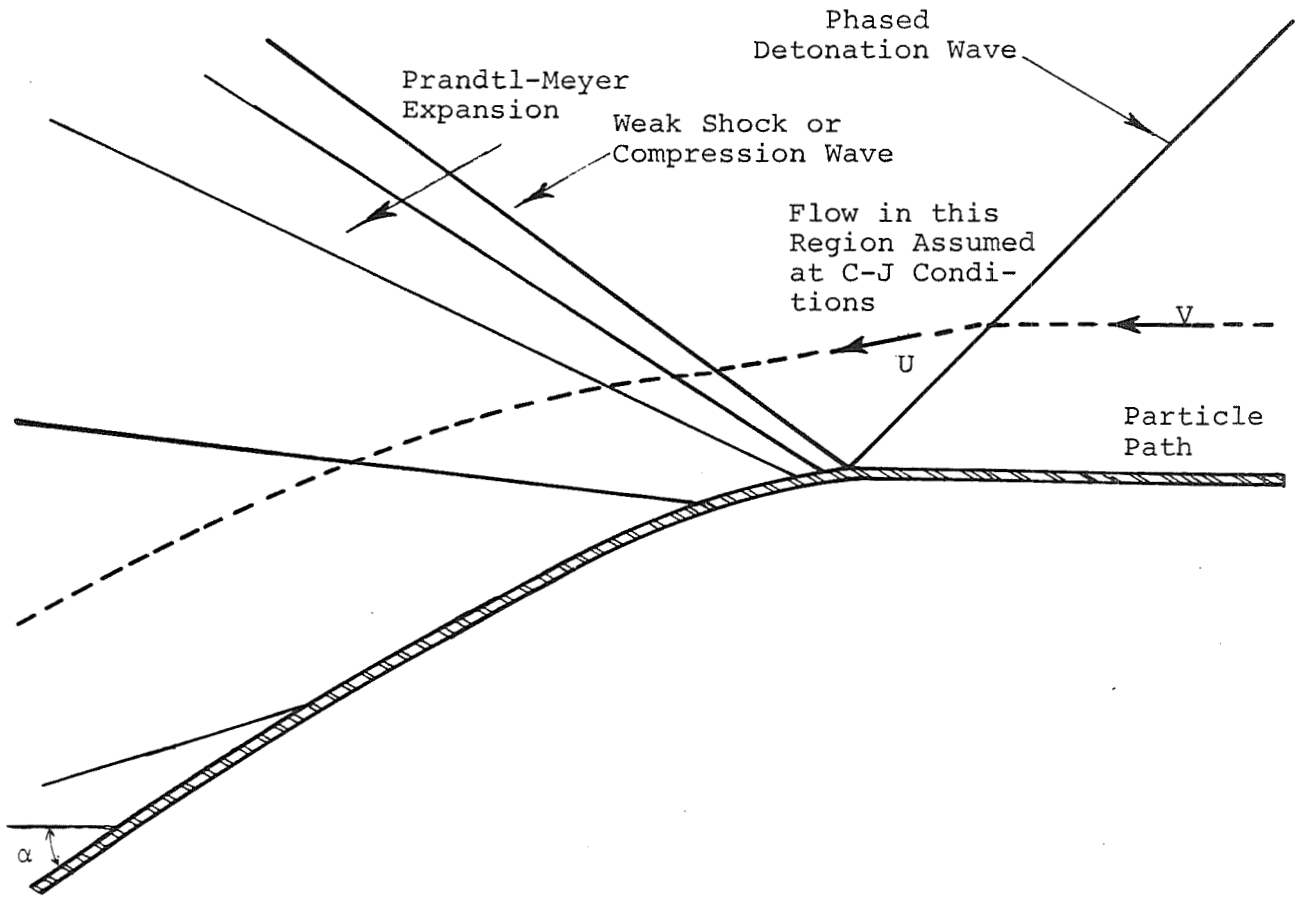

FIGURE 6. INTERACTION OF A TILTING (PHASED) DETONATION WAVE WITH A THIN PLATE. (SHOWN IN THE FRAME OF REFERENCE IN WHICH THE DETONATION IS STATIONARY)

Prandtl-Meyer compression followed by a Prandtl-Meyer expansion. This approximation can be shown to give good results even in the worst case of normal impact against an infinitely massive plate (Reference 4).

As shown in Figure 6, the detonation products undergo a Prandtl-Meyer compression followed by a Prandtl-Meyer expansion. Numerical calculation of terminal plate angle, α, as a function of the ratio of phase velocity to detonation velocity, V/D, is carried out in Reference 4 for both polytropic and Livermore equation-of-state descriptions* of the detonation products and are shown in Figure 7. The terminal angle is bounded and has a maximum for V/D > 1. In the limiting case of a detonation normally impacting a massless plate, the terminal velocity of the plate in laboratory coordinates is equal to the escape velocity of the detonation gases in one-dimensional flow, as would be expected.

From Figure 7 it can be seen that the terminal plate angle reaches a maximum at approximately V/D = 1.1, and that the terminal plate angle at V/D = 1.6 is still slightly greater than its value for an unphased (V/D = 1) detonation. For values of V/D > 3 the terminal plate angle is less than one half of the value for an unphased detonation.

The reason for this behavior is that as the detonation wave tilts, the directed kinetic energy of the detonation products is

---

*The Livermore equation of state is of the form

$$P = A\left(1 - \frac{w}{R_1 V}\right) e^{-R_1 V} + B\left(1 - \frac{w}{R_2 V}\right) e^{-R_2 V} + \frac{wE}{V}$$

where P is pressure, V is relative volume ρ_o/ρ, E is the chemical energy density of the explosive, and A, B, R_1, R_2, w are experimentally determined constants.

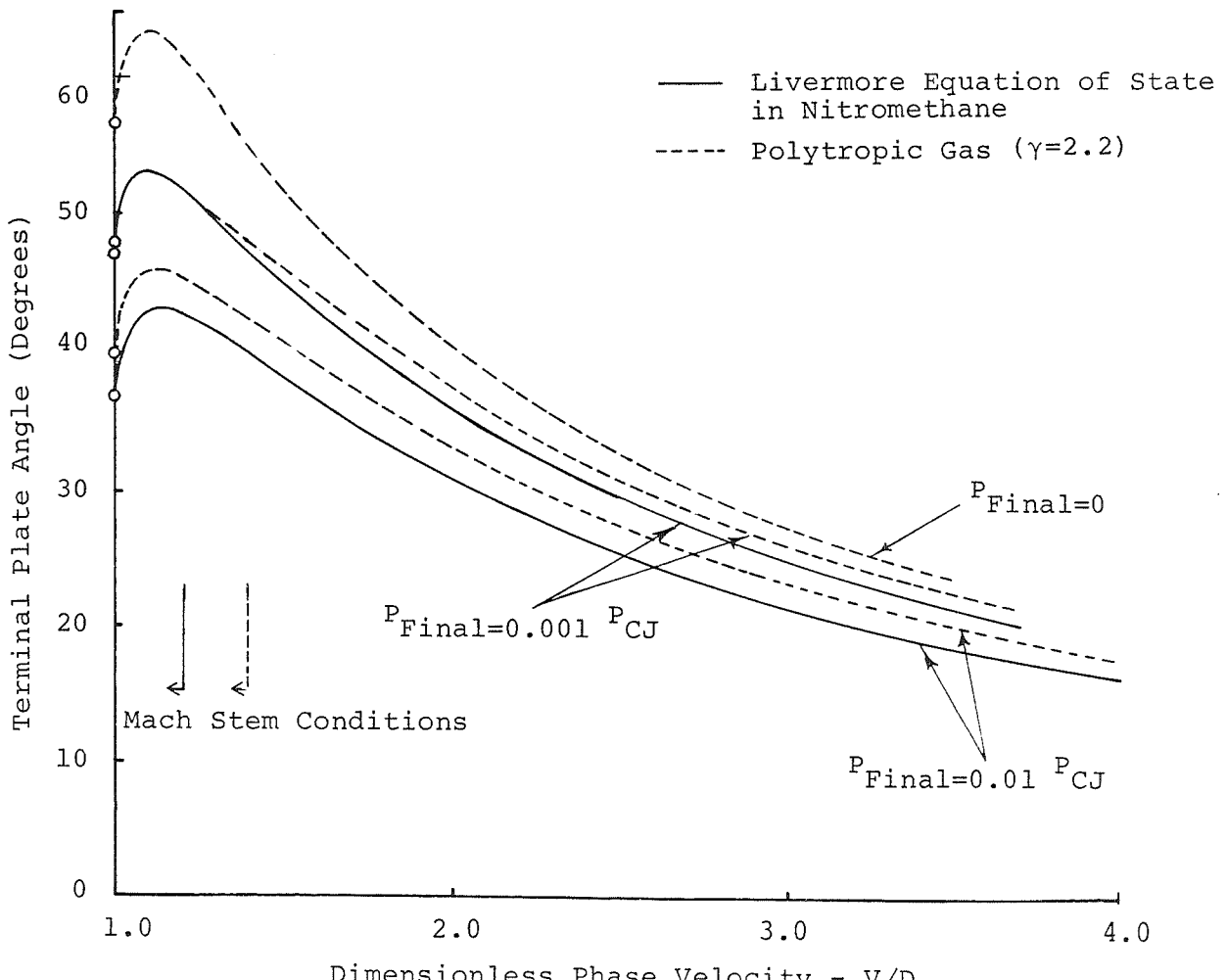

FIGURE 7. TERMINAL PLATE ANGLE AS A FUNCTION OF PHASE VELOCITY FOR VARIOUS RESIDUAL PRESSURES

available for accelerating the plate. The directed kinetic energy increases as the detonation wave tilts, causing the terminal plate angle to increase initially. However, the increased phase velocity, combined with the limited energy density of the explosive, begins to dominate and causes the terminal angle to begin to decrease. At infinite phase velocity the terminal angle is zero.

In the case of the explosive lens, the simplifying assumptions made for the above calculation do not apply. In particular, the explosive is not infinite, there is a large internal pressure in the tube, and the phase velocity is not constant but usually increases slowly in time. However, the tradeoff between directed kinetic energy and increasing phase velocity still exists and the above calculation is valuable as a figure of merit. That the terminal angle is approximately constant for $V/D < 2$ would seem to be a reasonable expectation in the case of the explosive lens. Based on this calculation, we would expect that the collapse or piston region would begin to elongate unrealistically for $V/D > 2$. With explosives such as Astrolite ($D = 8.6$ km/sec), this would indicate that piston velocites up to about 20 km/sec would be practical for launcher applications.

C. JETTING OF THE COLLAPSING PRESSURE TUBE

There are three phenomena that complicate the otherwise ideal operation of an explosive driver. Expansion of the pressure tube behind the shock wave and prior to the arrival of the detonation wave has been extensively studied experimentally and analytically and is discussed in Part A of this section. A second phenomenon is the growth of a boundary layer behind the shock. Since the boundary-layer gases receive little axial momentum when they encounter the piston, these gases tend to be trapped by the collapsing tube. The resultant leakage of boundary-layer gases ultimately limits the length of shocked gas obtainable with present driver designs.

This phenomenon is reported in Reference 3 and, since there has been little work done in this area under this contract, the subject will not be discussed here.

The third phenomenon encountered in explosive drivers is the possibility of forming a metallic jet upon collapse of the pressure tube. The theory of jetting is well established and can be found in References 3 and 4. A simple analysis will be presented here to illustrate the large effects that irreversible processes such as shock heating and plastic working have on the size of the jet formed. This analysis assumes only the conservation laws and the condition of steady state. The collapsing tube is shown schematically in Figure 8 in the frame of reference of the detonation wave.

From conservation of mass

$$MD = M_s D(1 - \varepsilon_s) + M_j D(1 - \varepsilon_j) \tag{2}$$

where M is mass/unit length of the collapsing tube, D is detonation velocity, subscript s denotes the slug of the collapsed tube, and subscript j denotes the jet. The velocities of the slug and jet are less than their classical value of D by some small amount, εD, due to irreversible processes. The irreversible energy deposited in the slug and jet as residual heat is subtracted from the energy of motion of the slug and jet in accordance with the first law of thermodynamics.

Similarly, for the conservation of momentum

$$MD \cos \theta \; D = M_s D^2 (1 - \varepsilon_s)^2 - M_j D^2 (1 - \varepsilon_j)^2 \tag{3}$$

where θ is the angle through which the tube is turned by the detonation (Figure 8).

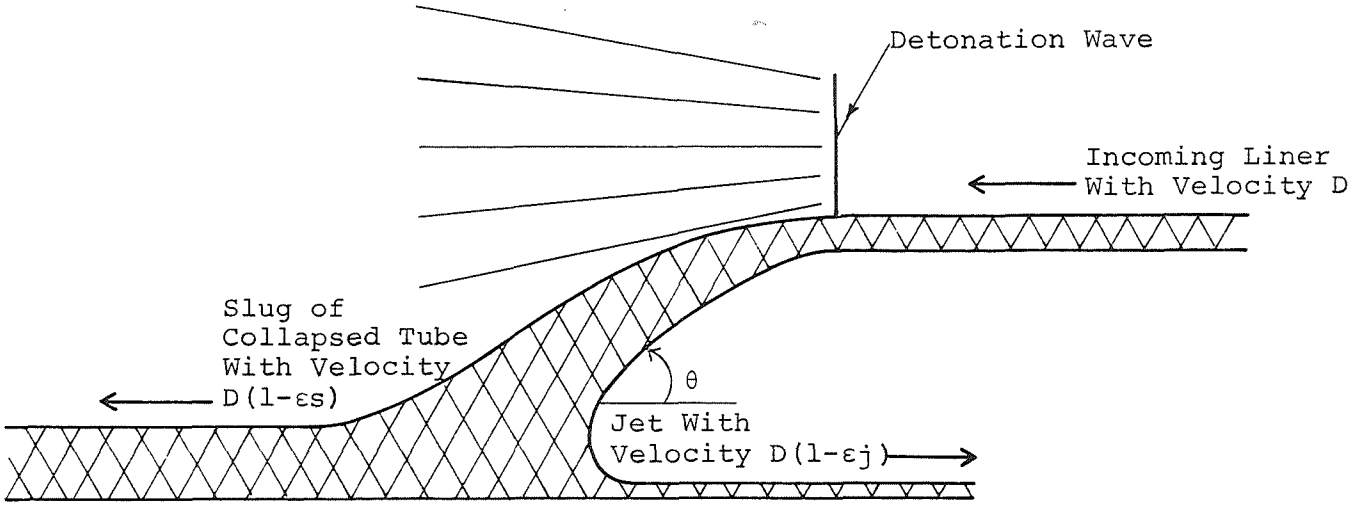

Slug and jet velocities are reduced by a small amount εD due to irreversible energy generated in the collapse process.

FIGURE 8. SCHEMATIC OF THE TUBE COLLAPSE PROCESS IN THE FRAME OF REFERENCE OF THE DETONATION WAVE

Solving Equations (2) and (3) for M_j/M,

$$\frac{M_j}{M} = \frac{(1 - \cos\theta) - \varepsilon_s}{(2 - \varepsilon_s - \varepsilon_j)(1 - \varepsilon_j)} \tag{4}$$

If $\varepsilon_j << 1$ and $\varepsilon_s << 1$

$$\frac{M_j}{M} = \frac{(1 - \cos\theta) - \varepsilon_s}{2} \tag{5}$$

which compares to the classical formula ($\varepsilon_s = \varepsilon_j = 0$)

$$\frac{M_j}{M} = \frac{(1 - \cos\theta)}{2} \tag{6}$$

Typically $(1 - \cos\theta)$ is small so that ε_s can have a significant effect on the mass of jet produced.

As mentioned previously, the velocity deficit, ε, arises when irreversible work is done in the collapse process. The irreversible work can be caused by various forms of plastic working or by shock heating of the metal if the collapsing liner is supersonic with respect to the frame of reference of the detonation wave (Reference 3). The irreversible work appears as heat and this is quite evident when picking up the collapsed pressure tube after an experiment.

The irreversible work may be expressed as

$$\Delta E = \frac{1}{2} D^2 - \frac{1}{2} D^2 (1 - \varepsilon_s)^2 \tag{7}$$

where this expression is evaluated along a stream tube which forms the slug of the collapsed tube. Therefore $\Delta E = D^2 \varepsilon_s$. Reference 4 considers the plastic shear work done in collapsing the tube by applying the two-dimensional steady equations of motion. The result is

$$W_p = \frac{2}{\sqrt{3}} \frac{Y}{\rho} |\Delta\alpha| \tag{8}$$

where Y is Von Mises yield strength, ρ is liner density, and $|\Delta\alpha|$ is cumulative angle through which the liner bends. From Figure 8 it is clear that $|\Delta\alpha| = 2\theta$.

If the irreversible work resulted only from plastic shear work

$$\Delta E = W_p$$

or

$$D^2 \varepsilon_s = \frac{2}{\sqrt{3}} \frac{Y}{\rho} 2\theta$$

Therefore

$$\varepsilon_s = \frac{4}{\sqrt{3}} \frac{Y}{\rho} \frac{\theta}{D^2} \tag{9}$$

From Equation (5)

$$\frac{M_j}{M} = \frac{(1 - \cos\theta) - \frac{4}{\sqrt{3}} \frac{Y\theta}{\rho D^2}}{2}$$

Using the small angle approximation $1 - \cos\theta = \theta^2/2$

$$\frac{M_j}{M} = \frac{\frac{\theta^2}{2} - \frac{4}{\sqrt{3}} \frac{Y\theta}{\rho D^2}}{2} \tag{10}$$

As an example consider a steel liner (Y = 6 kbar) collapsed by nitromethane (D = 6.3 km/sec) and a representative collapse angle of 10 deg:

$$\frac{M_j}{M} = \frac{0.0153 - 0.0008}{2}$$

Thus the jet mass is reduced by 5% from the contribution of plastic shear work alone. The contribution of bulk plastic work in the tube collapse process, for instance, should be considerably greater because of convergence effects.

The conclusion of this analysis is that small irreversible processes are important in the determination of tube jetting and should be included in any analysis of explosive driver performance. In an explosive driver, the internal pressure, the growth of a boundary layer, and all the irreversible processes occurring in the collapsing liner tend to suppress jetting. This is experimentally verified in the sense that jetting has never been a problem in the high pressure drivers used in launcher work.

SECTION III

GASDYNAMIC CYCLES FOR ACHIEVING VERY HIGH VELOCITIES

At the beginning of this year's program several methods of using explosively driven systems to achieve high velocities were considered. Three approaches using fairly well developed techniques were addressed. In this section these three types of gasdynamic cycles are described in detail with reference to calculations and experiments. The performance limits of each are pointed out.

A. SINGLE-STAGE LINEAR GUNS

With explosive drivers in their present state of development, very high enthalpy columns of driver gas may be generated. The schematic operation of this type of gun is shown in Figure 9. If the moving column of gas is brought to rest by a strong shock reflection, very high reservoir sound speeds may be produced. Using the strong shock relations for a perfect gas, the reservoir sound speed is found for a particular gas to be a function of the detonation velocity only

$$a_4 = \sqrt{\frac{(3\gamma-1)(\gamma-1)}{2}}\, D \qquad (11)$$

where a_4 is reservoir sound speed, γ is ratio of specific heat of driver gas, and D is driver detonation velocity. For helium ($\gamma = 5/3$) $a_4 = 1.15$ D and for hydrogen ($\gamma = 7/5$) $a_4 = 0.8$ D. Helium however is very nearly a perfect gas for driver pressures of several thousand atmospheres and driver detonation velocities of 5 to 8.6 km/sec, as shown by the Saha equation for helium in Figure 10.

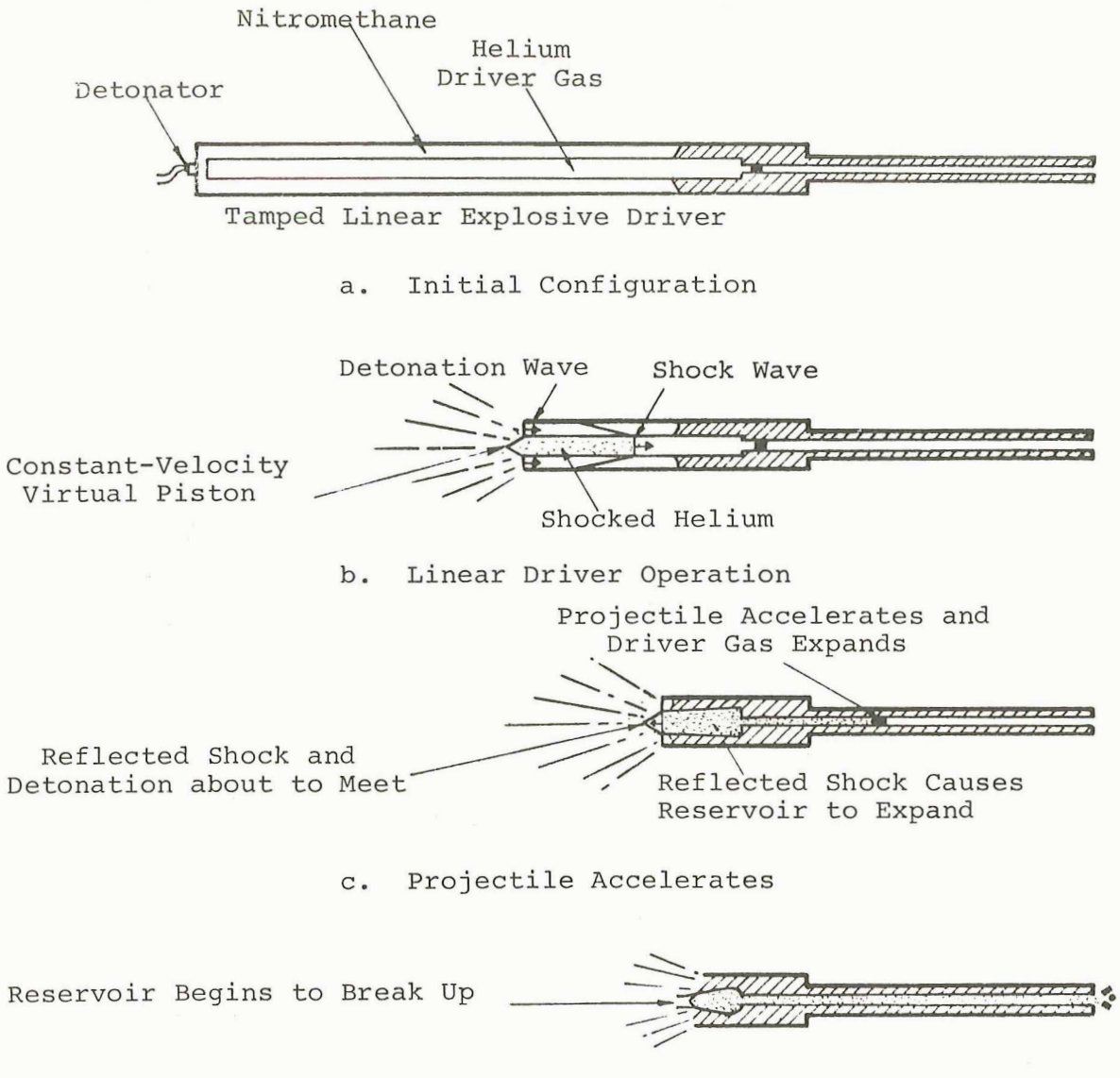

FIGURE 9. OPERATION OF A SINGLE-STAGE EXPLOSIVELY DRIVEN LAUNCHER

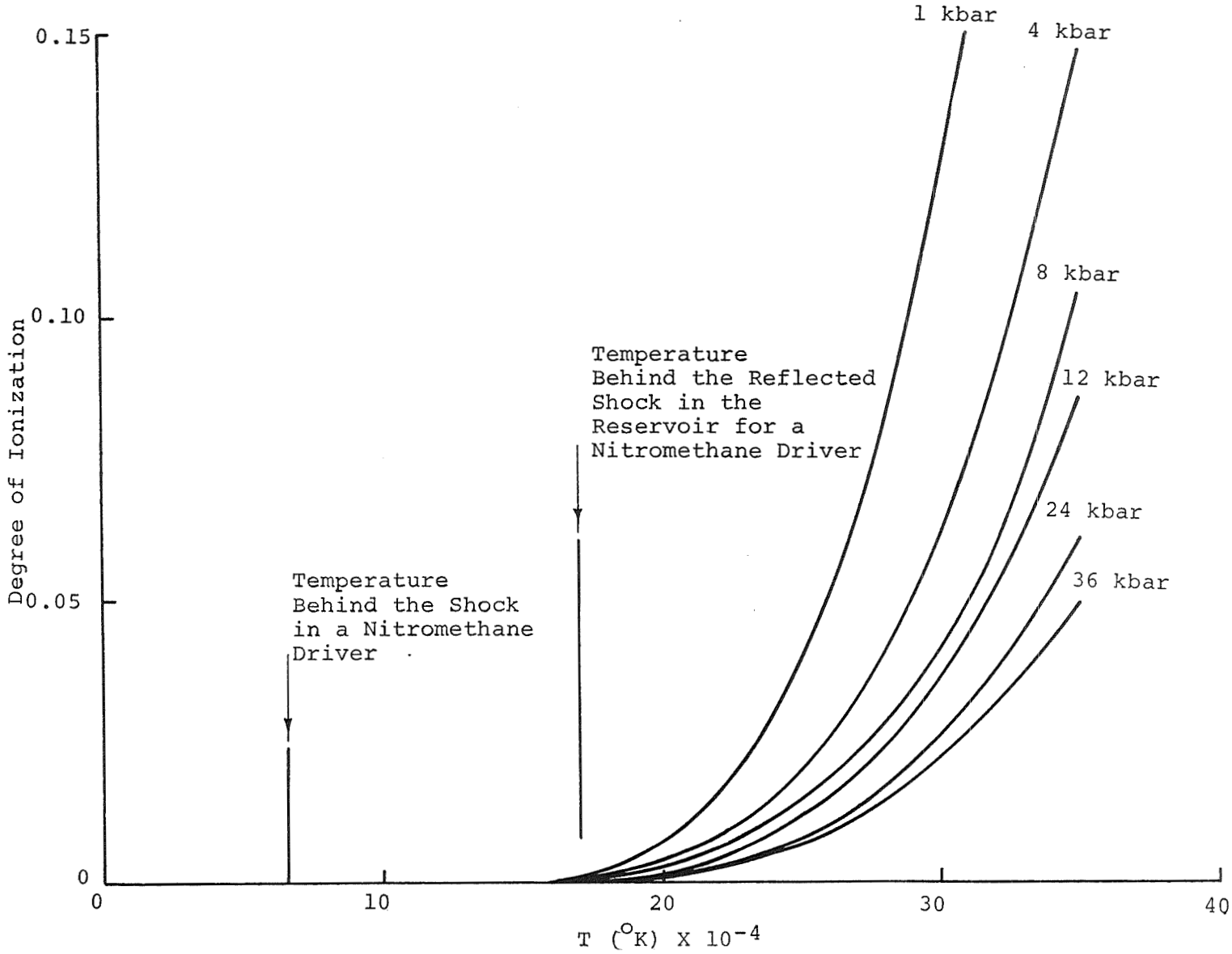

FIGURE 10. SAHA EQUATION FOR HELIUM

With nitromethane (D = 6.6 km/sec), reservoir escape speeds of 22 km/sec may be achieved using helium, as can be seen from the well-known relation for the unsteady escape speed for a gas expanding from a stationary reservoir

$$\hat{u} = \frac{2a_4}{\gamma-1} \tag{12}$$

Explosive drivers using helium ($\gamma = 5/3$), have been operated with gas pressures of 2 to 6 kbar for several years. If this gas is brought to rest by a strong shock reflection in the reservoir, pressures up to 36 kbar may be generated, as calculated by the equation

$$P_4 = \left(\frac{3\gamma-1}{\gamma-1}\right) P_2 \tag{13}$$

where P_4 is the pressure behind the reflected shock in the reservoir and P_2 is the pressure behind the driver shock. Therefore, with existing technology using a nitromethane driver, reservoir conditions of P_4 = 36 kbar and a_4 = 7.6 km/sec may be achieved. With these conditions to accelerate a 1/2-caliber long, 2-g projectile, it can be shown by applying the standard ballistic equations (References 5 and 6) that the final velocity would be 11.2 km/sec. Using another liquid explosive, Astrolite (D = 8.6 km/sec), to obtain reservoir sound speeds of 9.9 km/sec, the projectile velocity was calculated to be 12.8 km/sec. In these calculations the projectile is assumed to have an areal density of 1.1 g/cm^2. The barrel is 100 cm long and the driver-driven area ratio is taken as 2. The gas mass-to-projectile mass (G/M) ratio is assumed to be infinite. This assumption is valid in the examples cited above.

Although it would be desirable to lower the base pressures, operating the gun with reservoir pressures as high as 36 kbar is feasible with certain projectile shapes and materials. This has been demonstrated in References 2 and 7. However, to reduce model distortion and reservoir expansion (which is discussed later), it would be necessary to reduce the reservoir pressure. With the length of explosive drivers being limited by boundary-layer growth the assumption of infinite G/M ratio would no longer be valid with reduced driver pressures and the high performance estimates would not apply.

Two cases that are possible in an explosively driven gun operated with a limited length of shocked gas are now considered. In the first case the explosively formed piston remains closed when it stops, and in the second case the piston vanishes when it stops. This latter case may occur when the reflected shock from the breech interacts strongly with the piston.

Seigel (Reference 5) has calculated the performance of the gun for the case of the piston that remains closed. In this analysis, which will not be repeated here, he plots dimensionless velocity, $\bar{u} = u/a_4$, as a function of the ballistic parameter $\bar{x} = P_4 x/(\rho\ell)a_4^2$ for various values of the parameter G/M. Here u = projectile velocity, a_4 = reservoir sound speed, P_4 = reservoir pressure, x = barrel length, $(\rho\ell)$ = areal density of projectile, G = driver gas mass, and m = projectile gas mass. The curves for a driver-to-driven diameter ratio (D_{21}) of 2 are shown in Figure 11.

For the case of the open or vanishing piston, several computer solutions have been nondimensionalized and shown to correlate, not

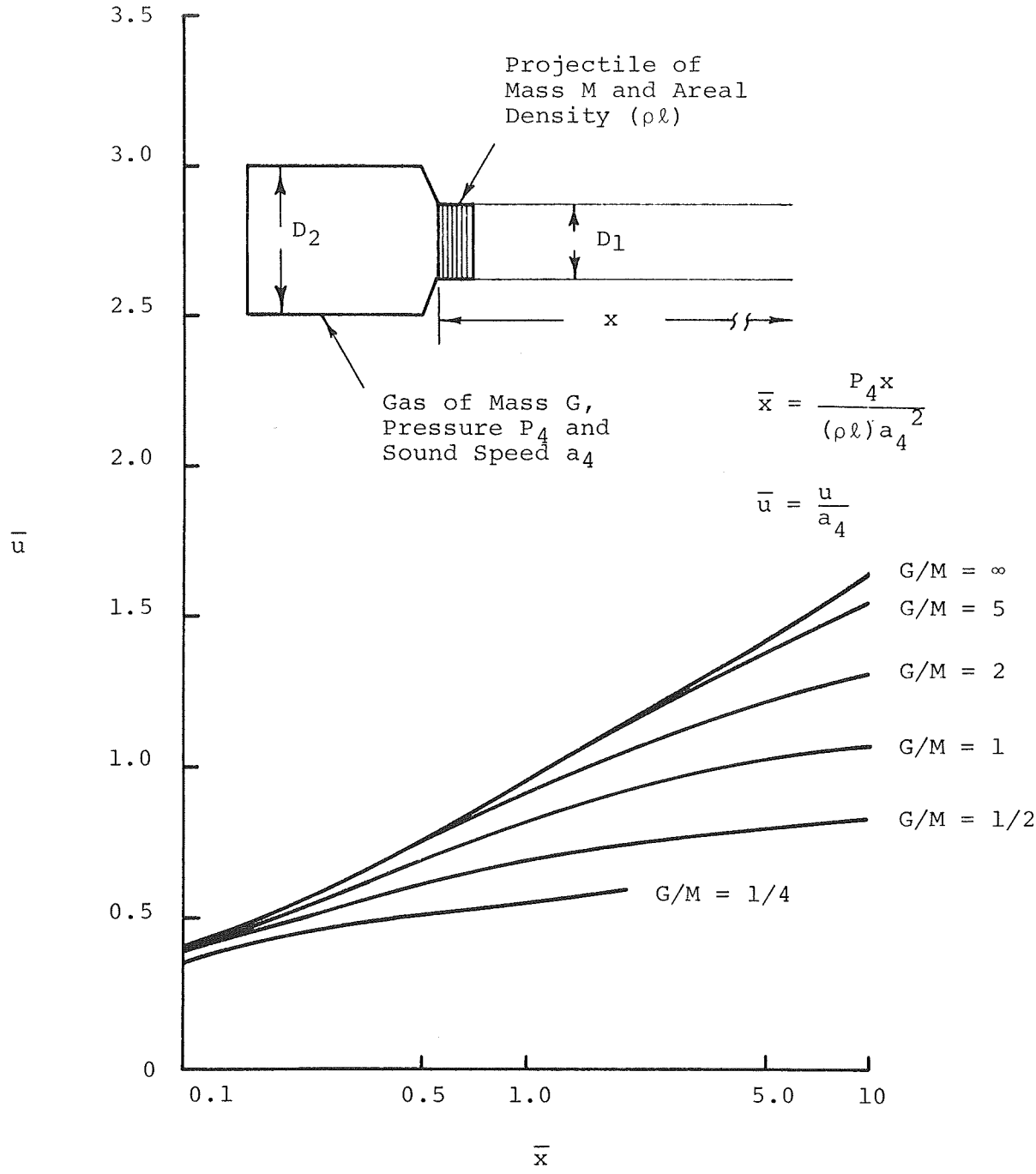

FIGURE 11. BALLISTIC EQUATIONS FOR A CLOSED RESERVOIR GUN WITH $D_{21} = 2$, $\gamma = 5/3$ (Reference 5)

with the G/M ratio, but rather with a dimensionless reservoir length parameter $L = x/x_o$ where x_o = reservoir length and x = barrel length. This correlation is shown in Figure 12, again for the driver-to-driven diameter ratio (D_{21}) of 2.

In the piston-stop or closed reservoir case where the G/M ratio is used, the limited mass of driver gas is felt when the rarefaction waves generated at the base of the accelerating projectile reflect from the end of the reservoir and overtake the accelerating projectile. The upstream end of the reservoir in this case, it should be noted, is stationary. In the open or vanishing piston case where the x/x_o ratio is used, the complete rarefaction generated when the piston "vanishes" dominates the problem. The rarefactions generated at the base of the accelerating projectile never reflect from the upstream end of the reservoir which is now formed by a head of the strong upstream-running rarefaction wave, which moves at nearly the characteristic velocity.

The analysis presented here is correct for a single-stage gun operating ideally. With the high sound speeds possible in the explosive guns, very high velocities (up to about 13 km/sec) should be possible. However, the high reservoir pressures cause the reservoir walls to expand; this unfortunately limits the velocities attainable through this approach. If the reservoir pressure is lowered to acceptable limits (for instance to the yield strength of the reservoir walls), the explosive gun is limited by a low G/M ratio because boundary-layer growth limits present driver performance.

Several designs of single-stage explosive guns have been tested experimentally. The G/M ratio in these guns is effectively infinite.

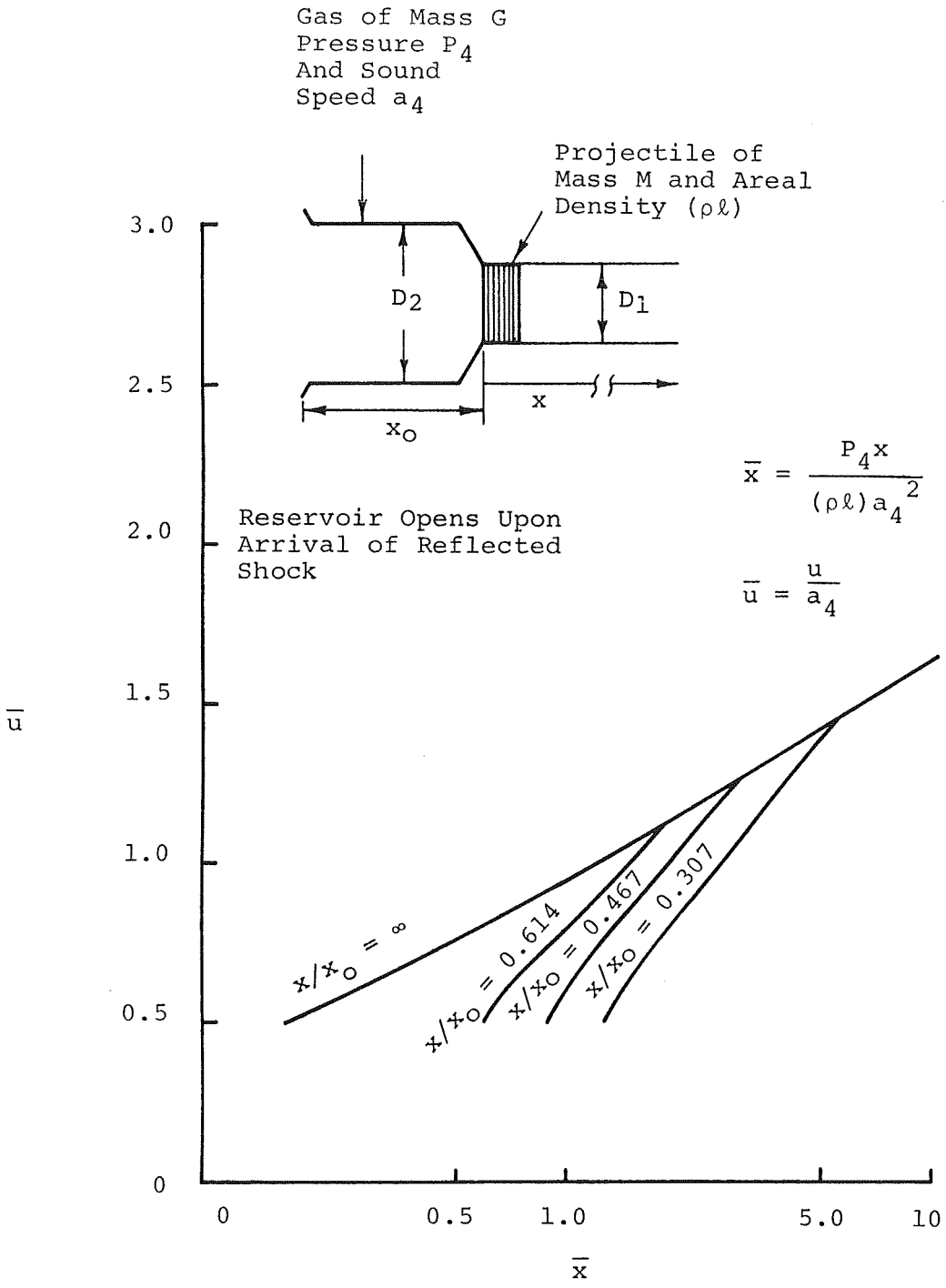

FIGURE 12. BALLISTIC EQUATIONS FOR AN OPEN-ENDED RESERVOIR GUN WITH $D_{21} = 2$, $\gamma = 5/3$

In all cases the predicted performance has not been achieved and a large fraction of this performance loss has been correlated with reservoir expansion during the launch cycle. The calculations and experiments supporting this conclusion are presented in Sections IV and V respectively.

B. TWO-STAGE SYSTEMS WITH CONSTANT BASE PRESSURE ACCELERATION

The most desired type of launcher operation is that in which the pressure on the base of the projectile is low and nearly constant. The theory for a complete two-stage, explosively driven system of the type shown schematically in Figure 13 is presented here. In the first stage, consisting of a linear explosively driven gun similar to that described in part A of this section, the projectile is accelerated in a controlled manner approximating a steady expansion of the reservoir gas. This is accomplished by using a large driver-to-driven diameter ratio as pointed out by Glass (Reference 6). The base pressure on the projectile is approximately that obtained through a steady expansion and this is valid until the flow Mach number behind the projectile reaches unity. This is expressed by the relation

$$\frac{P_3}{P_4} = \left[1 - \frac{\gamma-1}{2}\left(\frac{u_3}{a_4}\right)^2\right]^{\gamma/\gamma-1} = \left[1 + \frac{\gamma-1}{2} M_3^2\right]^{-\frac{\gamma}{\gamma-1}} \qquad (14)$$

where the subscript 3 refers to the gas conditions at the base of the projectile and the subscript 4 refers to the reservoir conditions.

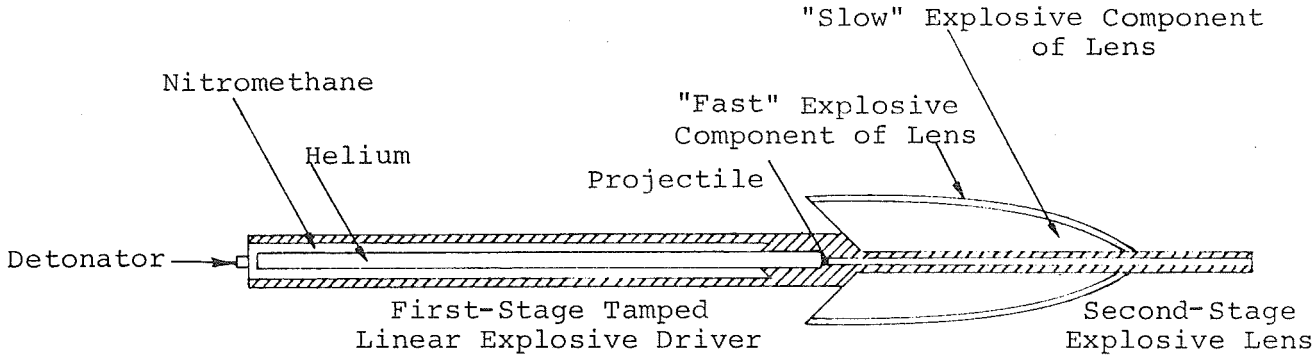

a. Initial Configuration

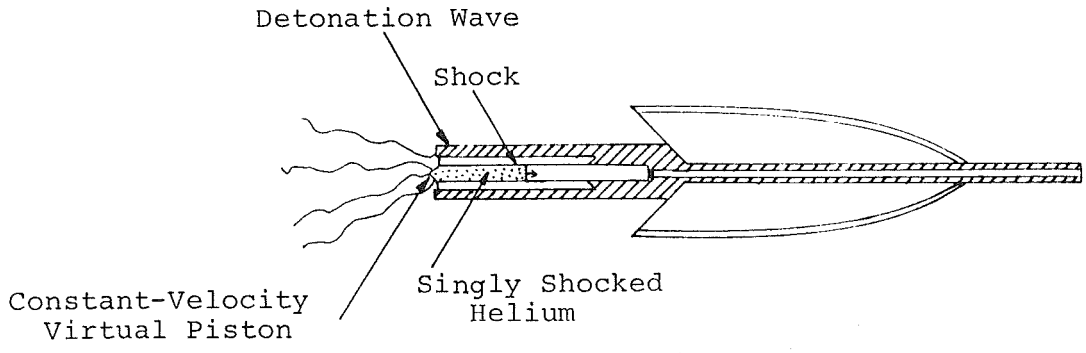

b. First-Stage Linear Driver Operation

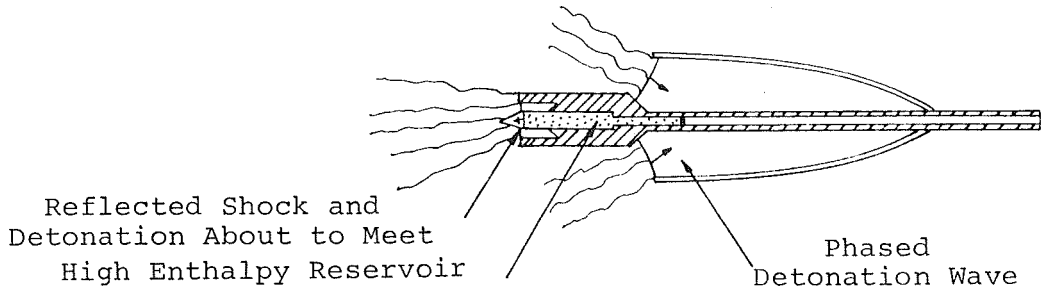

c. Second-Stage Initiated: Projectile and Driver Gas Being Injected into Explosive Lens

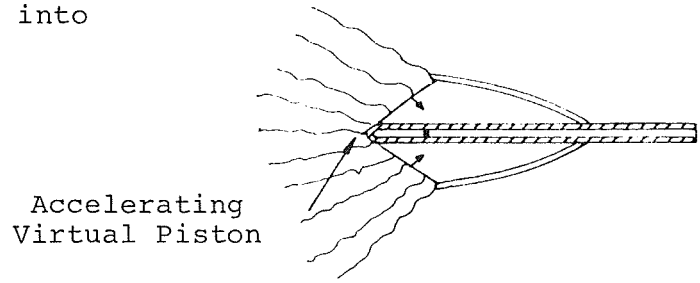

d. Explosive Lens Accelerates Projectile to Final Velocity

FIGURE 13. OPERATION OF A TWO-STAGE EXPLOSIVELY DRIVEN LAUNCHER

With this type of acceleration, the reduction in base pressure with increasing projectile velocity is minimized. With helium for example $P_3/P_4 = 0.488$ when $M_3 = 1$, which is the limit to which the equation is valid. In addition

$$\frac{dP_3}{du_3} = -\left[1 - \frac{\gamma-1}{2}\left(\frac{u_3}{a_4}\right)^2\right]^{1/\gamma-1}\left(\frac{\gamma u_3 P_4}{a_4^2}\right) \tag{15}$$

which gives the decrement in pressure as a function of increment in velocity. This is an important variable for consideration in augmentation. For the case of $u_3 = 5.5$ km/sec the quantities P_3/P_4, dP_3/du_3, and M_3 are plotted as functions of driver detonation velocity (D) in Figure 14 by expressing P_4 and a_4 in terms of D

$$P_4 = \left(\frac{3\gamma-1}{\gamma-1}\right)\left(\frac{\gamma+1}{2}\right)\rho_1 D^2 \tag{13}$$

$$a_4 = \sqrt{\frac{(3\gamma-1)(\gamma-1)}{2}}\ D \tag{11}$$

where ρ_1 = loading or initial gas density. Also of importance in augmentation are the position and time of the projectile when a given velocity and base pressure are achieved. These are obtained in the standard way using the equation

$$F = \frac{Md^2x}{dt^2} \tag{16}$$

or

$$P = (\rho\ell)\ \frac{d^2x}{dt^2}$$

where $(\rho\ell)$ is the areal density of the projectile.

For the position

$$P_3 = (\rho \ell)\ u\left(\frac{du}{dx}\right)$$

inserting

$$\frac{P_3}{P_4} = \left[1 - \frac{\gamma-1}{2}\left(\frac{u_3}{a_4}\right)^2\right]^{\gamma/\gamma-1} \tag{14}$$

and integrating we obtain

$$\frac{P_4 x}{(\rho \ell)\, a_4{}^2} = \left[1 - \frac{\gamma-1}{2}\left(\frac{u_3}{a_4}\right)^2\right]^{-\frac{1}{\gamma-1}} - 1 \tag{17}$$

This can be expressed in terms of driver detonation velocity and loading pressure by inserting

$$P_4 = \left(\frac{3\gamma-1}{\gamma-1}\right)\left(\frac{\gamma+1}{2}\right)\ \rho_1 D^2 \tag{13}$$

and

$$a_4 = \sqrt{\frac{(3\gamma-1)\,(\gamma-1)}{2}}\ D \tag{11}$$

For the case of $\gamma = 5/3$ (helium), $D = 6.6$ km/sec (nitromethane) and $u_3 = 5.5$ km/sec (a special case discussed later), the position of the projectile is plotted as a function of base pressure in Figure 15.

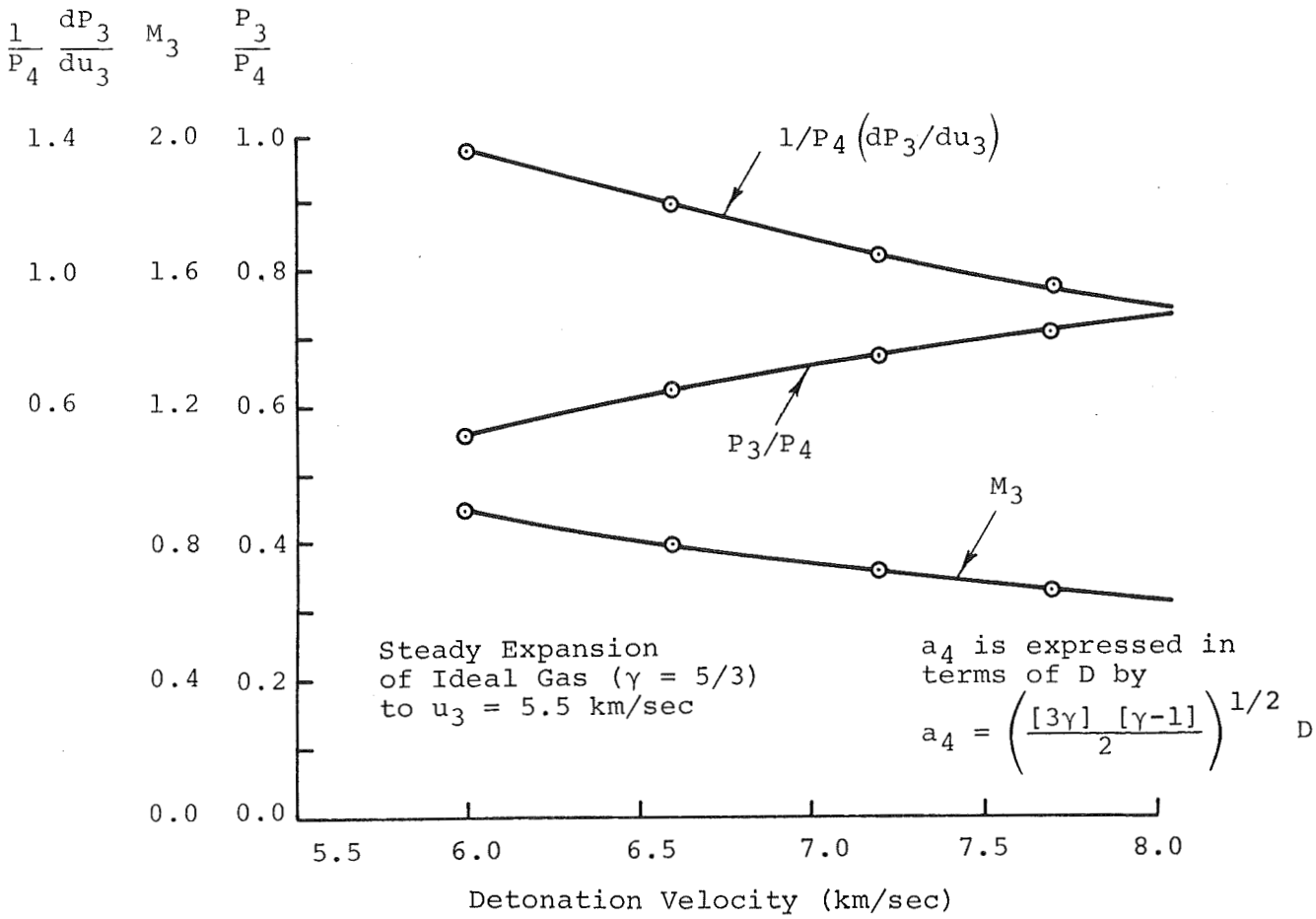

FIGURE 14. P_3/P_4, M_3, AND $1/P_4\ dP_3/du_3$ AS FUNCTIONS OF DRIVER DETONATION VELOCITY FOR A STEADY EXPANSION TO u_3 = 5.5 km/sec

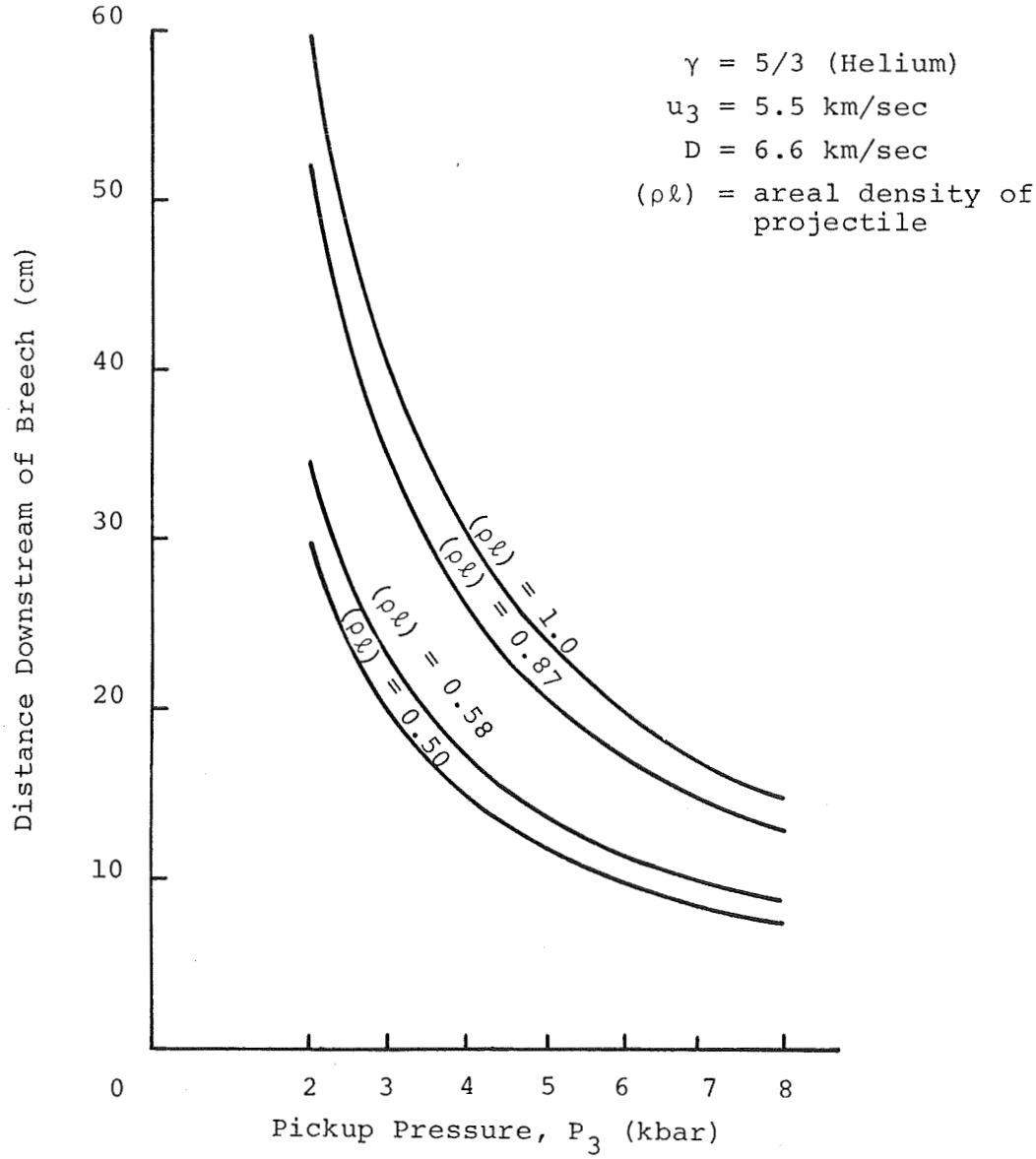

FIGURE 15. PROJECTILE LOCATION AT u_3 = 5.5 km/sec AS A FUNCTION OF BASE PRESSURE FOR A NITROMETHANE DRIVER AND A STEADY EXPANSION OF RESERVOIR GAS

In order to determine the corresponding time, the equation to be used is

$$P_3 = (\rho \ell)\left(\frac{du}{dt}\right)$$

Again

$$\frac{P_3}{P_4} = \left[1 - \frac{\gamma-1}{2}\left(\frac{u_3}{a_4}\right)^2\right]^{\gamma/\gamma-1}$$

To perform the integration P_3/P_4 is expanded in a binomial series. The result to four terms is

$$\frac{P_4 t}{(\rho \ell)} = u + \frac{\gamma}{6a_4^2} u^3 + \frac{\gamma(2\gamma-1)}{40a_4^4} u^5 + \frac{\gamma(2\gamma-1)(3\gamma-2)}{336a_4^6} u^7 + \ldots . \quad (18)$$

The series converges rapidly. The equation is plotted in Figure 16 for time as a function of P_3 for the case $\gamma = 5/3$, $u_3 = 5.5$ km/sec, and D = 6.6 km/sec. In Figures 14, 15, and 16 the velocity $u_3 = 5.5$ km/sec is chosen since this is a very likely choice of pickup velocity for the second stage. The second stage in this system would be an explosive lens (Reference 1), and the minimum starting velocity of this lens is the lowest velocity obtainable with the lens explosive (Figure 5). With diluted nitromethane this minimum velocity is around 5.5 km/sec.

For the case of a 0.94-cm-diam, 2/3-caliber long projectile of density 1.4 g/cm^3, the pickup conditions of $P_3 = 5$ kbar and $u_3 = 5.5$ km/sec are achieved at x = 21 cm and t = 70.5 μsec for a detonation velocity of 6.6 km/sec from Figures 15 and 16. The flow Mach number behind the projectile is $M_3 = 0.8$ and $dP_3/du_3 = 1.2\ P_4$. Since P_4 for this case is 8 kbar, a variation in pickup

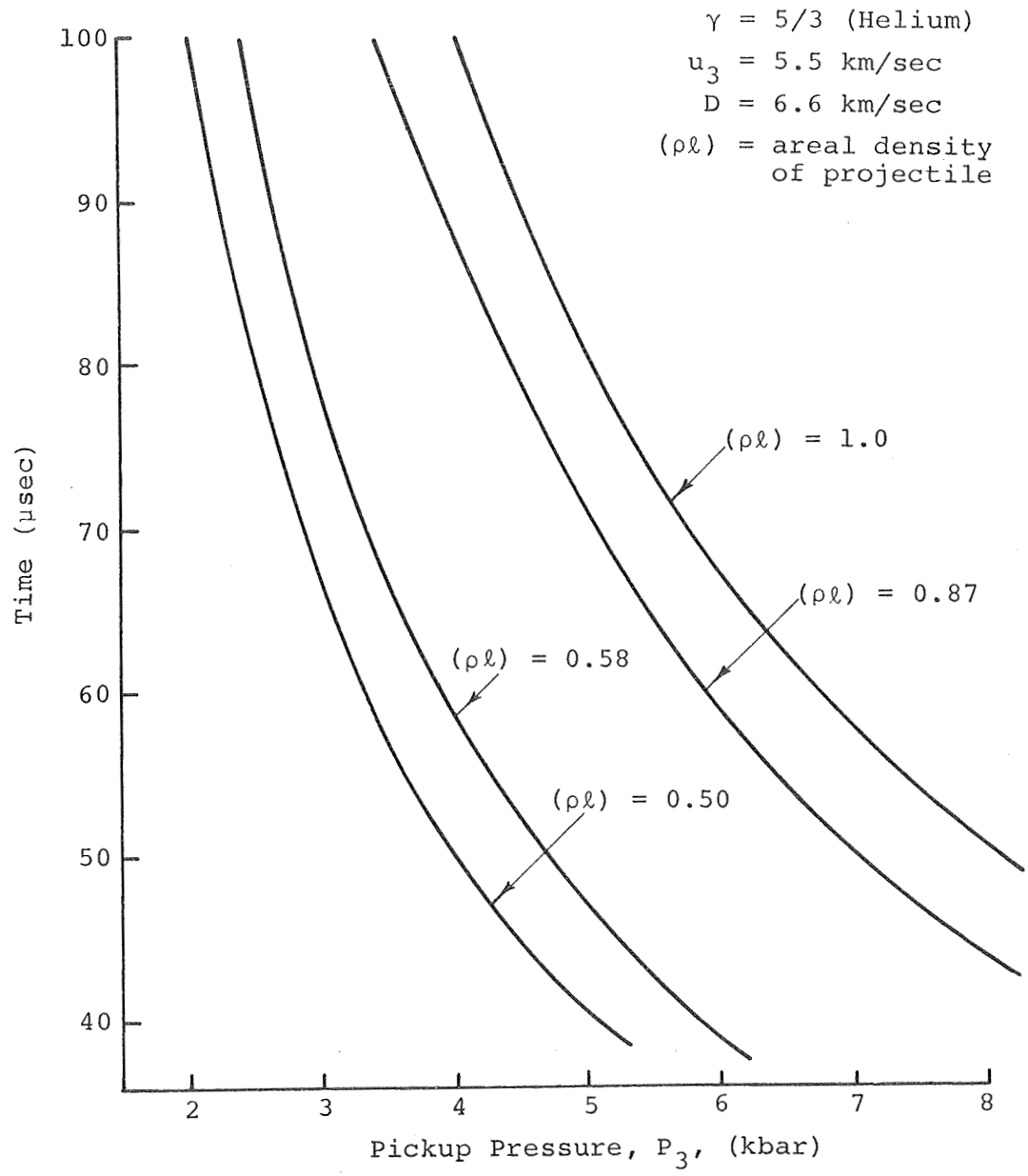

FIGURE 16. TIME TO ACCELERATE TO u_3 = 5.5 km/sec AS A FUNCTION OF BASE PRESSURE FOR A NITROMETHANE DRIVER AND A STEADY EXPANSION OF RESERVOIR GAS

velocity of ± 0.5 km/sec results in a change of pressure of approximately ± 0.48 kbar or ± 9.5% of the pickup pressure. If the gun were operated in the unchambered mode then the pickup pressure corresponding to a projectile velocity of 5.5 km/sec would be 2 kbar. A variation in pickup velocity of ± 0.5 km/sec results in a variation of ± 0.3 kbar in pickup pressure or ± 15% of the pickup pressure.

The advantages of operating the first stage in the infinite chambrage mode are clear. The variation of pickup pressure with pickup velocity and the decrease of pressure as the projectile accelerates are minimized. If the second-stage acceleration is constant, the entire gun cycle would be very close to the ideal constant base pressure system.

The second-stage acceleration is accomplished using an explosive lens such as described in Section II. This lens can provide a constant acceleration beginning at pickup conditions. Therefore, using the lens in conjunction with the above example, we could start with a constant base pressure of 5 kbar and continue the acceleration in a uniform manner from 5.5 km/sec to the final velocity. Using the results of Part B of Section II, velocities up to 20 km/sec should be possible.

The second-stage piston, which is explosively formed, is conically shaped and care must be taken to avoid an interaction between the projectile and the second-stage piston region. The second-stage gas dynamics are illustrated schematically in Figure 17. In this simple model, the second-stage gas is assumed to be isentropic and no boundary layer or jetting effects are assumed present.

The conservation of mass is written as

$$\left[\left(\frac{L_1}{3} + L_2\right)\rho\right]_p = \left(\frac{L_1}{3} + L_2\right)\rho \qquad (19)$$

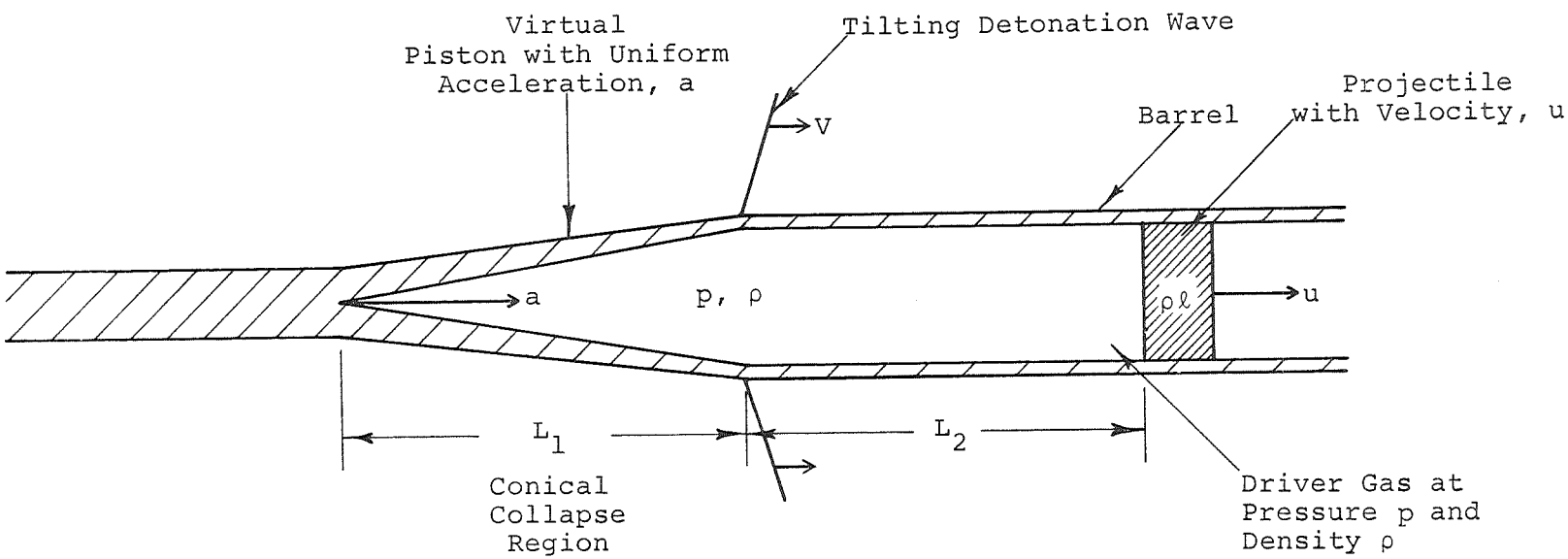

FIGURE 17. IDEAL SECOND-STAGE MECHANICS

where L_1 is length of gas in the collapse cone, L_2 is length of gas at barrel bore diameter, ρ is gas density, and subscript p denotes pickup conditions. For an isentropic gas

$$P = P_p\left(\frac{\rho}{\rho_p}\right)^{\gamma} \tag{20}$$

and for the piston with acceleration, a

$$P = \left[(\rho\ell) + \left(\frac{L_1}{3} + L_2\right)_p \rho_p\right] a \tag{21}$$

where $(\rho\ell) \equiv$ areal density of the projectile.

Combining these relations we obtain

$$\left(\frac{L_1}{3} + L_2\right) = \left(\frac{L_1}{3} + L_2\right)_p P_p^{1/\gamma} \left[(\rho\ell) + \left(\frac{L_1}{3} + L_2\right)_p \rho_p\right]^{-\frac{1}{\gamma}} a^{-\frac{1}{\gamma}}$$

or (22)

$$\left(\frac{L_1}{3} + L_2\right) \alpha\ a^{-\frac{1}{\gamma}}$$

When the second stage is matched to the pickup conditions provided by the first stage the quantity $(L_1/3 + L_2)$ should not change from its value at pickup. Equation (22) is plotted in Figure 18 for several values of γ. This graph gives the equilibrium value of $(L_1/3 + L_2)$ for any acceleration of the second-stage piston.

As the piston accelerates, the conical piston region tends to elongate (see Section II, Part B). Thus although $(L_1/3 + L_2)$

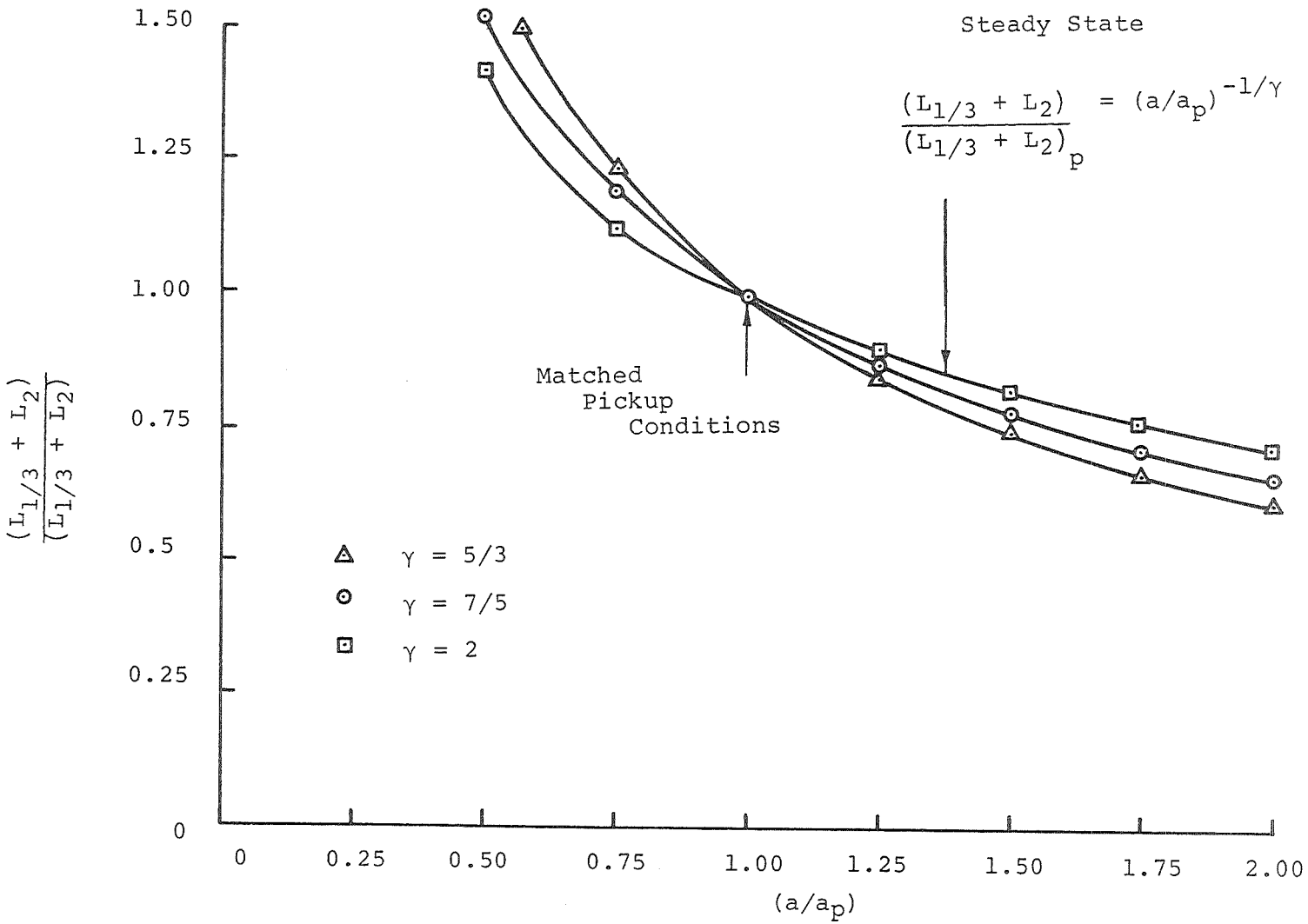

FIGURE 18. EQUILIBRIUM PROJECTILE-TO-PISTON DISTANCE AS A FUNCTION OF SECOND-STAGE ACCELERATION

remains constant for a constant acceleration, L_2 decreases and L_1 grows. The equation of motion of the piston for constant acceleration is

$$u = (u_o^2 + 2ax)^{1/2} \tag{23}$$

where u is second-stage piston velocity, u_o is initial second-stage piston velocity, and x is distance along barrel from initial position of the second-stage piston.

Using this equation along with Equation (19) and assuming $L_1 \propto u$, it can be easily shown that

$$x = \frac{u_o^2}{2a}\left[\left(1 + \frac{3L_2}{L_1}\right)_p^2 - 1\right] \tag{24}$$

is the condition for L_2 to vanish. This corresponds to the situation where the projectile encounters the second-stage conical piston region. In this situation all the second-stage driver gas now resides in the conical region.

Experiments have been carried out to test some of the ideas and calculations presented in this section. Preliminary tests to develop a first stage with effectively infinite chambrage were not completely successful. Even at low reservoir pressures of 8 to 10 kbar there seems to be a loss of reservoir pressure and temperature because of reservoir expansion. In addition, there can be some temperature loss due to flow contamination by the projectile or material eroded from the reservoir walls since the calculated gas temperature is nearly 16,500°K. The experiments in support of this approach, and the apparent performance limits are described in detail in Section V, Part B.

C. TWO-STAGE SYSTEMS WITH AUXILIARY PUMP CYCLE

It became evident that the high reservoir pressures possible with an explosive driver would be difficult to contain. Radial expansion of the reservoir walls under pressures up to 36 kbar act to reduce the amount of energy available in the reservoir. If we consider the effect of wall expansion alone on a stationary reservoir, the ratio of wall work (W) to initial reservoir enthalpy (H_o) is

$$\frac{W}{H_o} = \frac{\int_{r_o}^{r} P\, 2\pi r\, dr}{\pi r_o^2\, \rho_o C_p T_o} \tag{25}$$

If the pressure decays isentropically with wall expansion

$$P = P_o\left(\frac{r_o}{r}\right)^{2\gamma} \tag{26}$$

The result is

$$\frac{W}{H_o} = \frac{1}{\gamma}\left[1 - \left(\frac{r_o}{r}\right)^{2(\gamma-1)}\right] \tag{27}$$

For $\gamma = 5/3$ and a wall expansion of 15%, $W/H_o = 0.105$ or about 10% of the reservoir enthalpy has been used in wall work. As will be shown later, an expansion of 15% usually occurs quite early in the launch cycle of a high-pressure gun. Clearly a way must be found to prevent this energy loss.

One convenient method is to surround the reservoir with explosives and initiate the explosive when it is appropriate to

prevent reservoir wall expansion. This method may be extended to partially or completely collapse the reservoir walls, thereby adding energy to the reservoir gas and enhancing the performance of the gun over that expected, assuming ideal one-dimensional behavior. This method also allows a reduction in peak base pressures experienced by the projectile while still maintaining performance. As will be shown in the next section, the base pressure decays in the normal manner as the gas expands from the reservoir. The base pressure then begins to rise as the reservoir conditions are increased by the reservoir explosive or auxiliary pump cycle.

Coupling the variable reservoir conditions to a general solution of the projectile equation of motion is not easily done and recourse has been made to computer techniques. A computer program has been developed by Physics International for this application. A series of one-dimensional Lagrangian problems has been ganged to couple the description of wall motion with that of the dynamics of the driver gas and projectile. This computer program and several examples are discussed in the next section.

This technique of surrounding the reservoir of a single-stage gun with explosives has been tested experimentally and has proved successful. Velocities higher than those predicted with a one-dimensional analysis have been achieved. The addition of explosives around the reservoir has also proved useful in the design of a successful two-stage gun. These two types of guns are shown schematically in Figure 19. The auxiliary pump cycle is used to collapse the reservoir completely, thereby pumping most of the driver gas into the barrel behind the accelerating projectile. Gas pressures and projectile velocities in excess of minimum requirements for matching the first and second-stages can be generated.

There is one limitation to this approach, which has been of minor importance in the present fast-gun program. Initiation of the reservoir explosive (auxiliary pump cycle) must be timed so that the stress wave driven into the reservoir does not overtake and interact with the accelerating projectile. During this year's contract a 1.56-cm-diam, 0.5-caliber long lithium-magnesium projectile was used and in this case the projectile accelerated rapidly to a velocity greater than the stress wave velocity in the steel (~ 6 km/sec). The projectile always kept ahead of the stress wave in the steel and no damage from this source was ever observed. In another program 1.5-caliber long projectiles were accelerated to 5.5 km/sec. In this case, the auxiliary pump cycle had to be delayed to allow the projectile to keep ahead of the stress wave. Unfortunately the delay was long and the reservoir expansion reached nearly 35% before the auxiliary pump cycle could be started. By this time it was too late to reenergize the reservoir in time to enhance the performance of the gun.

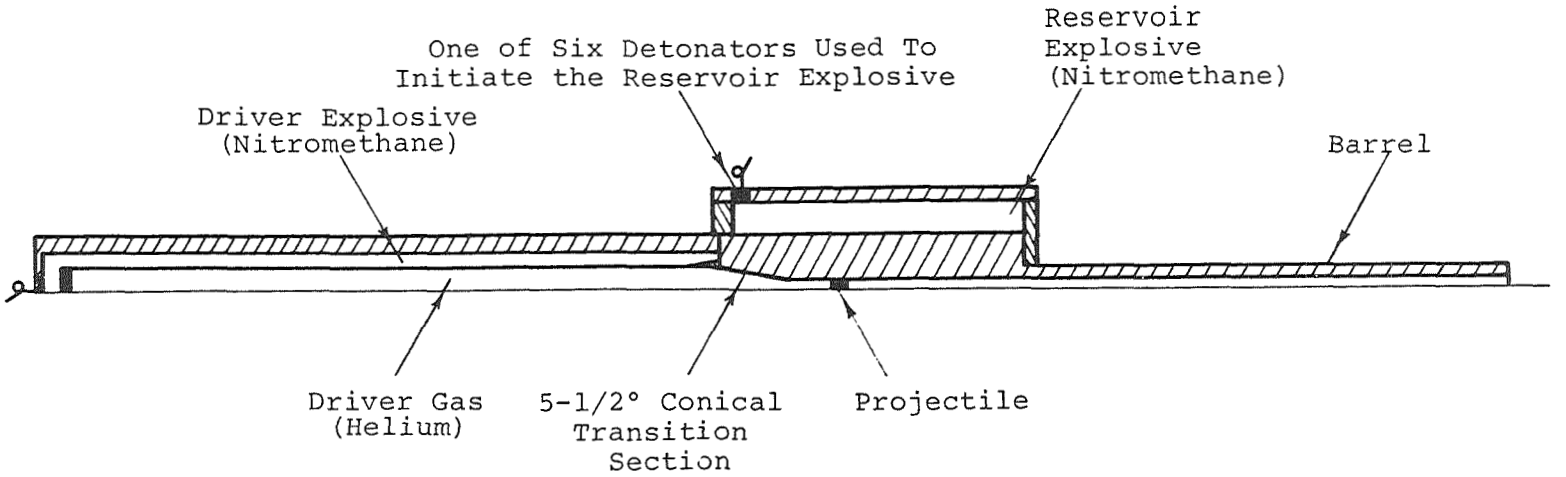

a. Single-Stage Explosively Driven Gun With Auxiliary Pump Cycle

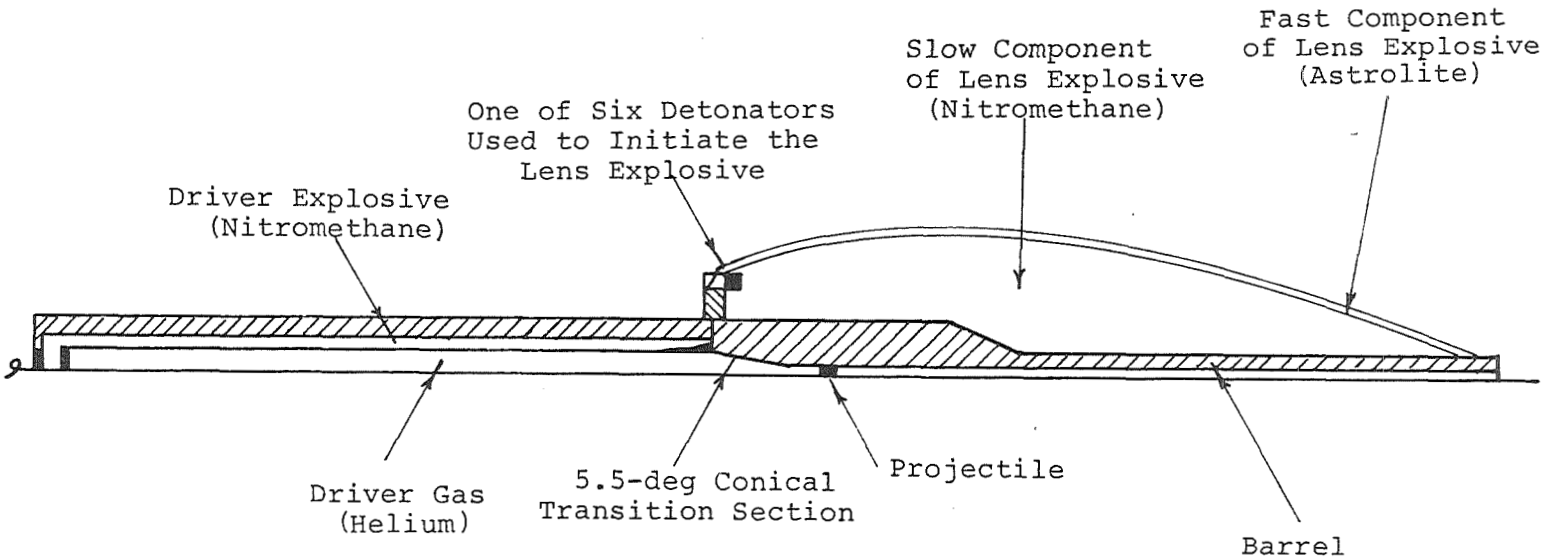

b. Two-Stage Explosively Driven Gun

FIGURE 19. SCHEMATICS OF ONE- AND TWO-STAGE GUNS WITH AUXILIARY PUMP CYCLES

SECTION IV

CALCULATION OF LAUNCHER OPERATION

This section describes a computer program that has been used to predict the performance of explosively driven guns. Several examples of the use of this program are presented. The performance of a single-stage gun, a single-stage gun with auxiliary pump cycle, and a two-stage gun with auxiliary pump cycle are calculated and compared to experiment. In the case of the single- and two-stage guns with auxiliary pump cycles, the performance calculations were carried out prior to the experiments and used to establish design criteria. These designs proved successful and were ultimately used to launch a 2-g projectile to 12 km/sec in both the single- and two-stage guns.

A. THE GANG-POD COMPUTER PROGRAM

In previous launcher development programs performance was calculated either by hand (References 5 and 6) or by Physics International's one-dimensional Lagrangian computer program, POD. This computer program included an elastic-plastic description of the projectile, and using the streamtube approximation, could simulate area changes. Predicted velocities, however, were always significantly higher (by 5 to 30%) than those observed. Radial expansion of the reservoir was felt to be the major cause of this performance loss since the reservoir pressures far exceeded the yield strength of the steel walls, often by an order of magnitude. Reservoir expansion histories have been measured using high-speed framing and streaking cameras (Reference 2). The measured expansion histories have been compared to simple analytic and one-dimensional Lagrangian computer calculations. A typical comparison

for a 24-kbar reservoir is shown in Figure 20. The steel is assumed to have a yield strength of 6 kbar in this case. It is seen that the measured expansion rates are accurately computed at early times; however, the observed expansion is substantially less at later times. The reason for the inability of this method to predict the complete reservoir expansion history is that the one-dimensional calculation in cylindrical geometry is not a valid representation of the reservoir expansion problem, which is axisymmetric and highly two-dimensional at late times.

One of Physics International's two-dimensional computer programs would be suitable for calculating reservoir expansion and coupling the effects of this expansion to the calculation of the launcher performance. Although such an approach is feasible, it is considered too expensive as a design aid. A complete performance calculation by this method would require approximately ten hours of computer time. It is, however, necessary to be able to calculate gun performance accurately since the successful operation of a two-stage system requires a detailed knowledge of the position, velocity, and projectile base pressure as a function of time.

To fill this need Physics International's one-dimensional POD code was modified in an attempt to approximately describe the wall motion. Point masses were placed at discrete points along the walls of the gun. These masses (Figure 21) were allowed to move in response to the average gas pressure under them. The radial motion of these points then modified the gas pressure in the zones under them. Attempts to calculate launcher performance were unsuccessful as it was not clear what mass to assign to the wall points. Since the wall velocity in a real gun is usually on the order of the wall sound speed, the wall motion is controlled by

$\bar{R}$ = dimensionless outer radius = $\frac{R}{r_o} - 1$

$\bar{r}$ = dimensionless inner radius = $\frac{r}{r_o} - 1$

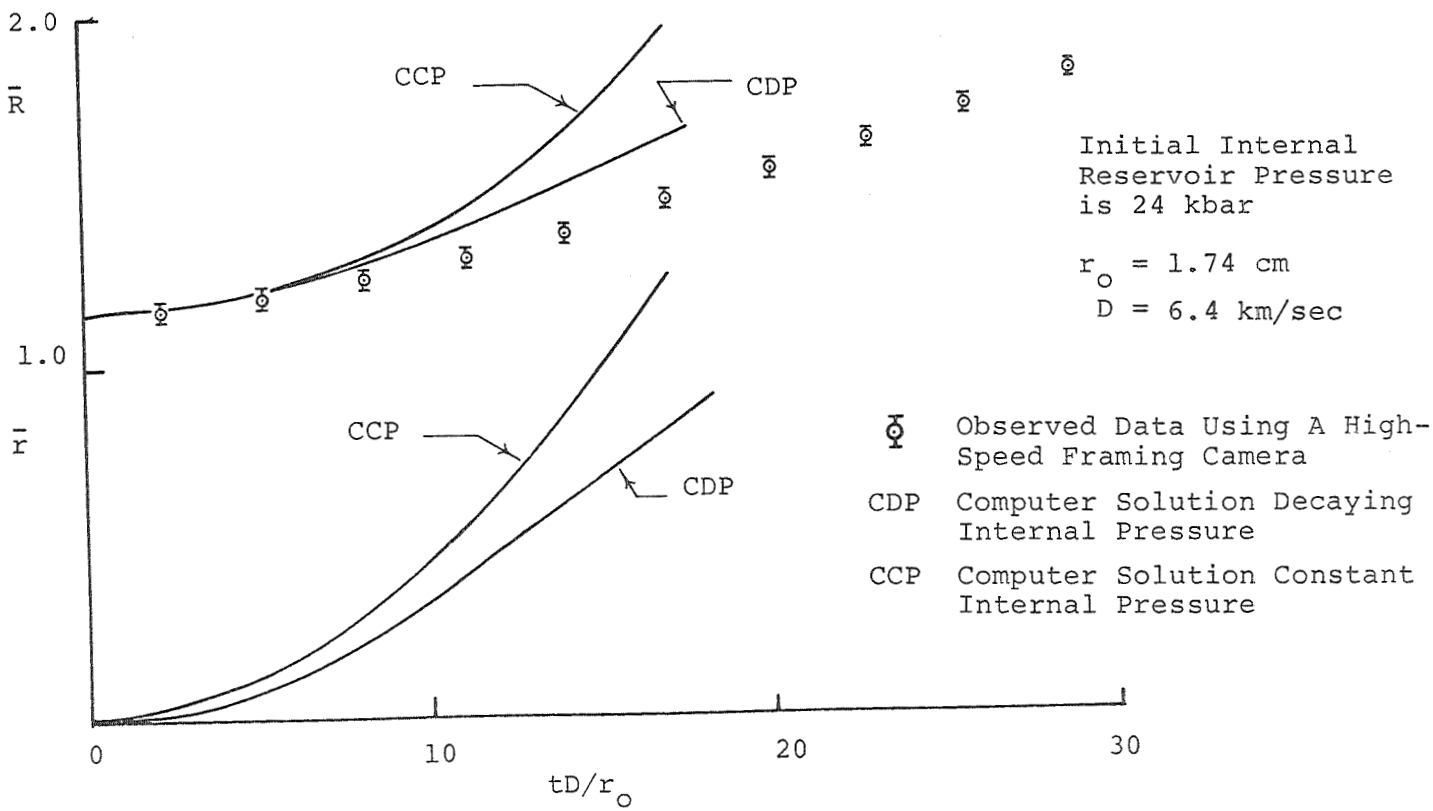

FIGURE 20. DIMENSIONLESS RADIUS-TIME PLOT OF RESERVOIR EXPANSION

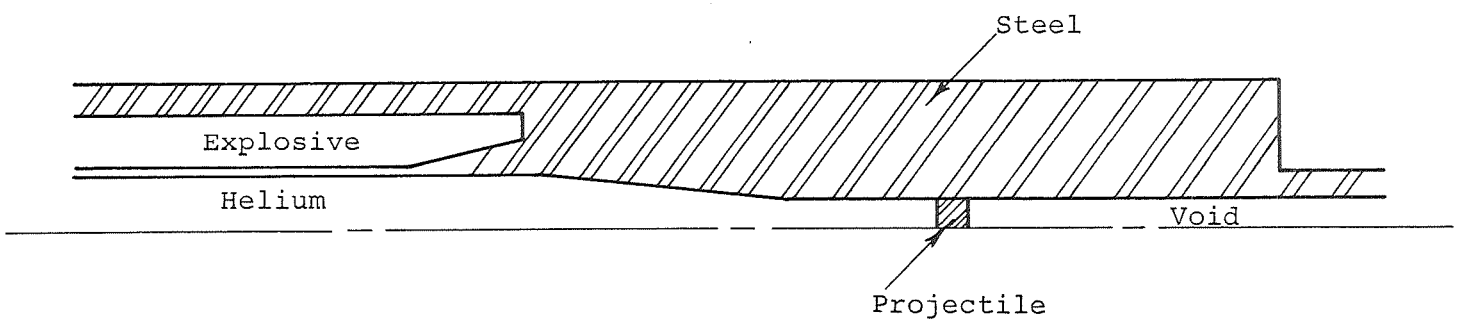

a. Configuration of a Typical Explosive Gun

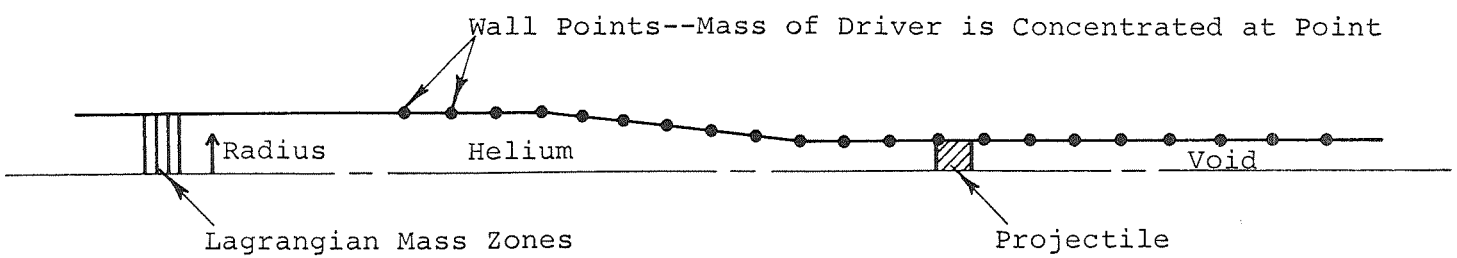

b. Representation of Gun on One-Dimensional Lagrangian Program (POD) with Moving Wall Option

FIGURE 21. EARLY ATTEMPT TO INCLUDE WALL MOTION IN THE CALCULATION OF GUN PERFORMANCE

the discrete waves reverberating in the wall. In the above method, the entire wall mass was concentrated at the wall point, with the result that the early wall motion was underestimated.

To overcome this difficulty, the concentrated wall mass points were replaced by one-dimensional Lagrangian calculations in cylindrical geometry (Figure 22). With this scheme, the wave propagation in the reservoir walls is properly accounted for. As in the previous approach, the gas pressure under the location of the wall calculation is used as a pressure profile for the wall motion calculation. Any motion of the wall then modifies the pressure in the gas under that wall point.

This program, called GANG-POD, can be further utilized to calculate the action of the auxiliary pump cycle. A wall calculation can consist of a layer of steel surrounded by a layer of explosive. This is illustrated in Figure 22. The explosive in the wall calculation can be initiated at any given time to reverse the motion of the reservoir walls. The effect of the collapsing reservoir wall is then automatically coupled to the gas and projectile dynamics in the axial calculation. Several examples of the use of this program are presented in Parts B and C of this section.

B. SINGLE-STAGE PERFORMANCE CALCULATIONS

An experiment was carried out in which a 6-kbar nitromethane driver was used to accelerate a 2-g, 1/2-caliber long projectile. The reservoir was fabricated from steel with a yield strength of about 4 kbar. The 3.48-cm-diam pressure tube was coupled to the 1.59-cm-diam barrel by a 5.5-deg conical transition section. The projectile was placed 2.8 diam downstream of the nozzle outlet plane. The outer diameter of the steel reservoir was 10.2 cm. In the experiment the projectile was accelerated to 7.8 km/sec. A

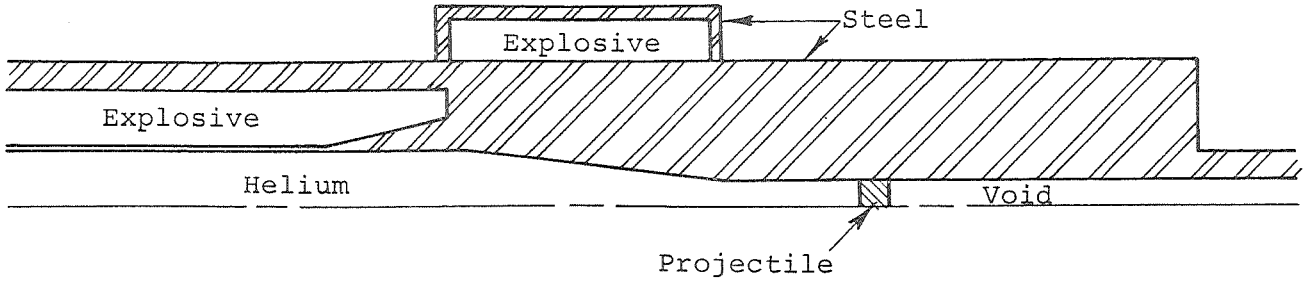

a. Configuration of a Typical Explosive Gun

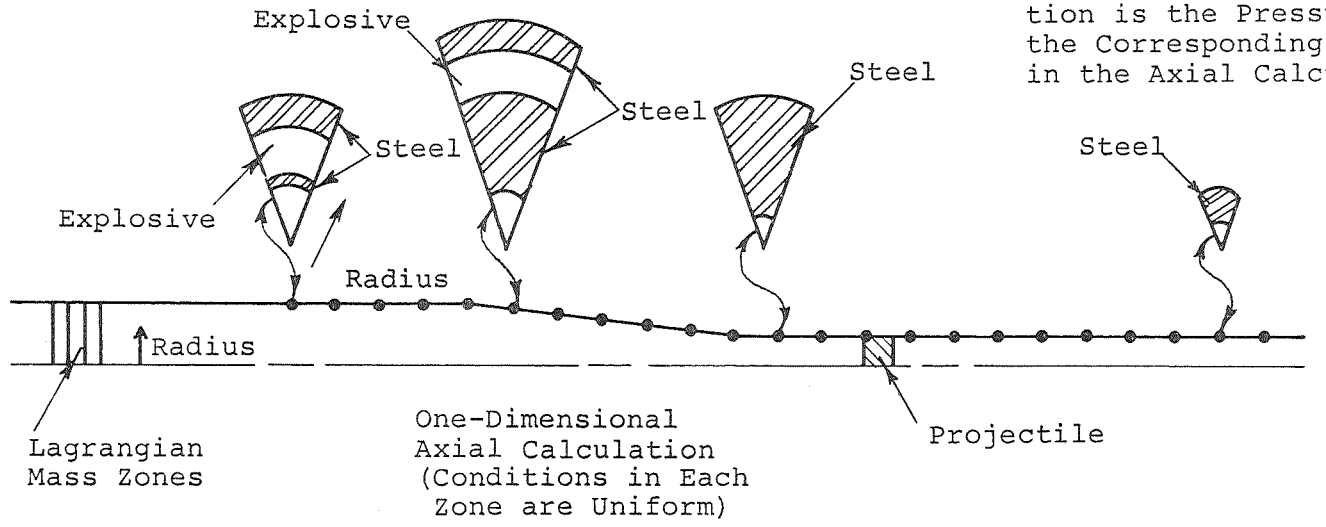

Pressure Applied to Interior Boundary of a Wall Calculation is the Pressure Under the Corresponding Wall Point in the Axial Calculation

b. Representation of Gun on GANG-POD Computer Program

FIGURE 22. GANG-POD COMPUTER PROGRAM TO INCLUDE WALL MOTION IN THE CALCULATION OF GUN PERFORMANCE

one-dimensional Lagrangian (POD) calculation of the launcher operation that assumed no wall motion yielded a muzzle velocity of 11.1 km/sec. The calculation is shown in the x-t plane of Figure 23. The calculation was repeated on the GANG-POD program, with a yield strength of 4 kbar assumed for the steel. The calculation, shown in Figure 24, predicted a muzzle velocity of 7.8 km/sec, which agreed with the velocity measured experimentally. Moreover, the predicted and observed muzzle exit times are in good agreement. The base pressure histories calculated by both the POD and GANG-POD programs are shown in Figure 25. Typical inner wall contours for the GANG-POD calculation are shown in Figure 26.

The success of this method and the insights gained from examining the calculation in detail led to the conclusion that considerable performance increase could be obtained by adding an auxiliary pump cycle to the gun. Therefore the calculation was repeated, this time with a layer of explosive surrounding the reservoir. The results of the calculation are shown in Figure 27. The initiation of the explosive was programmed to coincide with the arrival of the driver shock at the nozzle entrance plane. This timing ensured that the stress wave generated in the reservoir walls by the explosive would not overtake the accelerating projectile. The calculation, which was not carried to completion, did demonstrate that the initial expansion of the reservoir was under control. Based on the extrapolated trajectory (Figure 27), a muzzle velocity of 10 to 11 km/sec could be expected. In the actual experiment a muzzle velocity of 10.6 km/sec was observed. Typical inner wall contours for the calculation are shown in Figure 28. The projectile base pressure history is shown for comparison in Figure 25, and the effect of the auxiliary pump cycle can clearly be seen. Notice that the peak pressures generated in the launch cycle are the same as those where the auxiliary pump cycle was not used.

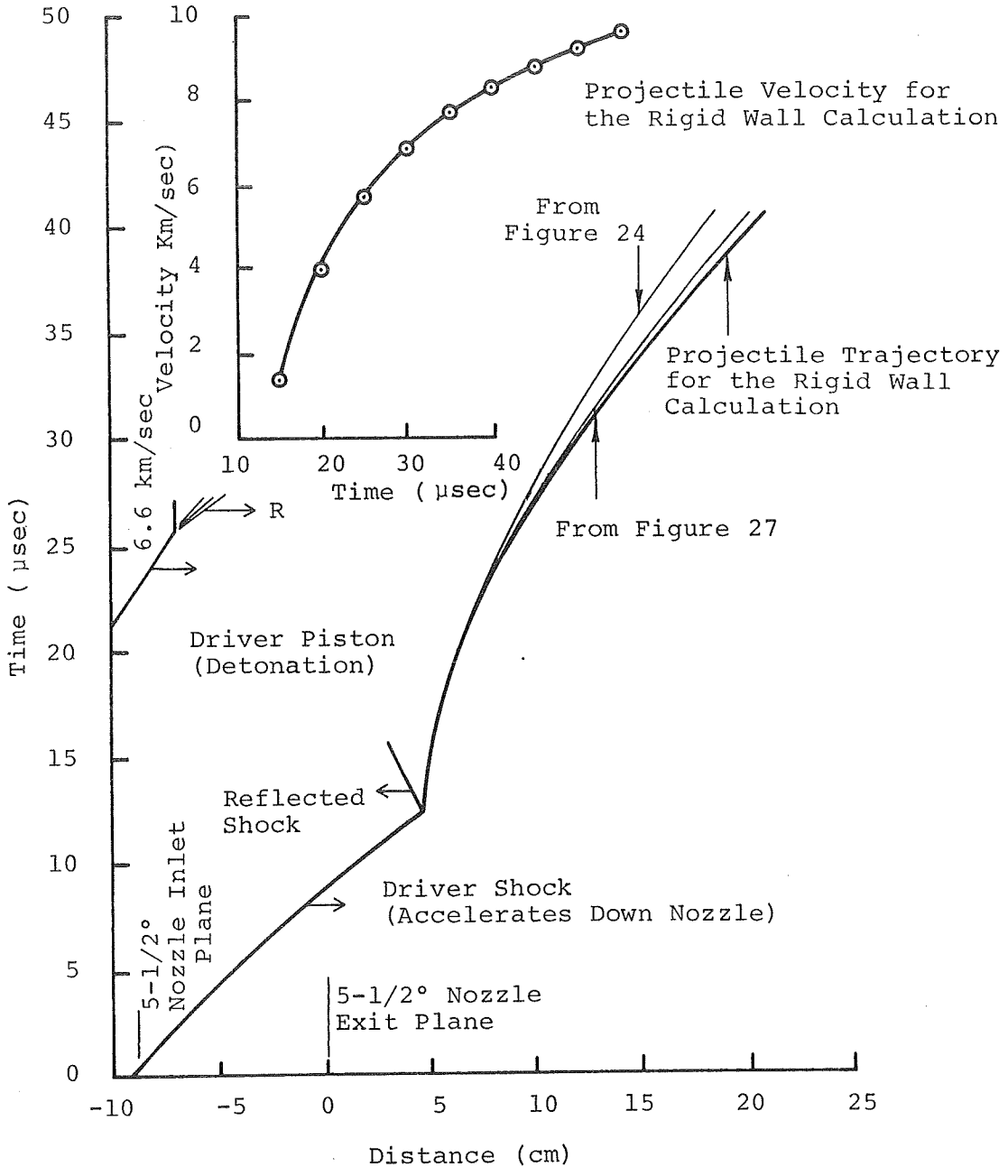

FIGURE 23. CALCULATION OF A HIGH-PRESSURE SINGLE-STAGE GUN USING ONE-DIMENSIONAL LAGRANGIAN CODE (POD)

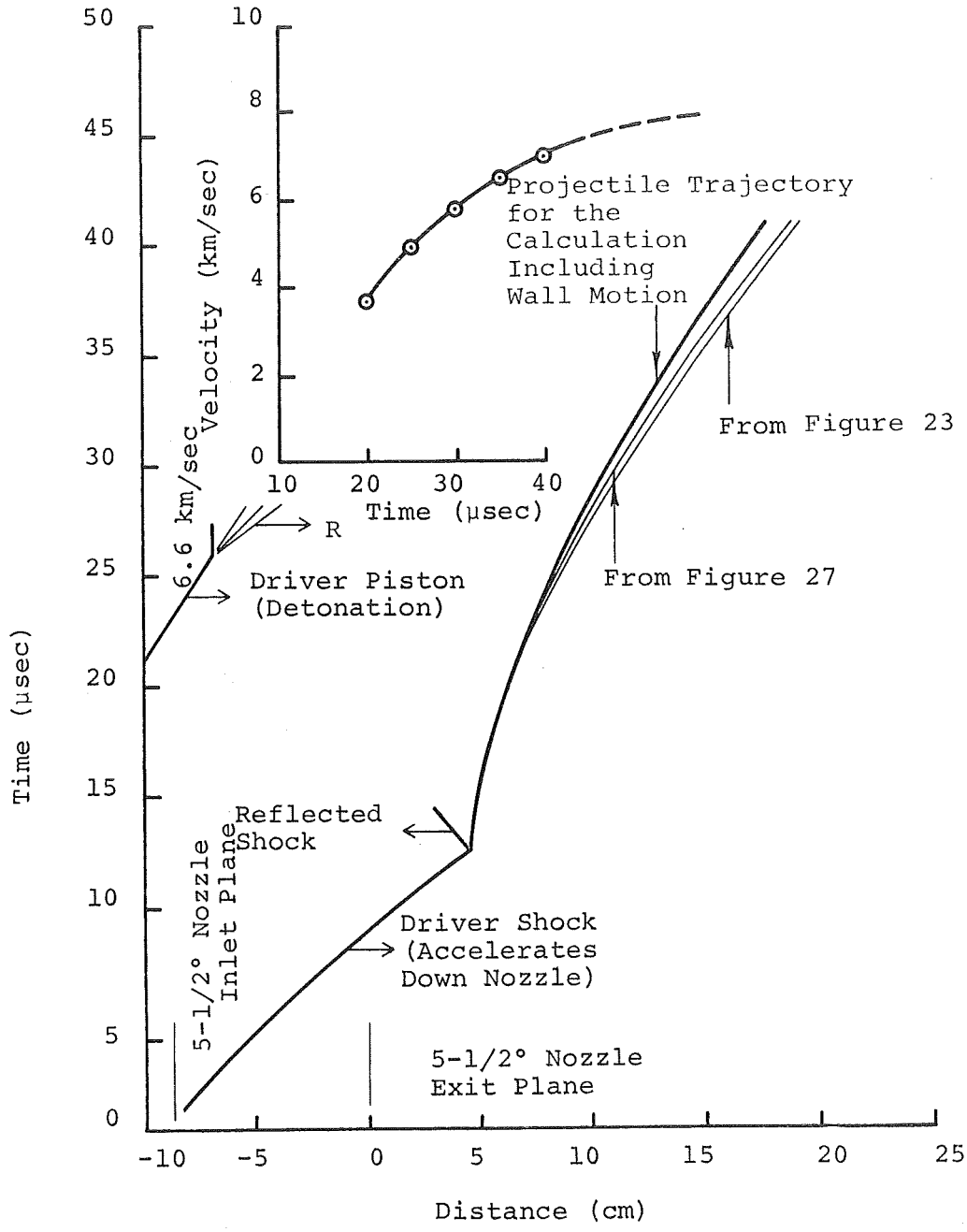

FIGURE 24. CALCULATION OF A HIGH-PRESSURE SINGLE-STAGE GUN USING THE GANG-POD COMPUTER PROGRAM

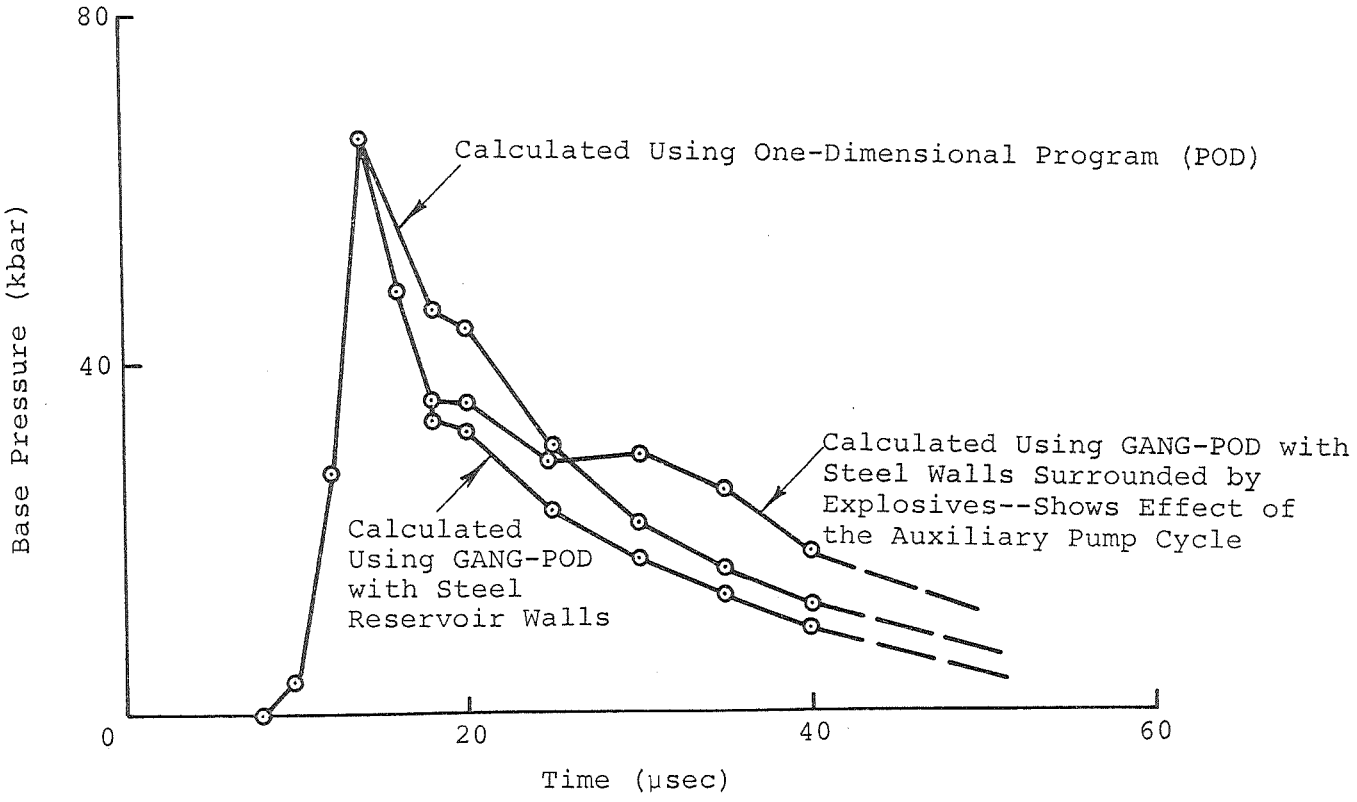

FIGURE 25. CALCULATED PROJECTILE BASE PRESSURE HISTORIES USING THE GANG-POD COMPUTER PROGRAM

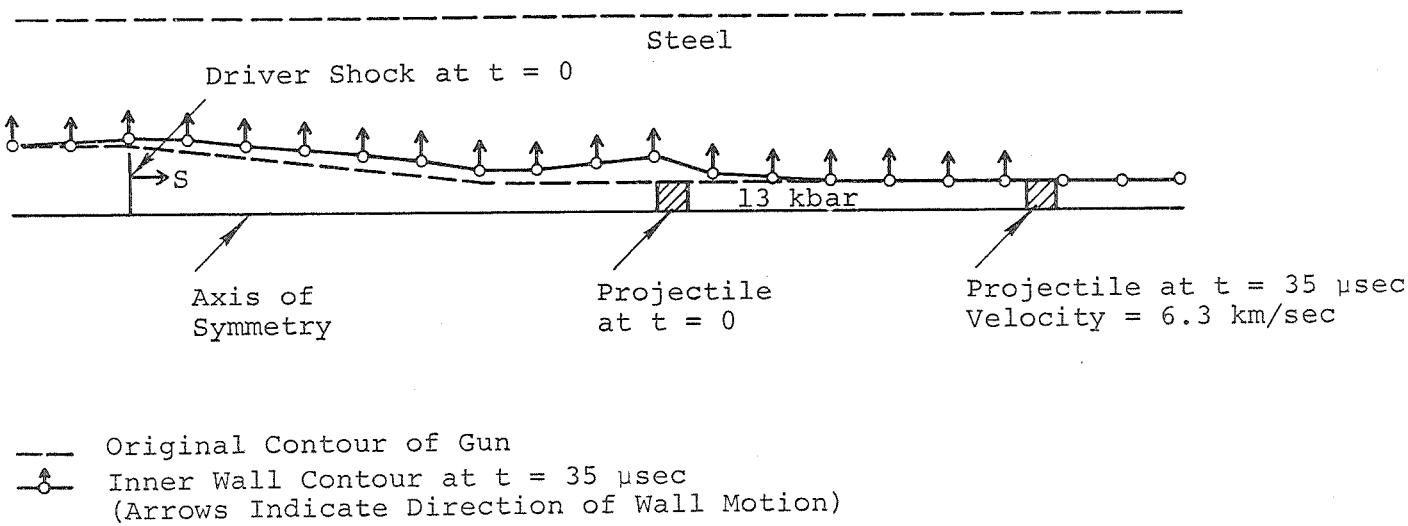

FIGURE 26. CALCULATED INNER WALL CONTOUR FOR A HIGH-PRESSURE SINGLE-STAGE GUN USING THE GANG-POD COMPUTER PROGRAM

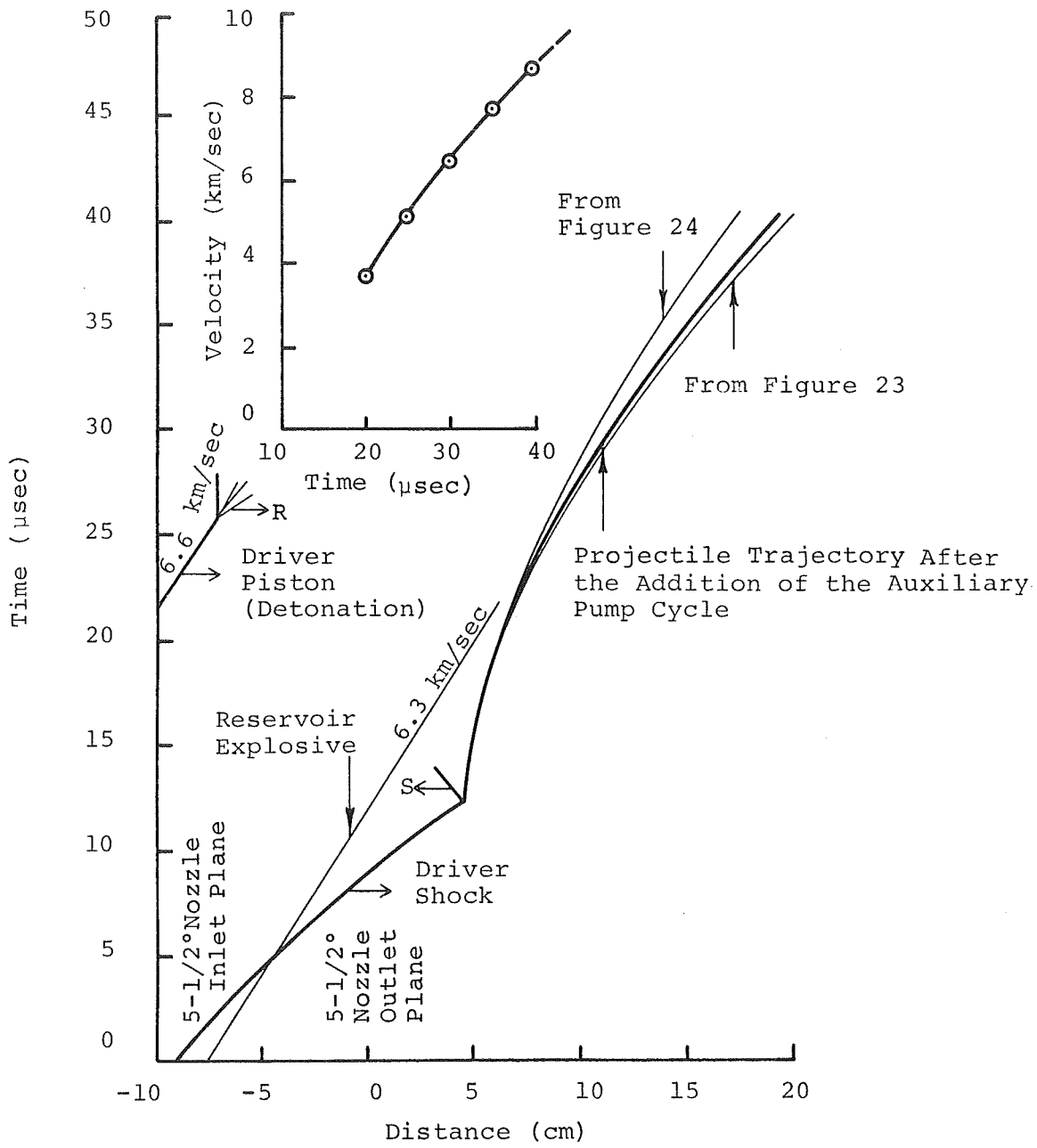

FIGURE 27. CALCULATION OF A HIGH-PRESSURE, SINGLE STAGE GUN WITH AUXILIARY PUMP CYCLE USING THE GANG-POD COMPUTER CODE PROGRAM

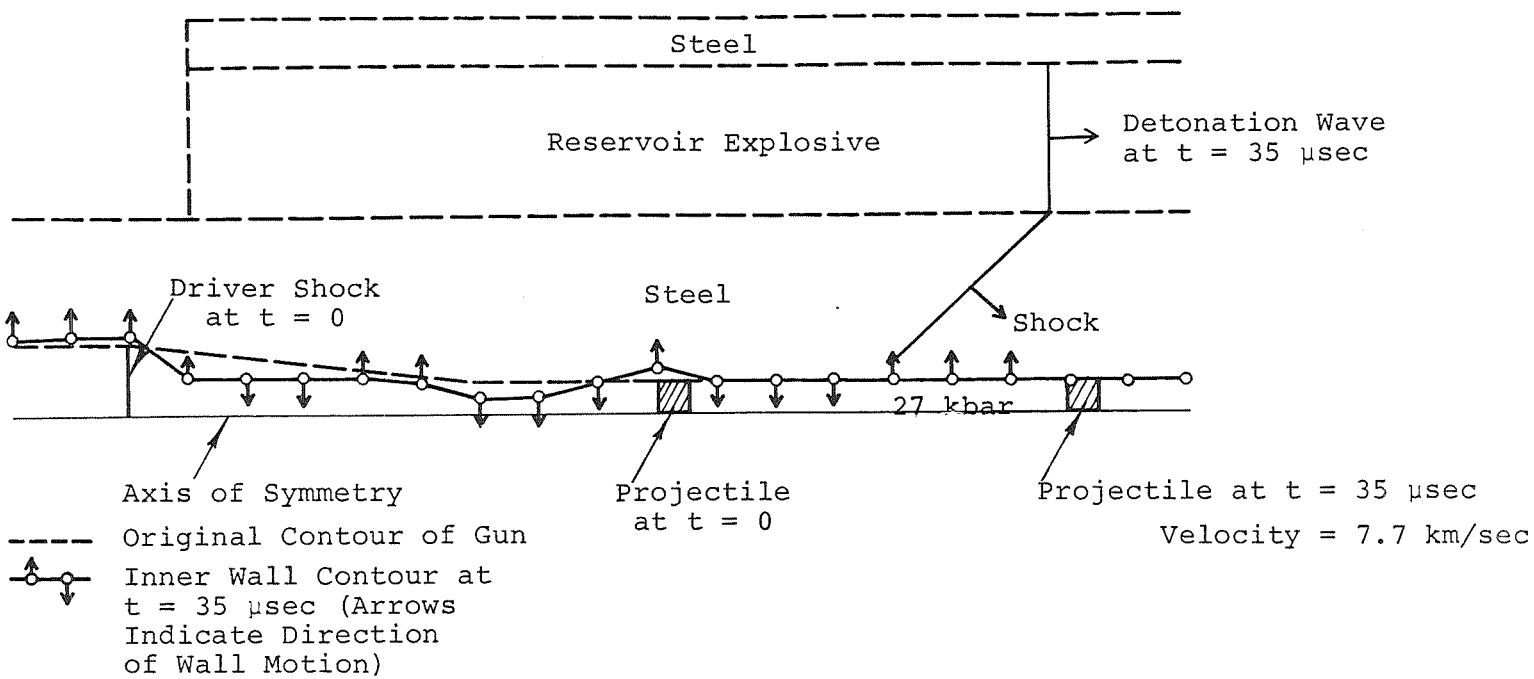

FIGURE 28. CALCULATED INNER WALL CONTOUR FOR HIGH-PRESSURE, SINGLE-STAGE GUN WITH AUXILIARY PUMP CYCLE USING THE GANG-POD COMPUTER PROGRAM

The above examples illustrate the accuracy of the GANG-POD program. Although the program is not a full two-dimensional code (the wall points are not coupled to each other), it does appear to provide a useful description of the launcher operation at a reasonable cost. A complete calculation, for instance, requires between 30 and 45 minutes of computer time, depending on the complexity of the problem.

C. TWO-STAGE PERFORMANCE CALCULATION

The calculation of the first-stage operation and the startup of the second stage is included here for two reasons: (1) It represents the calculated performance of the gun used to launch a 2-g model to 12.2 km/sec, and (2) it was the first use of the GANG-POD program as a design aid to determine when second-stage operation should begin.

In the calculation a 3-kbar nitromethane driver with a 3.48-cm-diam pressure tube was coupled to a 1.59-cm-diam barrel by a 5.5-deg conical transition section. The 2-g lithium-magnesium projectile was placed 4.5 cm (2.8 body diameters) downstream of the nozzle outlet plane. The 10.2-cm-diam steel reservoir was surrounded by a 3.8-cm layer of nitromethane. The 3.8-cm outer diameter of the barrel was surrounded by an effectively infinite layer of nitromethane. This simulates the second-state explosive lens. The situation is shown schematically in Figure 29. The steel was given a yield strength of 4 kbar.

The calculation begins with the driver shock at the nozzle inlet plane. After the calculation had proceeded for 8 μsec, projections showed that it would be safe to initiate the reservoir explosive. That is, the projectile would not be overtaken by the

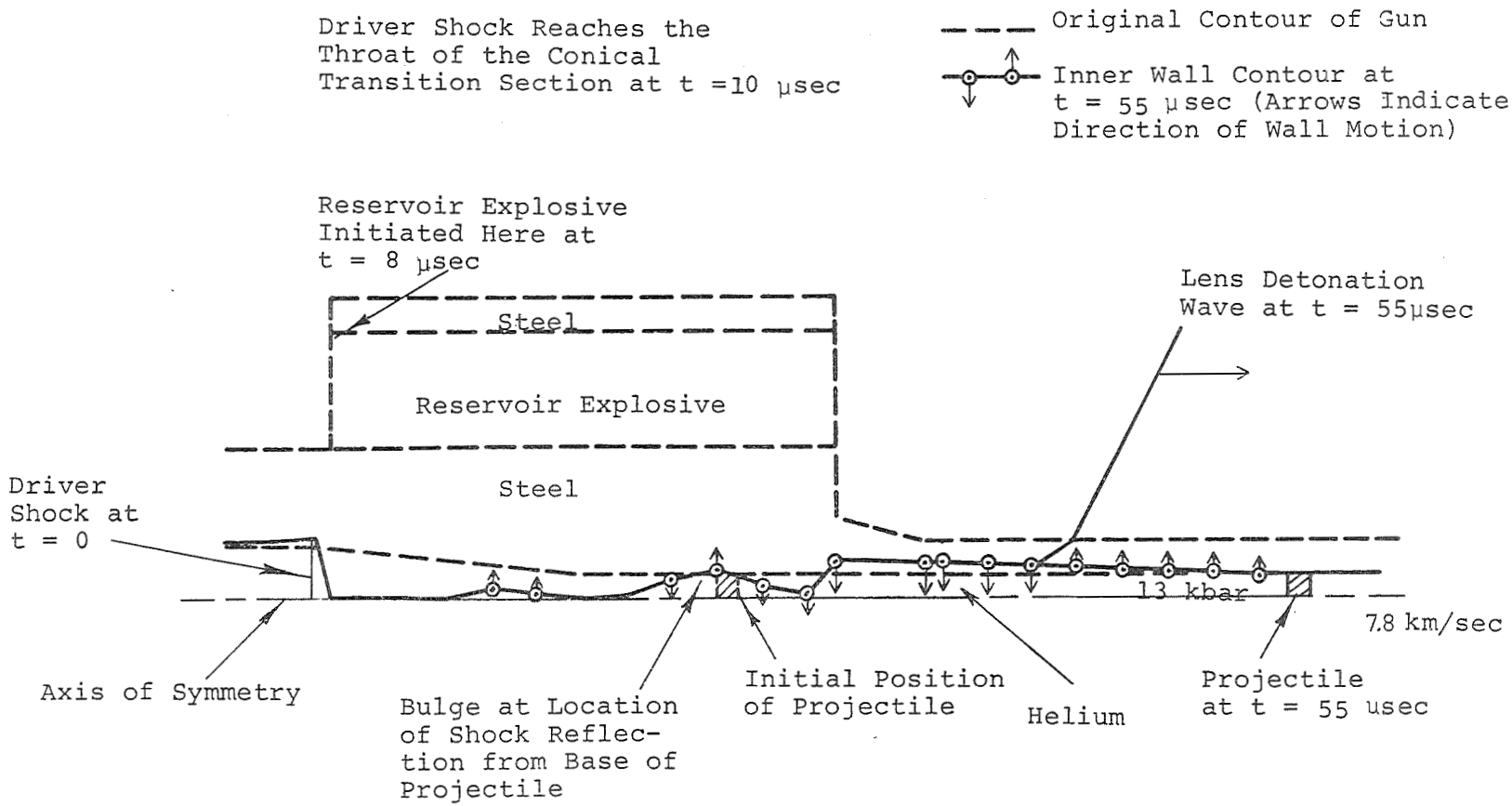

FIGURE 29. CALCULATED INNER WALL CONTOUR FOR A TWO-STAGE GUN WITH A 5.5-deg TRANSITION SECTION, USING THE GANG-POD COMPUTER PROGRAM

stress wave generated in the steel walls by the explosive. At this time the driver shock had just reached the nozzle exit plane and the projectile had not yet begun to accelerate. The problem was then run uninterrupted until t = 42 μsec. At this point inspection showed that the projectile was 10 cm into the second stage at a velocity of 5.7 km/sec and with a base pressure of nearly 20 kbar. The auxiliary pump cycle had forced a substantial amount of driver gas into the second-stage portion of the barrel. At this time the explosive surrounding the barrel was initiated. The problem was then run for another 14 μsec and terminated. At this time the projectile velocity was 7.9 km/sec and the base pressure was 13 kbar. The second-stage piston had not yet formed although the barrel walls were accelerating inward. Enough information had been obtained to design the second-stage explosive lens so that the projectile would never be overtaken by the accelerating second-stage piston. The results of the calculation are shown in Figures 29, 30, and 31. In the plot of projectile base pressure as a function of time, the effect of the auxiliary pump cycle is quite evident. The effect of the second-stage piston formation has not as yet been communicated to the projectile. The inner wall contours shown in Figure 29 illustrate that nearly all the driver gas is forced into the second-stage portion of the barrel. From the point of view of any augmentation scheme this is considered a desirable feature. In fact, the high pressures generated in the barrel by the auxiliary pump cycle appear to be making it very difficult for the explosive surrounding the barrel to collapse the barrel rapidly.

The calculation was not carried to completion because there were not enough wall points available to describe the entire second-stage gasdynamic cycle. If necessary, the calculation can be completed by reassigning wall problems and discarding those problems in that portion of the collapsed reservoir.

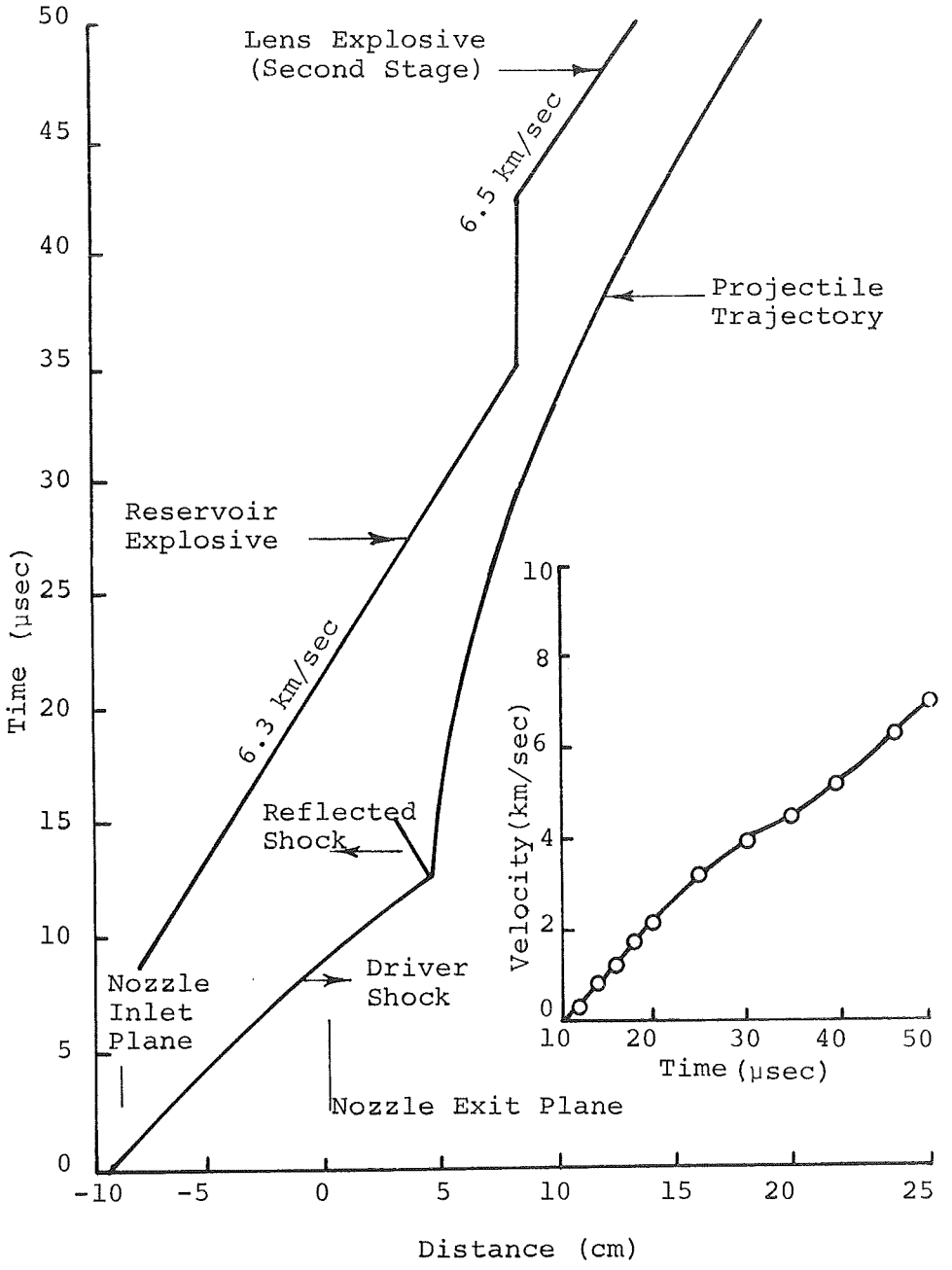

FIGURE 30. CALCULATION OF THE START-UP OF A TWO-STAGE GUN USING THE GANG-POD COMPUTER PROGRAM

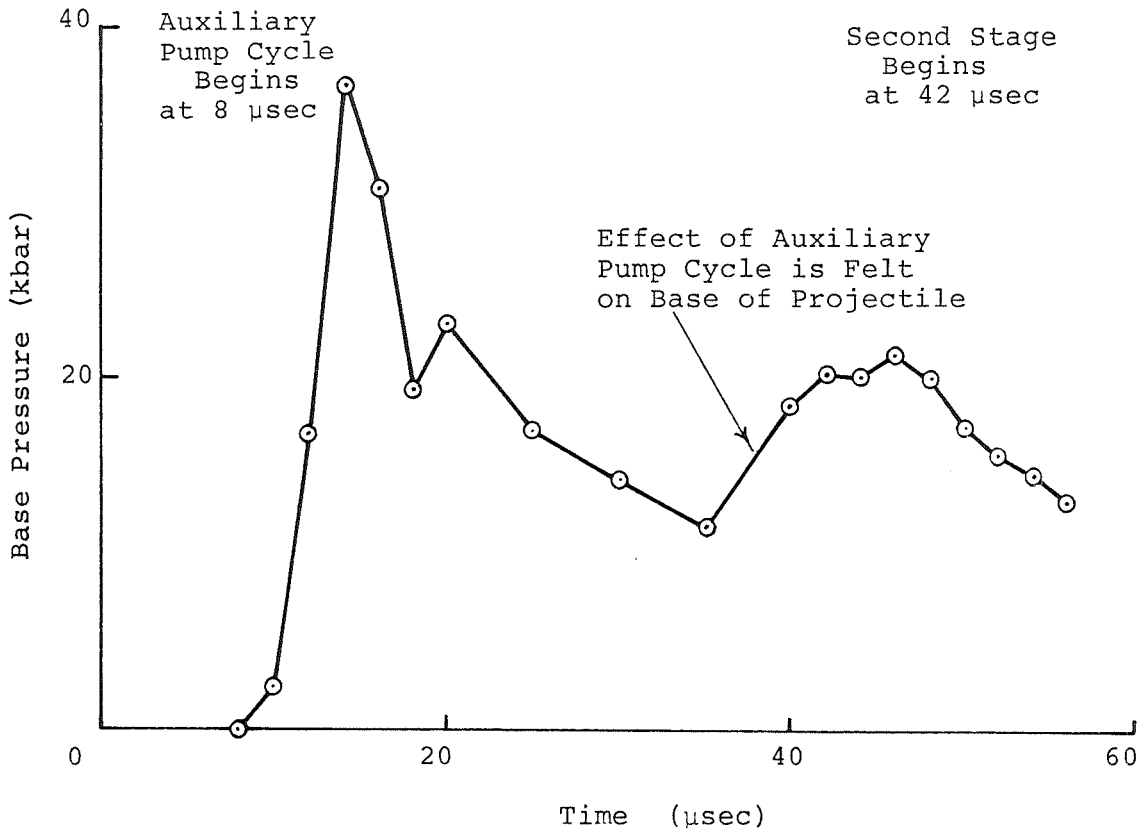

FIGURE 31. CALCULATED BASE PRESSURE FOR INITIAL ACCELERATION OF TWO-STAGE GUN

It is appropriate to include here another example of the GANG-POD program as a design aid in the launcher program. The original first-stage experiments utilized a 3-kbar nitromethane driver coupled to the barrel by an abrupt area change. Calculations showed that during the operation of the auxiliary pump cycle, the breech section was first collapsed at the area change, trapping a large fraction of the driver gas in the reservoir. The inner wall contours calculated by GANG-POD that demonstrate this are shown in Figure 32. By using a 5.5-deg conical nozzle to couple the driver and barrel, it was felt a more natural reservoir collapse would result during the auxiliary pump cycle. Figure 28 shows the inner wall contours calculated for the case of the 5.5-deg nozzle. It is evident that more of the driver gas is pumped into the barrel and made available for second-stage augmentation.

Use of the nozzle rather than the abrupt area change at the breech results in higher performance; however, the peak pressures in the case of the nozzle (30 kbar) are higher than those in the case of the abrupt area change (18 kbar). This was not considered serious in this program as projectiles have been accelerated intact in the same geometry with peak pressures up to 60 kbar.

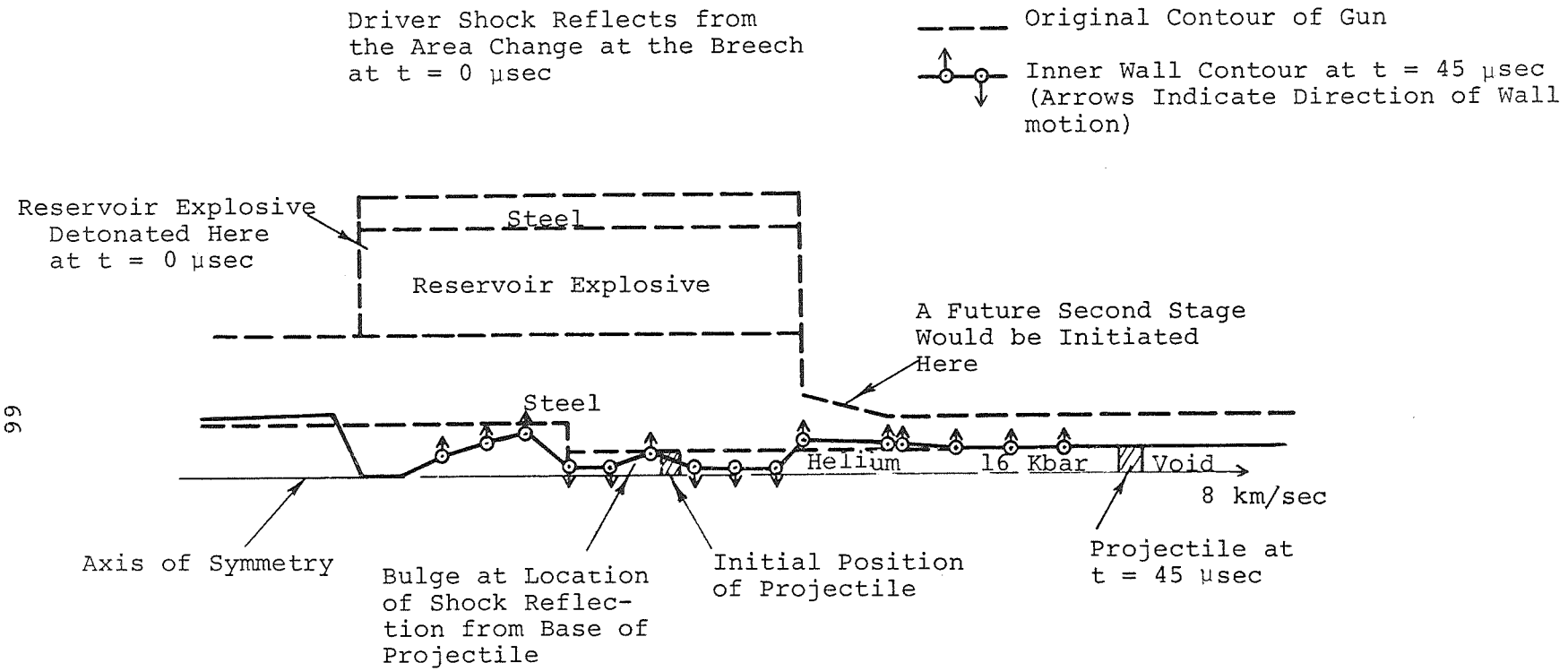

FIGURE 32. CALCULATED INNER WALL CONTOUR FOR AN ABRUPT AREA CHANGE GUN DESIGN WITH RESERVOIR EXPLOSIVE, USING THE GANG-POD COMPUTER PROGRAM

SECTION V

LAUNCHER EXPERIMENTS

In this section, the experiments supporting the calculations presented in Section III are described. Three approaches were made during this year's program and two of them have proved successful. The first approach was to use a single-stage, explosively driven gun to accelerate a projectile to 12 km/sec. This goal was accomplished by adding an auxiliary pump cycle to the gun. The second approach was an attempt to develop a low-pressure, first-stage gun with large chambrage. This first stage would be matched to the second stage which is an explosive lens, to provide a nearly constant base pressure acceleration to very high velocities. This approach was not completely successful in preliminary tests. The third approach was to test a complete two-stage system based on the knowledge gleaned from the single-stage experiments. These tests were successful and a 2-g projectile was launched to 12.2 km/sec with reasonably low base pressures.

A. HIGH-PRESSURE, SINGLE-STAGE EXPERIMENTS

The purpose of these experiments was twofold. First, it would be advantageous to develop a simple single-stage gun capable of accelerating 2-g models to 12 km/sec. Second, the knowledge gained by extending the limits of single-stage gun technology could be used to help design the first stage of a two-stage system that would operate at considerably lower pressure levels. The single-stage experiments, which led to the development of a single-stage gun capable of accelerating a 2-g projectile to 12 km/sec, will now be briefly outlined.

The first single-stage experiments utilized a 6-kbar nitromethane driver with a 3.48-cm-diam pressure tube. This driver was coupled to a 1.59-cm-diam barrel by a massive reservoir section. The driver-to-driven transition was accomplished by an abrupt area change and

the 2-g projectile was placed successively at the area change and then two and three body diameters downstream of the area change in three separate experiments. The predicted velocity in all three cases was 10.8 km/sec and the different initial projectile positions were tested to determine the best position for reducing deformation of the projectile. The range radiographs of the three projectiles are shown in Figures 33, 34, and 35. The observed velocities were 8.1, 9.3, and 8.3 km/sec respectively. The failure to achieve the predicted velocity of 10.8 km/sec was attributed to excessive expansion of the reservoir during the launch cycle (Figure 20). Moreover, adding mass to the outside of the reservoir in an attempt to control wall expansion did not improve the performance (Table I).

As far as projectile integrity is concerned, the best initial location of the projectile is 3 diam downstream of the area change. At this location the initial pressure loading of the projectile was most uniform. This problem has been studied previously and the calculated and experimental results of this investigation are shown in Figure 36. The calculations were carried out using a two-dimensional coupled Eulerian-Lagrangian computer program (ELK). In the case of the projectile at two diameters downstream of the area change, the calculation predicted a grossly nonuniform initial loading with a very high pressure applied to the center of the projectile. In the comparison experiment the projectile was launched with a hole in its center.

One other experiment was carried out to investigate this type of gun. The driver-driven transition was changed from an abrupt area change to a 5.5-deg conical nozzle. The two-dimensional flow down this nozzle was calculated using Physics International's two-dimensional coupled Eulerian-Lagrangian program (ELK), and it was

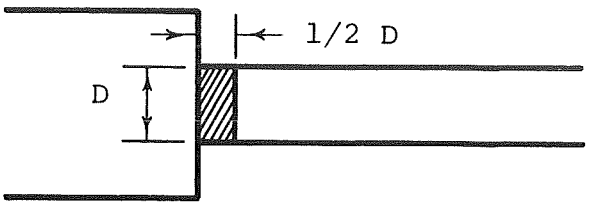

Initial Position
of Projectile
(D = diameter)

Direction of Flight

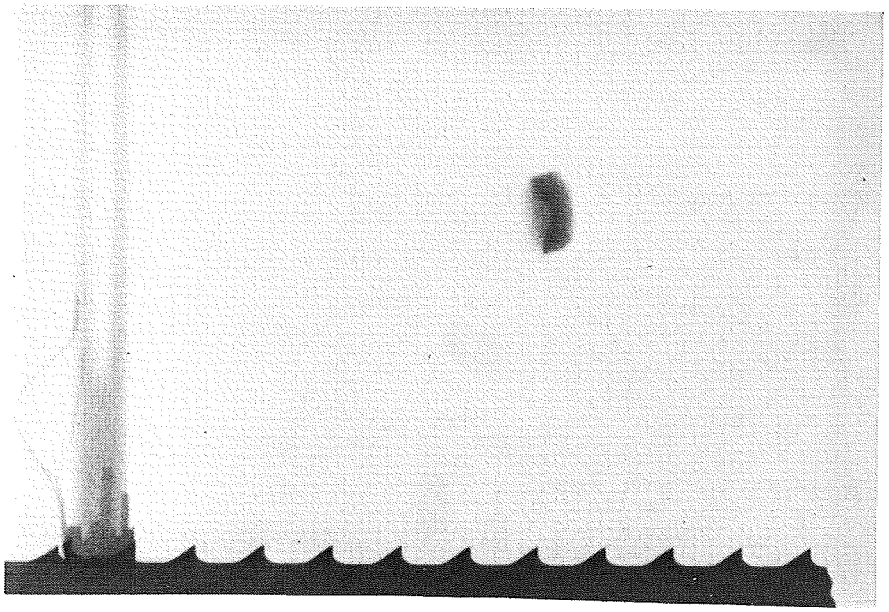

1.27 cm

Model is 112 body diameters down-
stream of the muzzle. (Range
atmosphere is air at 1 atm.)

FIGURE 33. RANGE RADIOGRAPH OF A 2-g, 1/2-caliber LONG PROJECTILE LAUNCHED TO 8.1 km/sec (Shot 397-3)

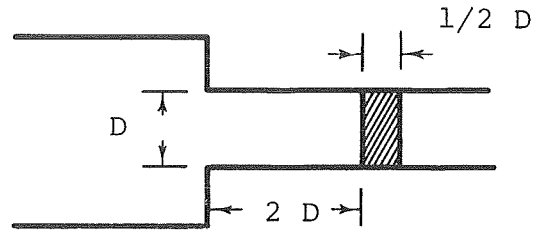

Initial Position
of Projectile
(D = diameter)

Direction of Flight

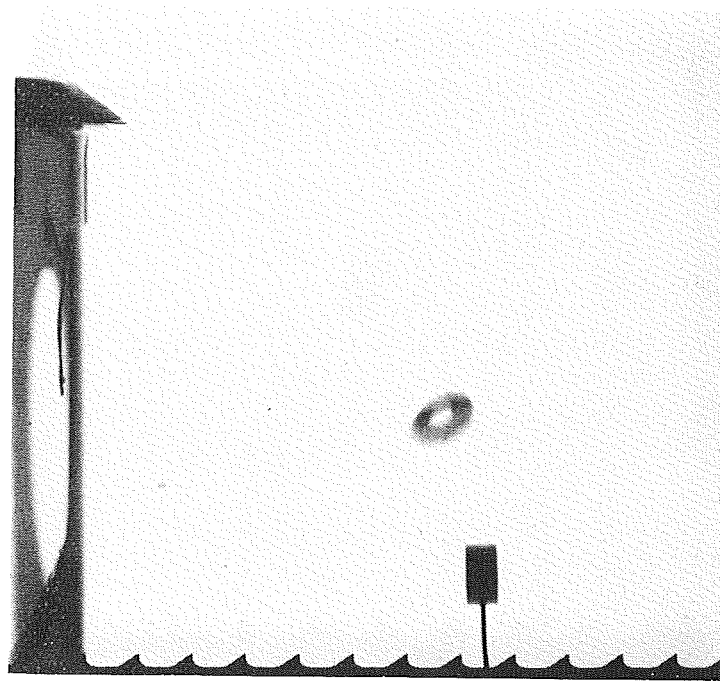

Model is 63 body diameters down-
stream of the muzzle. (Range
atmosphere is air at 1 atm.)

FIGURE 34. RANGE RADIOGRAPH OF A 2-g, 1/2-caliber LONG PROJECTILE LAUNCHED TO 9.35 km/sec (Shot 351-111)

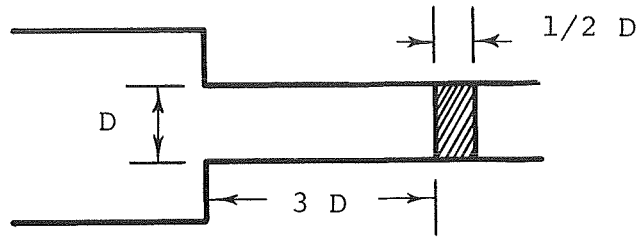

Initial Position
of Projectile
(D = diameter)

Direction of Flight

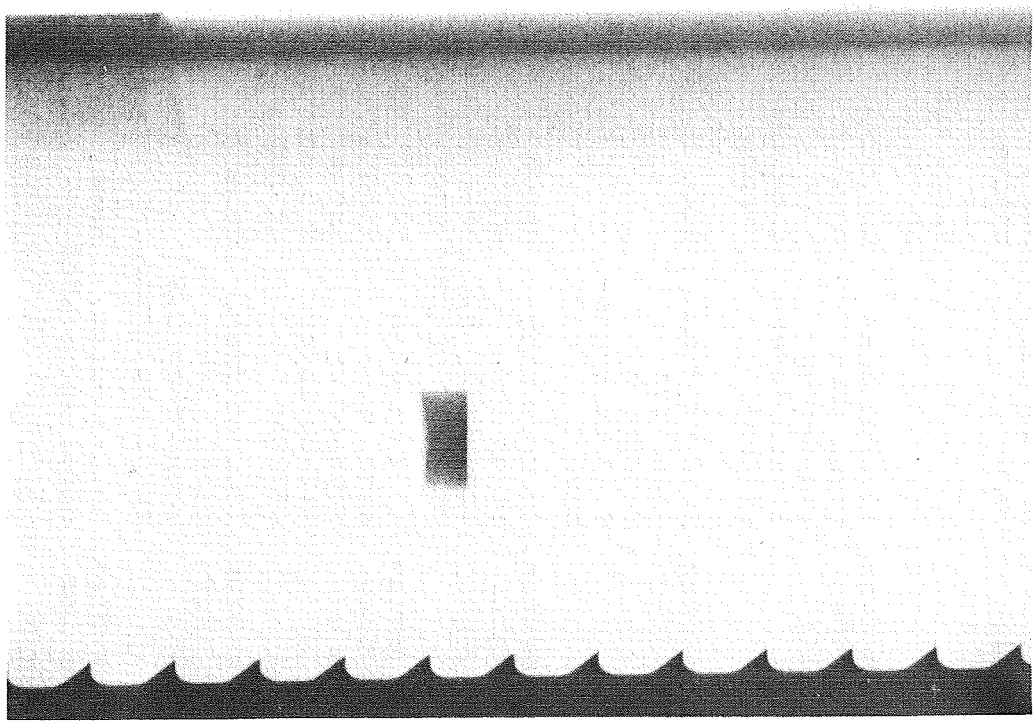

1.27 cm

Model is 113 body diameters down-
stream of the muzzle. (Range
atmosphere is air at 5 mm Hg)

FIGURE 35. RANGE RADIOGRAPH OF A 2-g, 1/2-caliber LONG PROJECTILE LAUNCHED TO 8.3 km/sec (Shot 397-1)

TABLE I

SUMMARY OF HIGH-PRESSURE, SINGLE-STAGE EXPERIMENTS

Experiment Number	Driver	Projectile	Reservoir	Breech	Final Velocity	Comments
351-111	6-kbar nitro-methane driver	1.59-cm-diam, 1/2 caliber long, 2 g	21.5-cm-diam lead	Abrupt 4:1 area change. Projectile placed 2 diameters downstream	9.3	Projectile launched with hole in center.
397-1	6-kbar nitro-methane driver	1.59-cm-diam, 1/2 caliber long, 2 g	10.2-cm-diam steel surrounded by 5.1-cm layer of lead	Abrupt 4:1 area change. Projectile placed 3 diameters downstream	8.3	Projectile in excellent condition.
397-2	6-kbar nitro-methane driver	1.59-cm-diam, 1/2 caliber long, 2 g	10.2-cm-diam steel surrounded by 1.27 cm explosive	Same as 397-1	8.3	Projectile in excellent condition. Explosive initiated late in launch cycle.
397-3	6-kbar nitro-methane driver	1.59-cm-diam, 1/2 caliber long, 2 g	10.2-cm-diam steel surrounded by 5.1 cm layer of lead	Abrupt 4:1 area change. Projectile placed at area change	8.1	Projectile in good condition.
397-5	6-kbar nitro-methane driver	1.59-cm-diam, 1/2 caliber long, 2 g	10.2-cm-diam steel surrounded by 5.1-cm layer of lead	5-1/2° nozzle transition. Projectile placed 4.5 cm downstream of nozzle exit.	7.8	Projectile in good condition.
397-7	6-kbar nitro methane driver	1.59-cm-diam, 1/2 caliber long, 2 g	10.2-cm-diam, steel surrounded by 3.8 cm of explosive.	Same as 397-5	10.6	Projectile in good condition.
397-9	6-kbar nitro methane driver	1.59-cm-diam, 1/2 caliber long, 2 g	10.2-cm-diam, steel surrounded by 3.8 cm of explosive	Same as 397-5	12.0	Explosive extended further down the barrel. Projectile may have been broken.

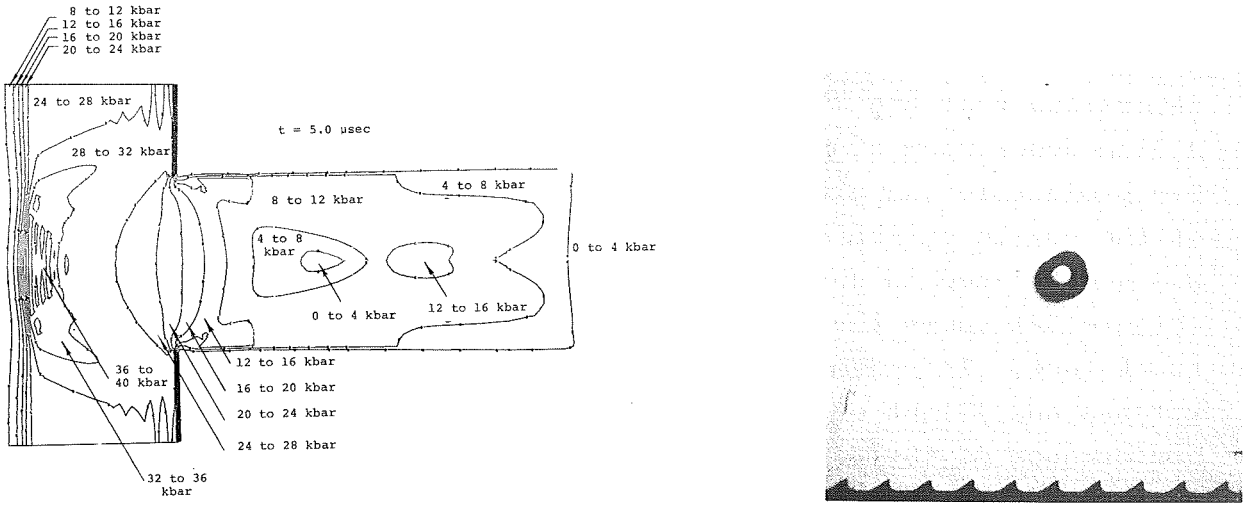

a. Projectile in flight that was initially located two diameters downstream of the area change. The calculated pressure distribution at the beginning of acceleration is shown.

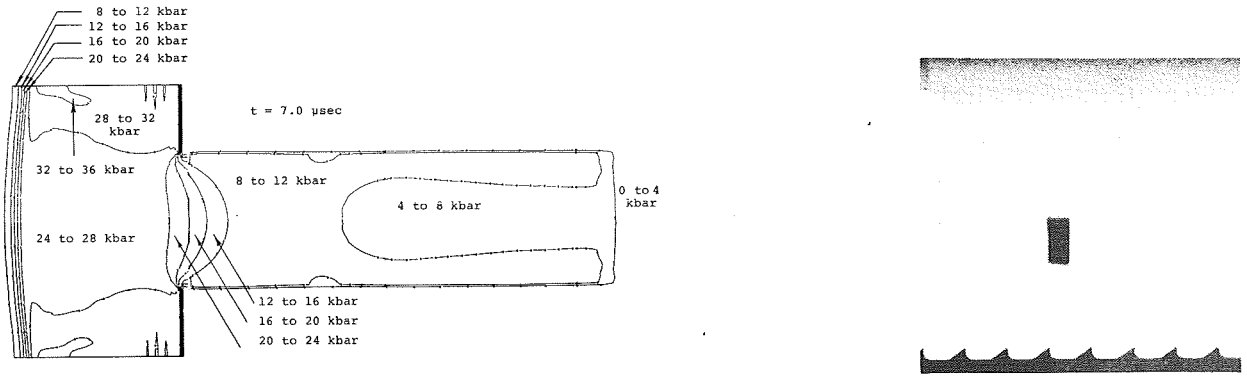

b. Projectile in flight that was initially located three body diameters downstream of the area change. The calculated pressure distribution at the beginning of the acceleration is shown.

FIGURE 36. TWO-DIMENSIONAL GAS DYNAMICS AT AN ABRUPT AREA CHANGE IN A BREECH

determined that the flow became reasonably uniform between 2 and 3 diam downstream of the nozzle outlet plane (Figure 37). The 2-g projectile was placed 4.5-cm (2.8 body diameters) downstream of the nozzle outlet and in the subsequent experiment the projectile was accelerated in good condition to 7.8 km/sec. The range radiograph (Figure 38) shows the projectile intact but with some damage to the front face. This damage was later attributed to the violent muzzle release and flight of the projectile into air at 1 atm. Again, the performance of the gun appeared to be limited by expansion of the reservoir. In this particular design with the conical transition section, the peak base pressures experienced by the projectiles were nearly 60 kbar (Figure 25).

In this last experiment good correlation was obtained in the performance calculation using the GANG-POD computer program that included the effects of reservoir wall motion during the launch cycle. It was concluded from these experiments that the gas even at pressures of 36 to 60 kbar could be controlled and used to accelerate an intact projectile. However, velocities of 10 to 12 km/sec could not be achieved because of reservoir expansion during the launch cycle.

The next step in the single-stage gun program was to use explosives to control the early reservoir expansion. The launcher described above with the 5.5-deg conical nozzle was modified to include a 3.8-cm layer of explosive around the 10.2-cm-diam steel reservoir. The arrangement was duplicated on the GANG-POD computer program (Figure 27) and the performance calculation indicated a muzzle velocity between 10 and 11 km/sec. The initiation of the reservoir explosive was timed to coincide with the arrival of the driver shock at the nozzle inlet plane (Figure 27). This timing

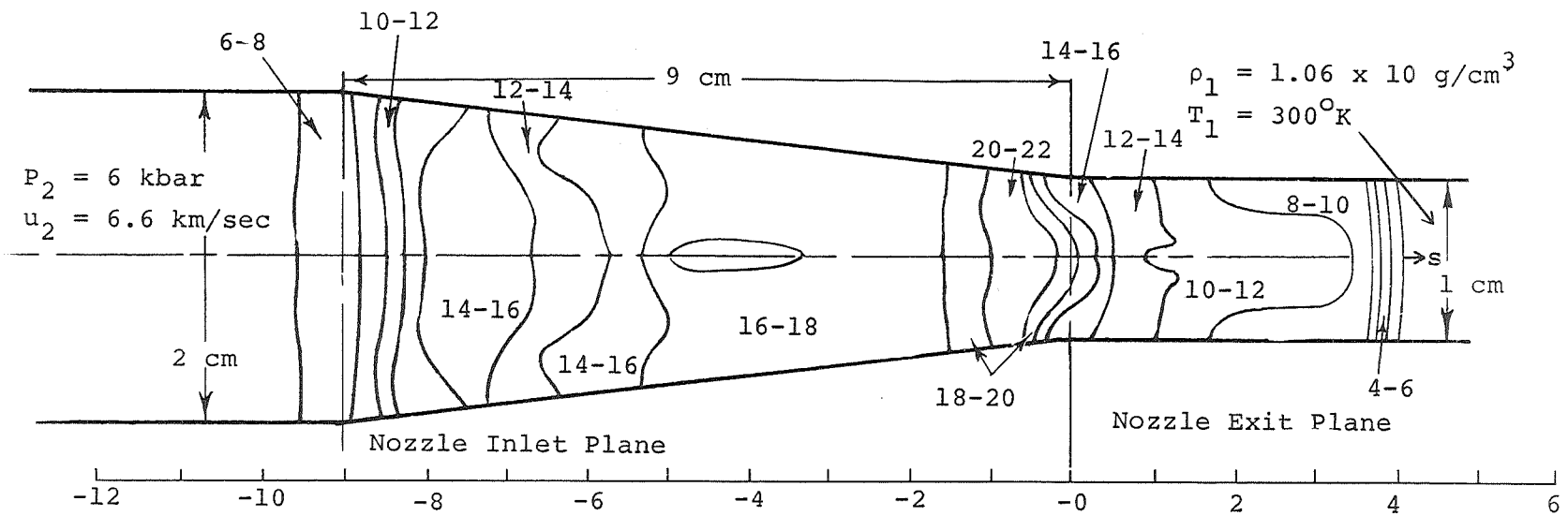

FIGURE 37. TWO-DIMENSIONAL GAS DYNAMICS IN A 5.5-deg CONICAL TRANSITION SECTION. (Isobaric contours of the flow behind a 6-kbar shock at Mach 8.8 in Helium calculated by a two-dimensional coupled Eulerian Lagrangian computer program ELK)

Direction of Flight →

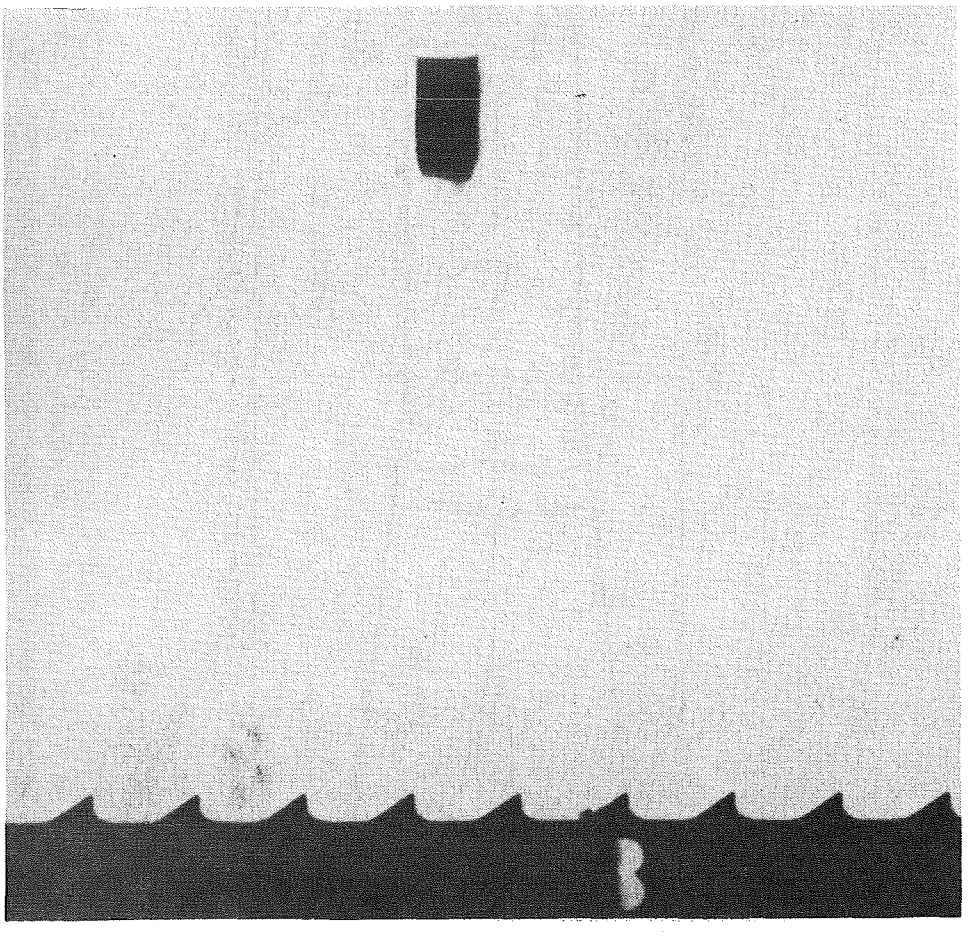

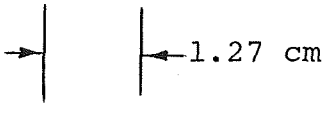

Model is 31 body diameters down-stream of the muzzle. (Range atmosphere is air at 1 atm.)

FIGURE 38 RANGE RADIOGRAPH OF A 2-g, 1/2-caliber LONG PROJECTILE LAUNCHED TO 7.8 km/sec BY HIGH PRESSURE SINGLE STAGE GUN (Shot 397-5)

would ensure that the accelerating projectile would not be overtaken by stress waves generated in the reservoir walls by the explosive.

The projectile was accelerated intact to 10.6 km/sec; however, the projectile was launched into air at one atm and the muzzle release and subsequent flight were quite violent. During the flight, for example, the stagnation pressure and temperature were computed to be about 1.2 kbar and 7800^{o}K respectively. The range radiograph taken 200 diam downstream of the muzzle shows the projectile intact but badly ablated (Figure 39). In fact, in Figure 39 the ablation products are faintly discernible streaming from the upper edge of the projectile. The white blots are a result of debris impact on the film, which was left unprotected to obtain a high-resolution X ray.

This experiment was repeated with two modifications. The reservoir explosive was extended farther downstream in an attempt to achieve better performance. The range atmosphere was changed from air at 1 atm to helium at 1 atm to reduce the damage due to muzzle release and the subsequent flight down the range. Unfortunately, when this experiment was carried out, the range radiographs were lost. The target showed a large impact, indicative of an intact projectile; however, the streaking camera suggested the projectile may have been broken. The velocity was recorded as 12 km/sec, and the observed performance of this system is shown in the x-t plane in Figure 40.

This test ended the single-stage gun experiments. It was demonstrated that high velocities were possible if reservoir expansion were controlled. Other experiments have shown that the nitromethane (D = 6.6 km/sec) in the explosive driver can be

Model is 200 body diameters downstream of the muzzle. (Range atmosphere is air at 1 atm.)

FIGURE 39. HIGH RESOLUTION RANGE RADIOGRAPH OF A 2-g, 1/2-caliber LONG PROJECTILE LAUNCHED TO 10.6 km/sec BY A HIGH PRESSURE GUN WITH AUXILIARY PUMP CYCLE (Shot 397-7)

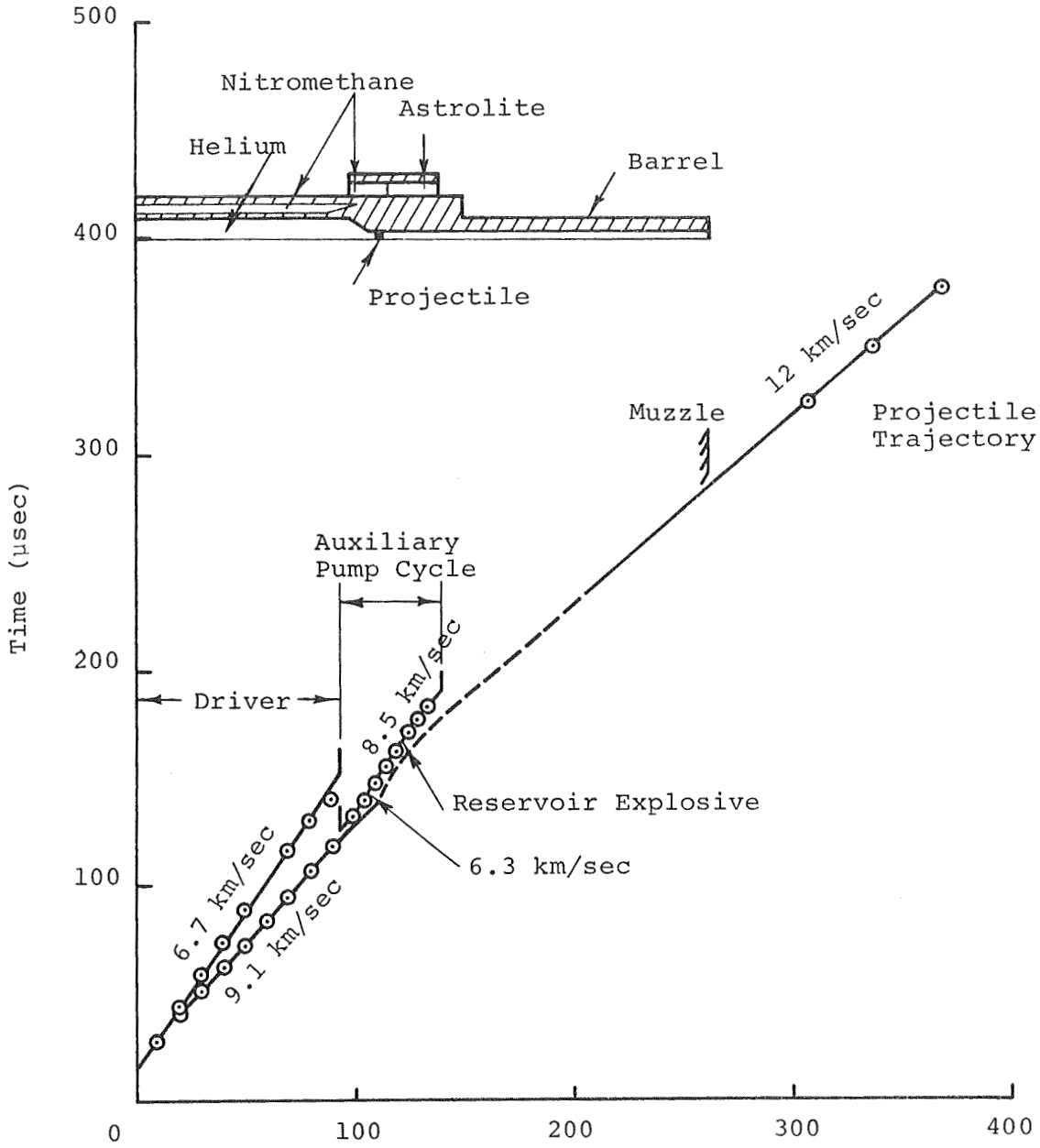

FIGURE 40. OBSERVED PERFORMANCE OF A HIGH-PRESSURE SINGLE-STAGE GUN WITH AUXILIARY PUMP CYCLE (Shot 397-9)

replaced by Astrolite, (D = 8.6 km/sec), with no modifications to the driver design. If the driver is operated at the same pressure, the use of Astrolite results in significantly higher sound speeds ($a_4 \propto D$). Therefore, it is felt that the performance of high-pressure, single-stage guns can be improved further simply by changing the driver explosive. Such a gun would be useful for impact work; however, it should be kept in mind that equal or better performance can be obtained by two-stage guns, which operate at about one-half the peak base pressures.

B. LOW-PRESSURE FIRST-STAGE EXPERIMENTS

Two designs of low-pressure first-stage launchers are described. The first design embodies the principles described in Part B of Section III, in which the first-stage acceleration is approximated by a steady expansion of the reservoir gas. The second design evolved from the results of the high-pressure single-stage experiments. An auxiliary pump cycle is used to pump most of the driver gas into the second stage. It is this design that was chosen for the successful two-stage experiments.

Two experiments to develop the low-pressure large area ratio gun were carried out. In these experiments a 1.67-kbar nitromethane driver with a 3.48-cm-diam pressure tube was coupled to a 0.95-cm-diam barrel by an abrupt 13:1 area change. This large area change results in an unsteady reservoir expansion, which can be approximated by a steady expansion to Mach 1 and then an unsteady expansion to final velocity. The 2/3-caliber long projectile was placed at the area change. The predicted velocity for this experiment was 7.6 km/sec; the observed velocity was 5.5 km/sec. The performance of the gun was monitored in detail and is shown in the x-t plane in Figure 41. The experiment was repeated with extensive modifications

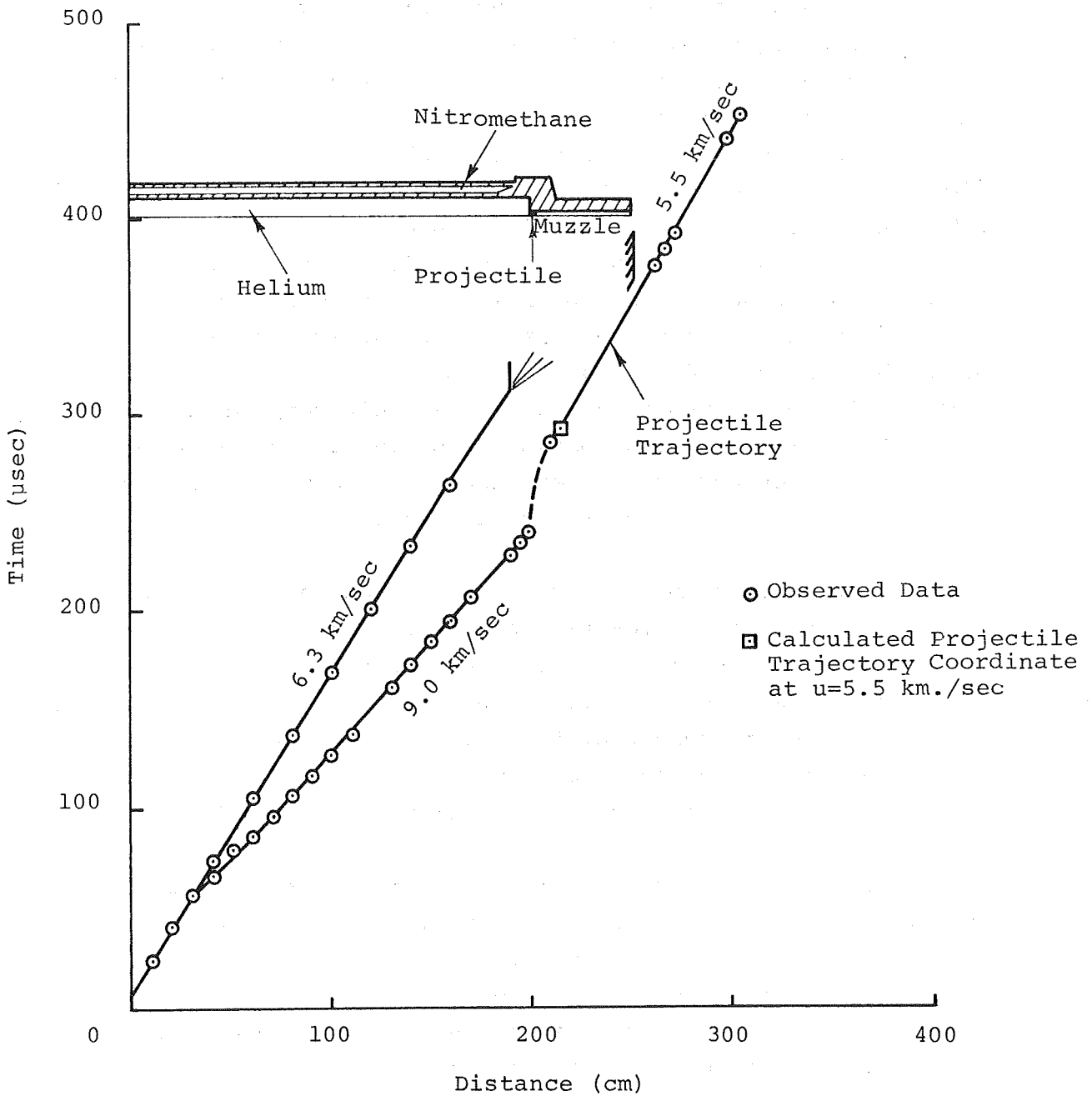

FIGURE 41. OBSERVED PERFORMANCE OF A LOW-PRESSURE 13:1 AREA RATIO FIRST-STAGE GUN (Shot 351-108)

to the breech design, because breech collapse was suspected during the critical part of the launch cycle. The results of this experiment were identical to the first and the projectile was again launched intact to 5.5 km/sec (Figure 42). The breech section was recovered and found to be slightly expanded. The framing camera record of the gun during operation showed no noticeable reservoir expansion, but did show expected barrel expansion. It is speculated that even with reservoir pressures as low as 10 kbar, some reservoir and barrel expansion was present and contributed to the performance loss. This particular design, which relied heavily on "ideal" gas dynamics, could also be affected by cooling of the reservoir gas (peak reservoir temperatures are 16,500^{o}K) because of flow contamination by projectile material lost by friction during acceleration down the barrel and by erosion products from the walls of the reservoir and barrel.

The above experiments were discontinued and the investigations into high-pressure single-stage guns were carried out as reported in Part A of this section. After the program to develop a high-pressure single-stage gun, effort was redirected again toward developing a low-pressure gun, this time with controlled reservoir expansion. This gun would serve as the first stage of a two-stage system. These experiments are summarized in Table II.

In one of the first experiments of this series, a 3-kbar nitromethane driver with a 3.48-cm-diam pressure tube was coupled to a 1.59-cm-diam barrel with a 5.5 deg conical transition section. The 2-g projectile was placed 4.5-cm downstream of the nozzle outlet plane. No explosives were used to surround the reservoir. The projectile was launched intact to 8 km/sec, as shown in the x-t plot of performance (Figure 43). This velocity, incidentally, was

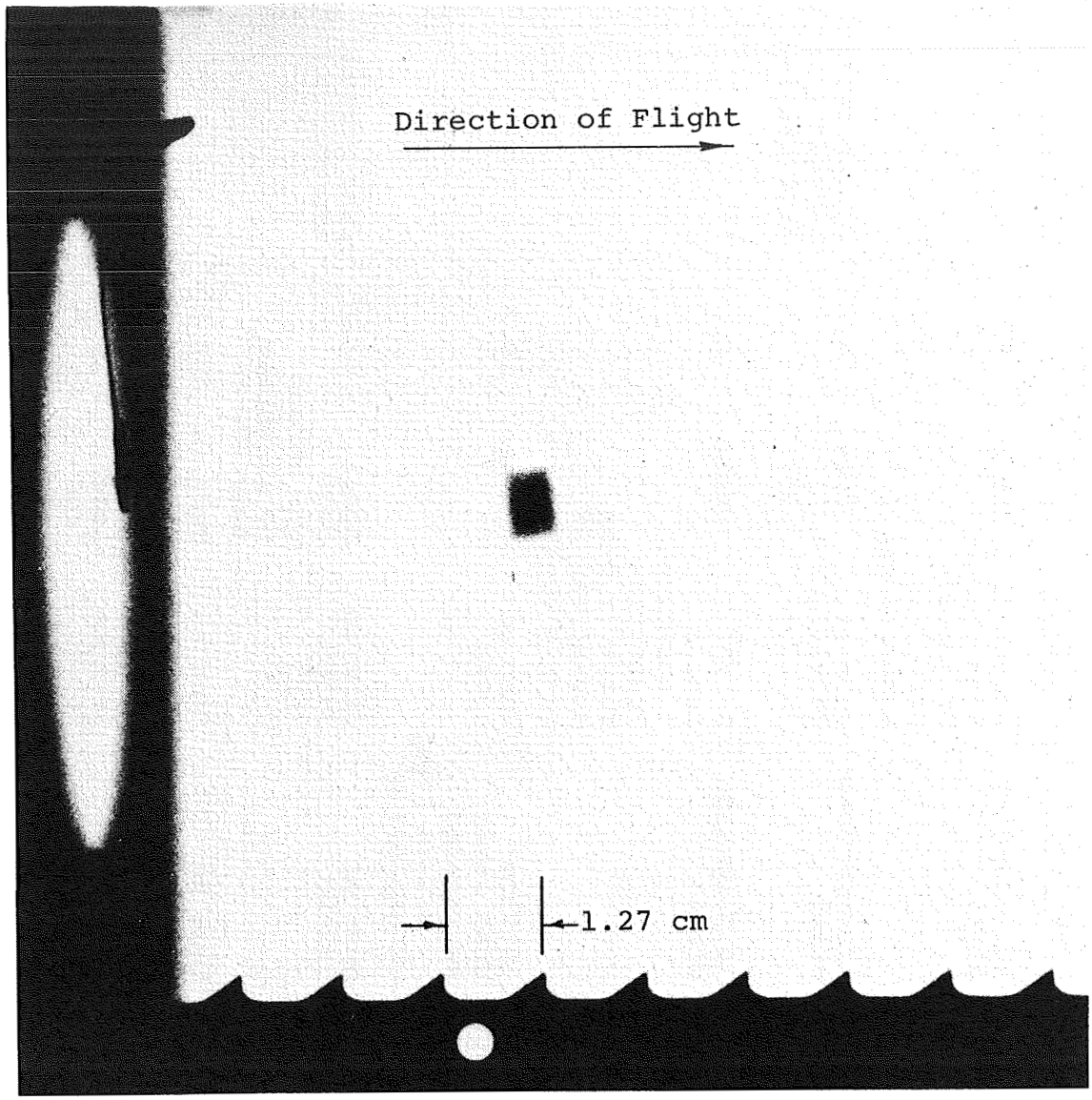

FIGURE 42. RANGE RADIOGRAPH OF A 0.67 gm, 2/3-LONG PROJECTILE LAUNCHED TO 5.5 km/sec BY A LOW PRESSURE FIRST STAGE GUN (Shot 351-108)

TABLE II

SUMMARY OF ONE- AND TWO-STAGE EXPERIMENTS

Experiment Number	Driver	Projectile	Reservoir	Breech	Lens	Final Velocity	Comments
351-103	1.6-kbar nitro-methane driver	0.95-cm-diam, 2/3 caliber long, 0.66 g	10.2-cm-diam steel	Abrupt 13:1 area change. Projectile placed at area change.	None	5.5	
351-108	1.6-kbar nitro-methane driver	0.95-cm-diam, 2/3 caliber long, 0.66 g	10.2-cm-diam steel	Same as 351-103	None	5.5	Breech design changed from Shot 351-103
397-8	3-kbar nitro-methane driver	1.59-cm-diam, 1/2 caliber long, 2 g	10.2-cm-diam steel	5-1/2° nozzle transition. Projectile placed 4.5-cm downstream of nozzle outlet.	None	8.0	
397-10	3-kbar nitro-methane driver	1.59-cm-diam, 1/2 caliber long, 2 g	10.2-cm-diam steel surrounded by 3.8-cm layer of explosive	Same as 397-8	None	10.2	
397-11	3-kbar nitro-methane driver	1.59-cm-diam, 1/2 caliber long, 2 g	Same as 397-10	Same as 397-8	Accel. from 6.3 km/sec to 12 km/sec over 100 cm	12.0	Lens worked improperly
397-12	3-kbar nitro-driver	1.59-cm-diam, 1/2 caliber long, 2 g	Same as 397-10	Same as 397-8	Same as 397-11	12.2	
397-13	3-kbar nitro-methane driver	1.59-cm-diam, 1/2 caliber long, 2 g	Same as 397-10	Same as 397-8	Accel. from 6.3 km/sec to 14 km/sec over 80 cm	11.5	Lens initiated late to avoid overtaking the projectile

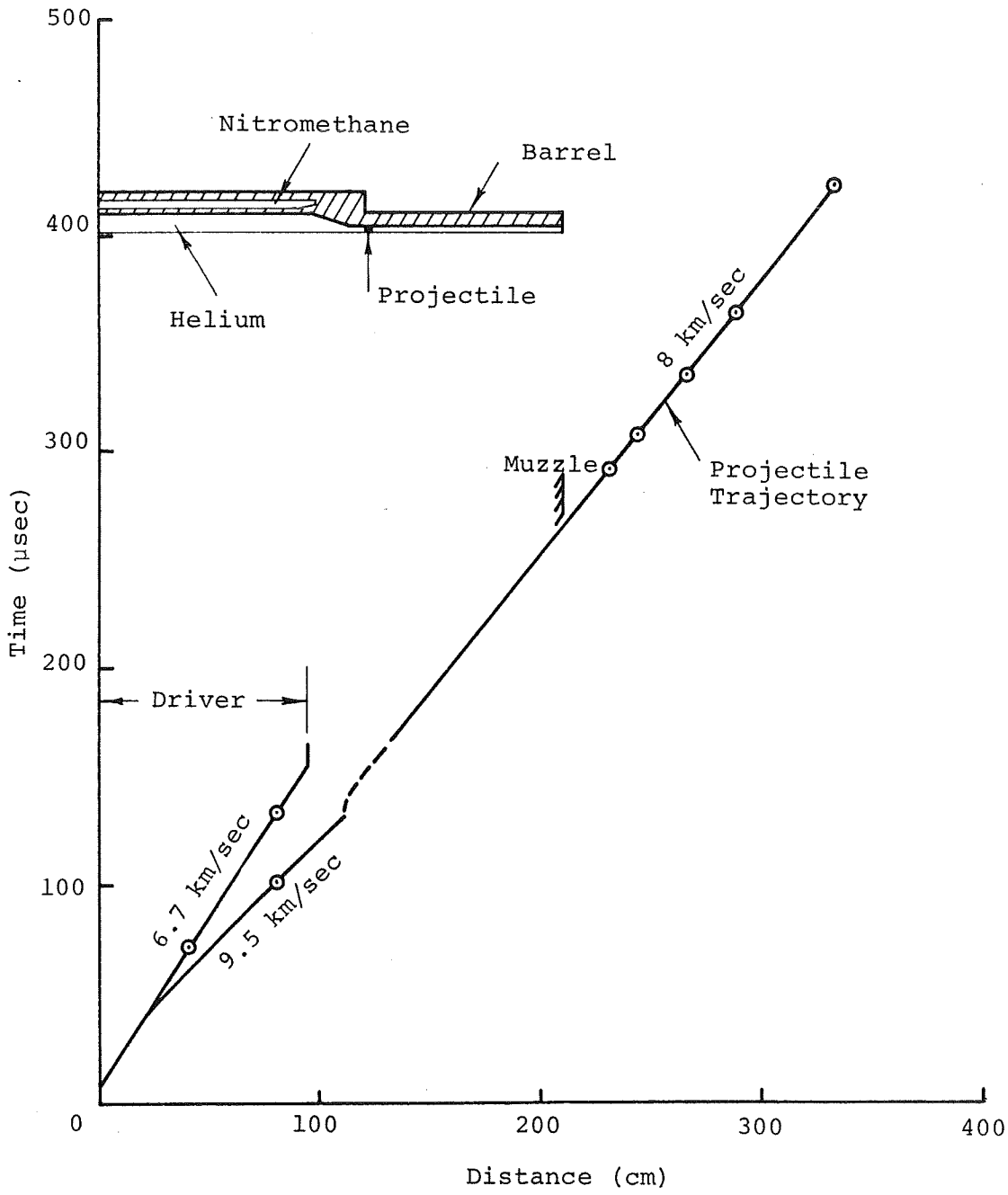

FIGURE 43. OBSERVED PERFORMANCE OF A LOW-PRESSURE FIRST-STAGE GUN WITHOUT AUXILIARY PUMP CYCLE (Shot 397-8)

about the same velocity recorded for the same gun operated at twice the pressure. Because of radial expansion of the reservoir and barrel, there appears to be an optimum operating pressure beyond which performance increases are negligible.

This experiment was repeated with the addition of a 3.8-cm layer of nitromethane around the 10.2-cm-diam steel reservoir. The addition of the auxiliary pump cycle resulted in a projectile velocity of 10.2 km/sec, or an increase in muzzle velocity of about 28%. The projectile was accelerated into a range containing air at 1 atm and is shown in the range radiograph of Figure 44. The damage to the front of the projectile has been attributed to violent muzzle release and subsequent flight into air at 1 atm. The performance of this launcher is shown in the x-t plane of Figure 45. A typical framing camera record (Figure 46) shows the barrel rupturing 30 μsec after the passage of the projectile. This rupture occurs after the second stage, which when added, would begin to operate and does not present a problem. In fact, this rupture was expected based on expansion data from the GANG-POD computer calculation (Figure 29). The rupture does indicate the high gas pressures in the barrel and the timing of the rupture coincides with the predicted surge of reservoir gas from the auxiliary pump cycle.

This experiment concluded the development of the low-pressure first-stage gun. Augmentation conditions required to provide proper matching of the first stage with the second stage are generated. Based on calculation and supported by experiment, the second stage could be started when the projectile is between 5 and 6 km/sec and the gas pressure behind the projectile is 20 kbar. With the completion of the first-stage development, the remaining experiments were directed toward investigating second-stage augmentation techniques.

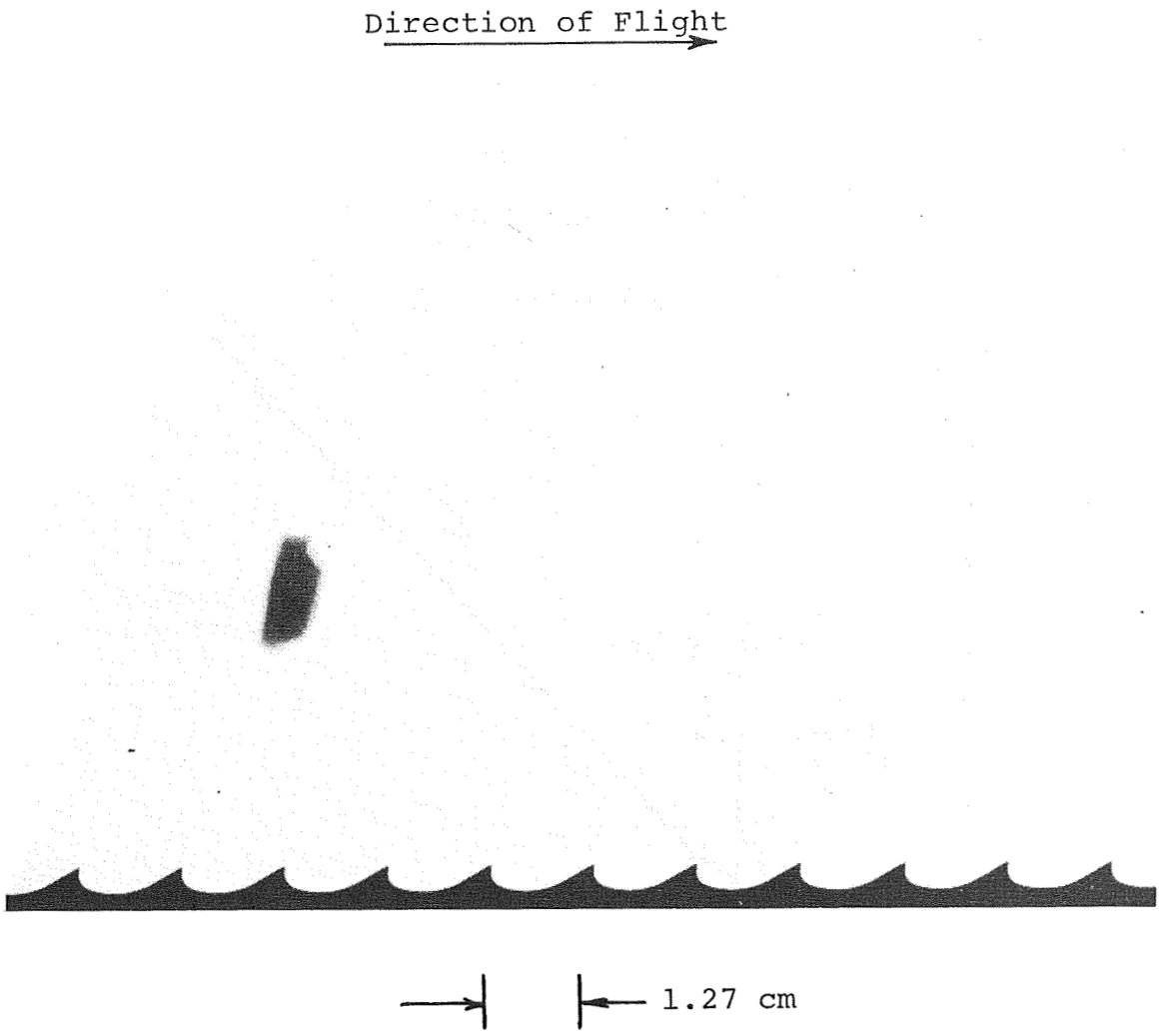

Model is 78 body diameters downstream of the muzzle.
(Range atmosphere is air at 1 atm.)

FIGURE 44. RANGE RADIOGRAPH OF A 2-g, 1/2-caliber LONG PROJECTILE LAUNCHED TO 10.2 km/sec BY THE FIRST-STAGE GUN WITH AUXILIARY PUMP CYCLE (Shot 397-10)

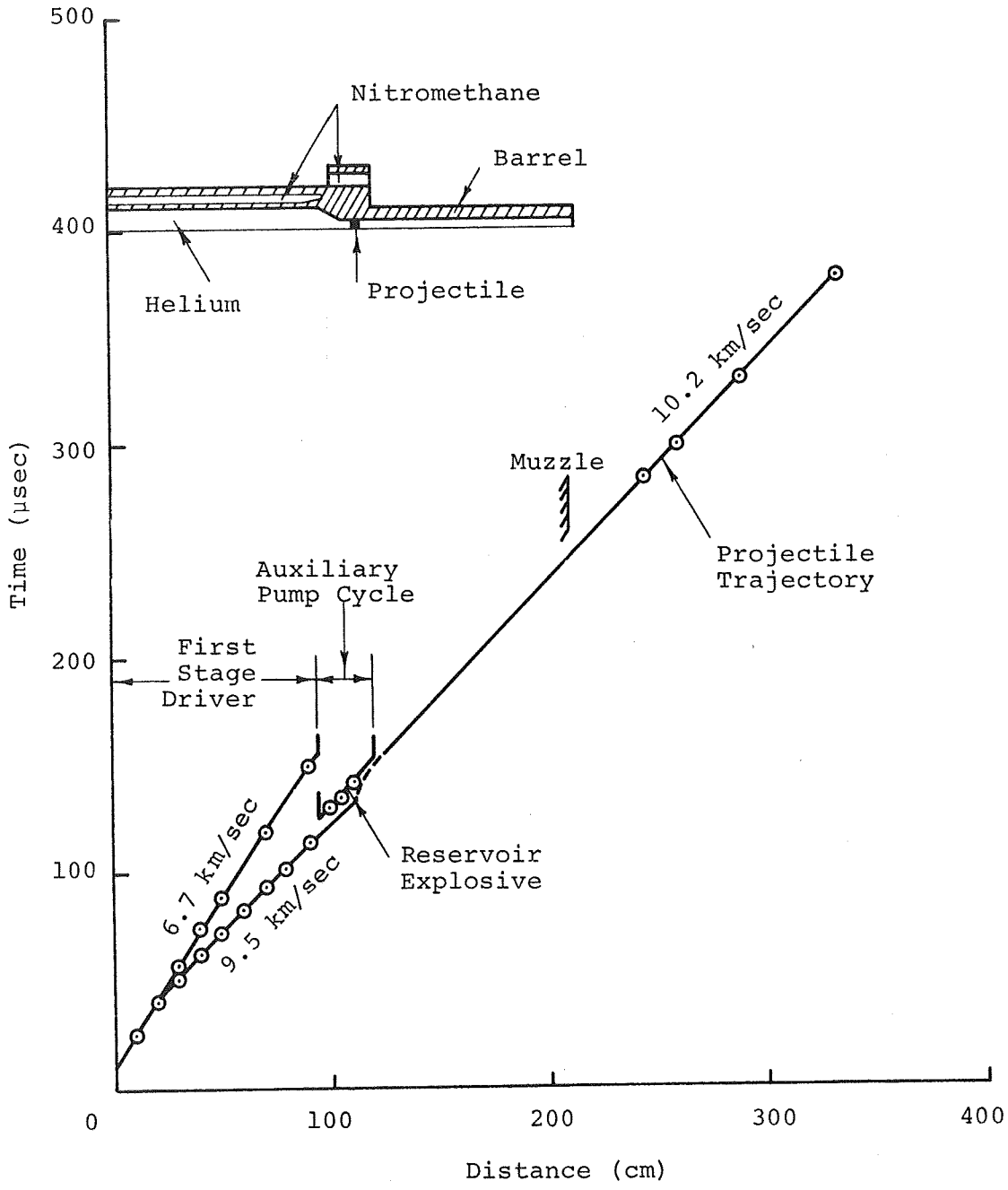

FIGURE 45. OBSERVED PERFORMANCE OF A LOW-PRESSURE FIRST-STAGE WITH AUXILIARY PUMP CYCLE (Shot 397-10)

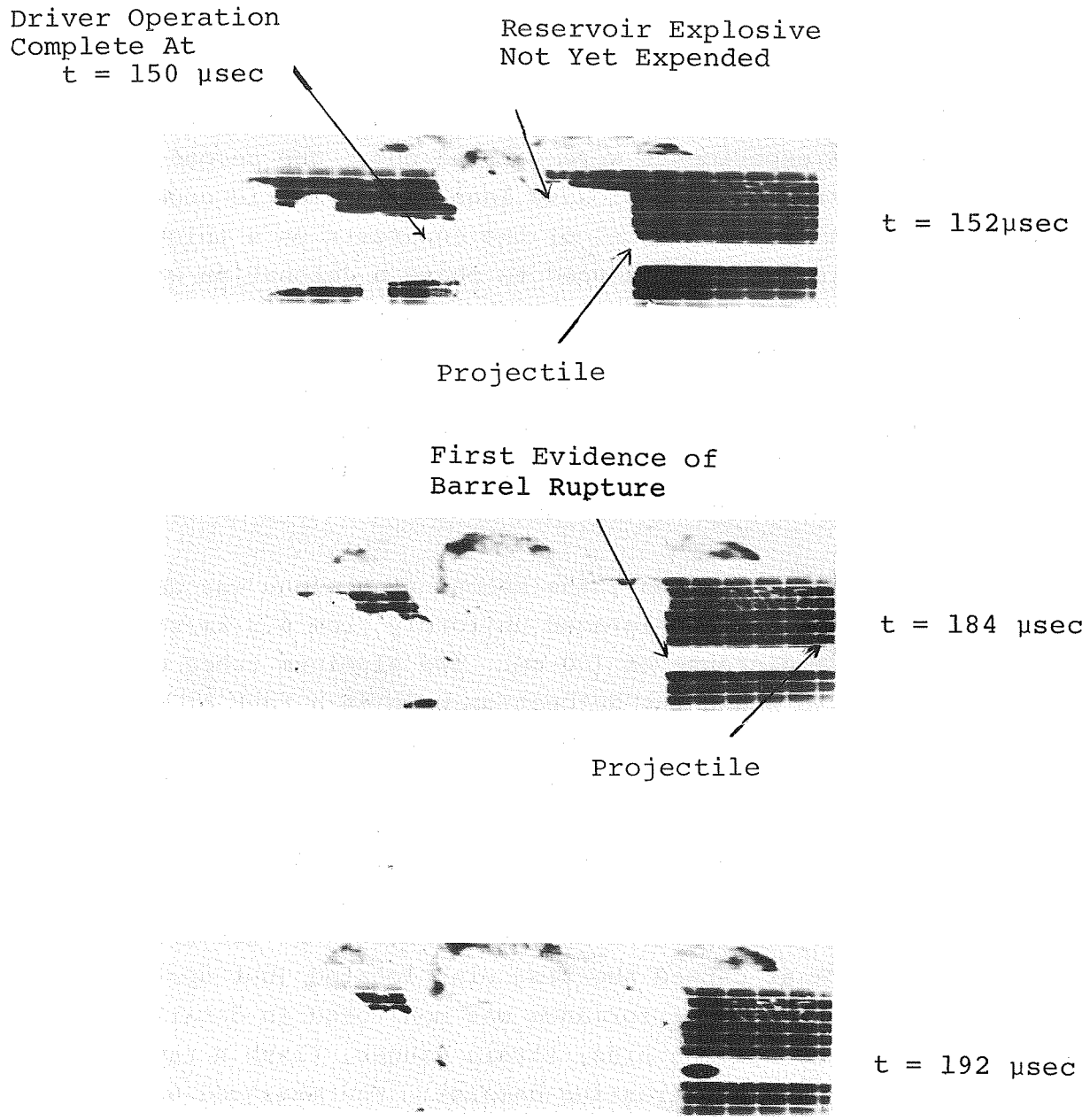

FIGURE 46. HIGH-SPEED FRAMING CAMERA RECORD OF FIRST-STAGE WITH AUXILIARY PUMP CYCLE (Shot 397-10)

C. TWO-STAGE LAUNCHER EXPERIMENTS

Using the low-pressure first stage with auxiliary pump cycle, three two-stage experiments were carried out. The second stage of each gun consisted of an explosive lens in asymmetric geometry. As shown in Figure 47, the barrel of the gun rests on a thick steel plate. An explosive lens is used to phase a detonation wave in the explosive surrounding the barrel and crush the barrel behind the accelerating projectile. While the collapse process is not symmetric, there is more than sufficient energy in the explosive to collapse the barrel. The asymmetric second-stage design was chosen for ease of fabrication, to reduce costs, and to allow a high-speed framing camera to record the operation of the lens.

In the first experiment, the second-stage lens was designed to form a piston that accelerated uniformly from 6.3 km/sec to 12 km/sec over a distance of 100 cm. Two aluminum tubes of Astrolite were used to phase the detonation wave in a tank of nitromethane (Figure 47). Initiation tests were conducted and showed that the Astrolite could indeed initiate sensitized nitromethane.

The timing of the second-stage initiation and the auxiliary pump cycle was determined from the computer calculation (Figure 30). The reservoir explosive and lens were initiated by the arrival of the driver shock at capped shorting pins located just upstream of the nozzle inlet. Gun performance was monitored in detail by ionization and pressure sensing pins, strain gauges, flash X rays, and high-speed framing and streaking cameras. The measured performance is shown in the x-t plane of Figure 48. The projectile was launched in good condition at 12 km/sec into helium at one atm. The range radiograph of the projectile (Figure 49) shows the projectile tumbling, probably because the barrel was not perfectly straight and the stagnation pressure on the projectile in flight was moderately high (0.2 kbar). Unfortunately, the Astrolite initiated the nitromethane in the lens intermittently, for reasons that are not yet

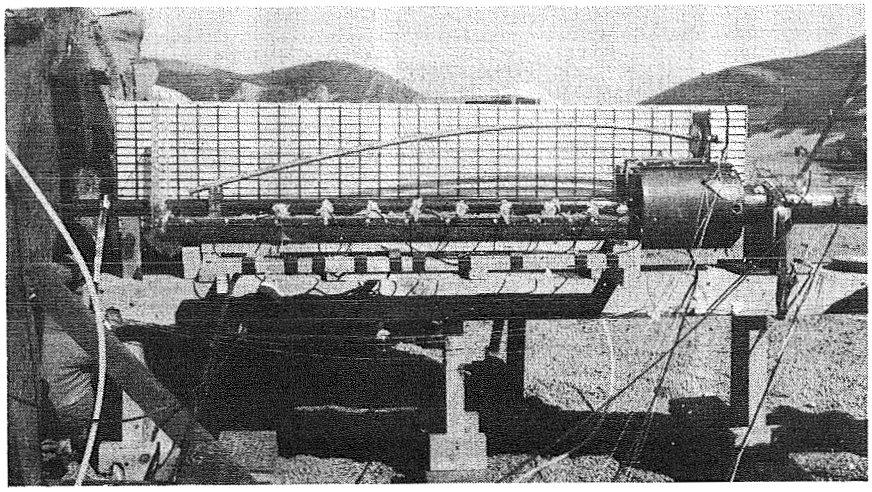

a. Shot 397-11 Showing Second Stage Lens

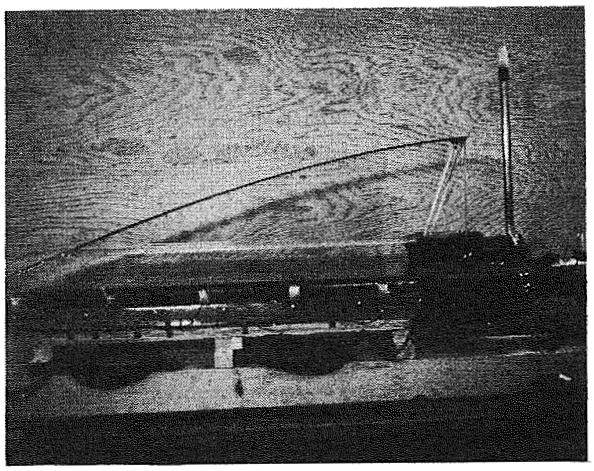

b. Shot 397-12 Showing Modified Lens Design

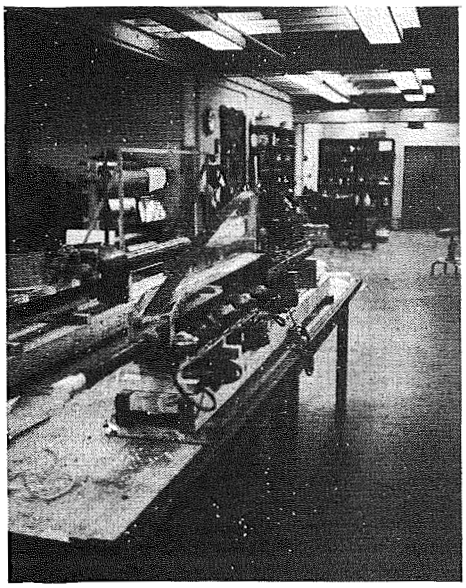

Construction of 397-12 and 397-13

FIGURE 47. TWO STAGE EXPLOSIVELY DRIVEN GUNS TO LAUNCH 2g PROJECTILES TO 12 km/sec

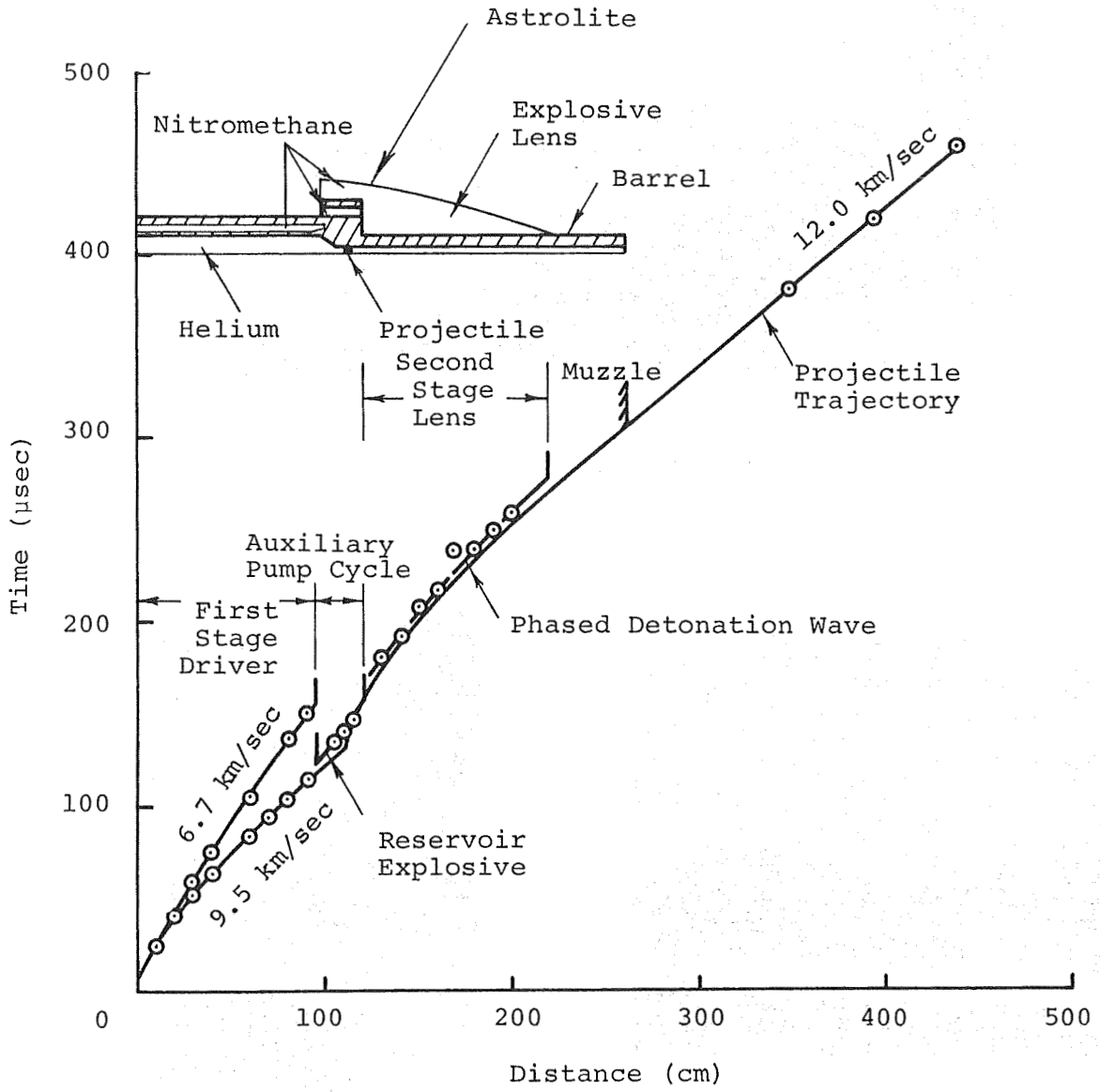

FIGURE 48. OBSERVED PERFORMANCE OF A TWO-STAGE GUN (Shot 397-11)

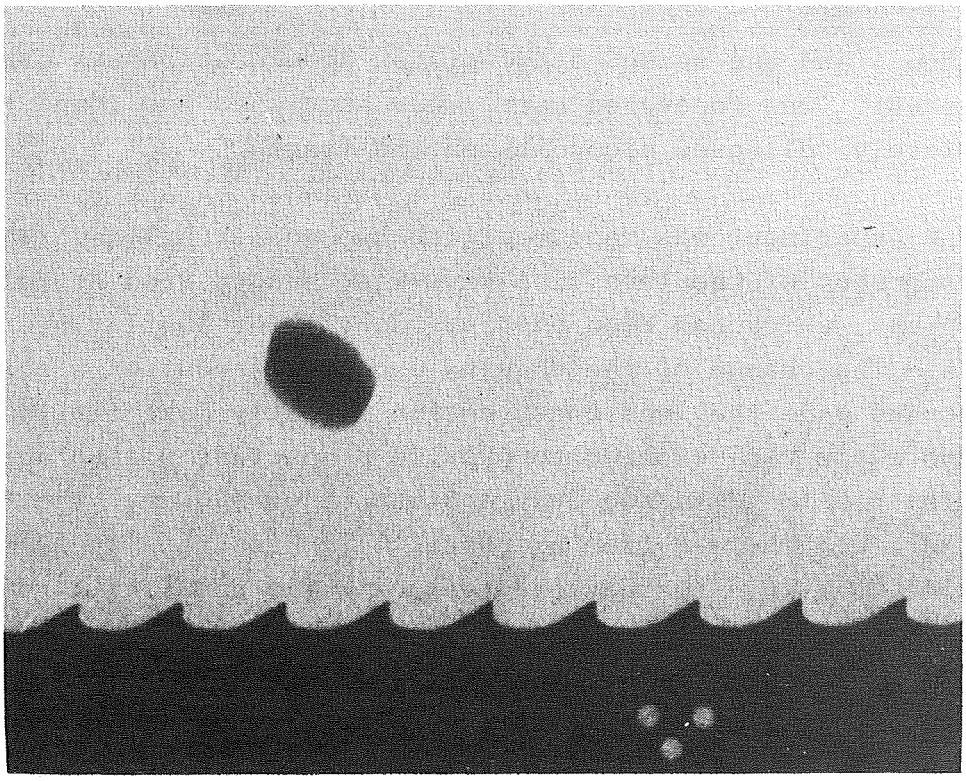

Model is 87.5 body diameters downstream of the muzzle. (Range atmosphere is Helium at 1 atm)

Figure 49. RANGE RADIOGRAPH OF A 2-g, 1/2-caliber PROJECTILE LAUNCHED TO 12 km/sec BY A TWO-STAGE EXPLOSIVELY DRIVEN GUN (Shot 397-11)

understood, and the second-stage piston acceleration was erratic (Figure 48). The recovered barrel was sectioned and found to be incompletely collapsed along its entire length.

The experiment was repeated with two modifications. The fast component of the lens explosive was changed from Astrolite to EL506-A8, which had been used previously for initiating nitromethane. The change of the phasing explosive required a new lens contour and made the lens construction slightly more difficult. The lens again was designed to provide a constant piston acceleration from 6.3 to 12 km/sec over a distance of 100 cm. The range atmosphere was changed from helium at 1 atm to argon at 20 mm Hg to reduce the range stagnation pressure while ensuring a reasonably bright streaking camera record.

The projectile was accelerated to 12.2 km/sec (Figure 50), but unfortunately it collided with a dummy projectile mounted in the range. Because of this alignment error no X rays of the projectile were obtained. The streaking camera record showed one bright continuous line up to the position of the dummy projectile. At this point the streak broadened rapidly as a result of the collision. X rays of the fragmented particles were used to reconstruct the origin of the breakup. The projected trajectories of the pieces came together at the position of the dummy projectile, again confirming that projectile breakup was a result of an alignment error. The evidence seems to indicate that the projectile was launched intact. The operation of the explosive lens was flawless, as shown in the sequence of framing camera records of Figure 51. Again, the sectioned barrel showed incomplete collapse over the entire length.

In the final experiment of the program, the lens was modified to provide a second-stage piston acceleration from 6.3 to 14 km/sec over a distance of 80 cm. Based on the results of the previous two

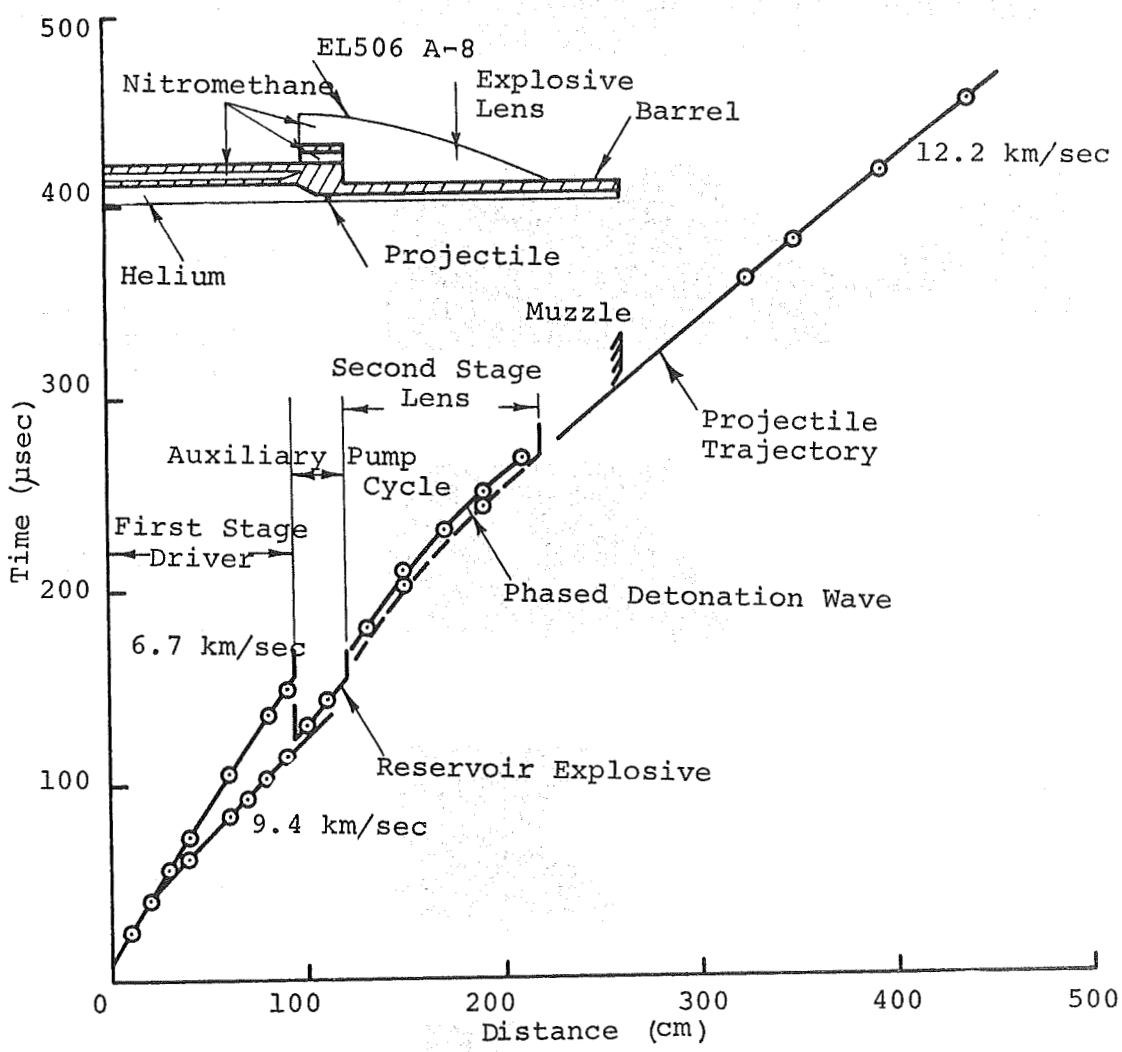

FIGURE 50. OBSERVED PERFORMANCE OF A TWO-STAGE GUN (Shot 397-12)

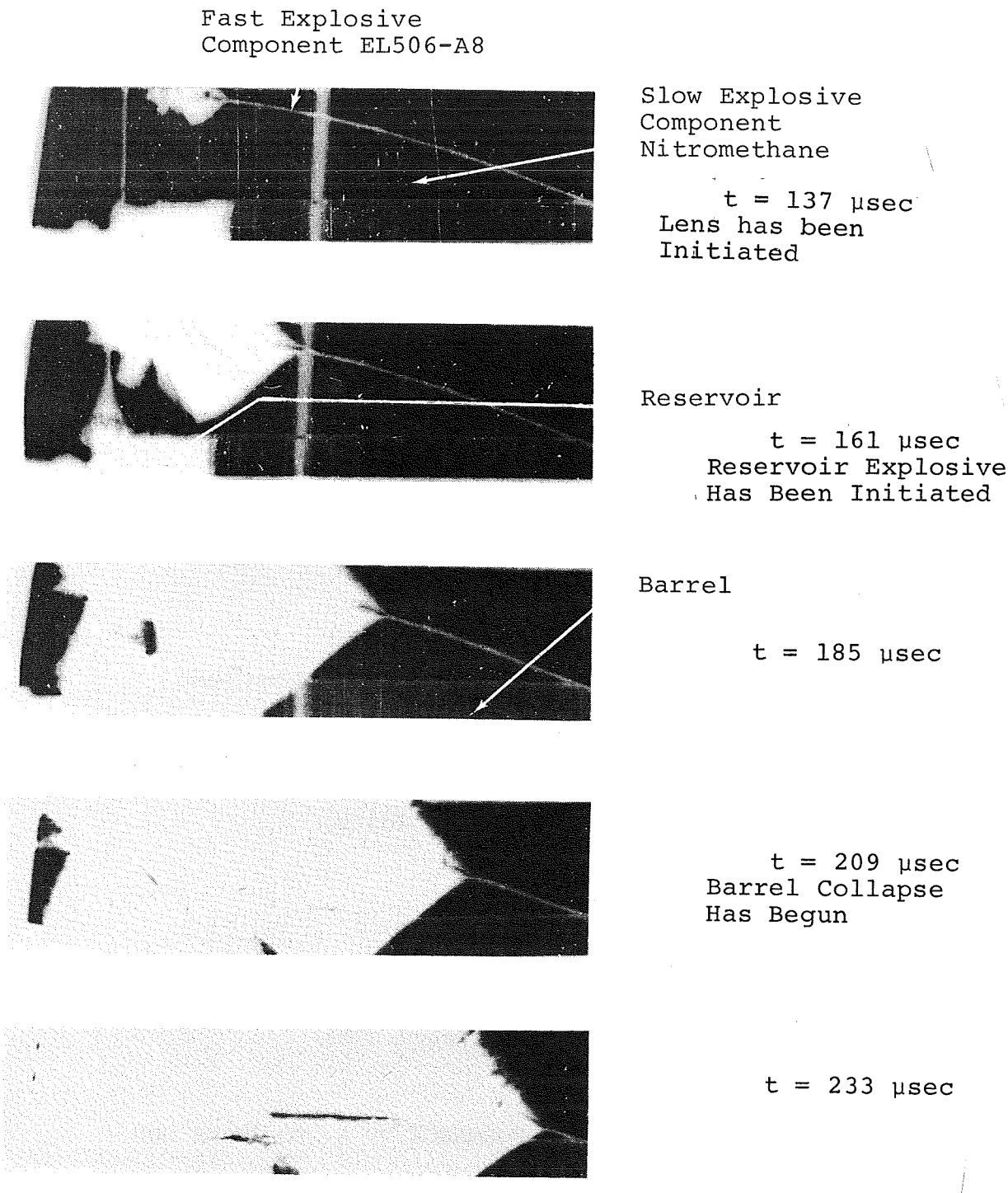

FIGURE 51. HIGH SPEED FRAMING CAMERA RECORD OF SECOND STAGE EXPLOSIVE LENS OPERATION (Shot 397-12)

experiments, it was felt that the second-stage augmentation would not be as successful as originally anticipated. Therefore, the initiation of the lens in this experiment was delayed somewhat to ensure that the phased detonation did not overtake and destroy the accelerating projectile.

The experiment was carried out and the projectile was accelerated to 11.5 km/sec in good condition (Figure 52). The measured velocity (Figure 53) was somewhat low, probably because of the delay in second-stage initiation. Again, the recovered barrel was sectioned and found only partially collapsed.

The results of the three two-stage experiments described above suggest a fourth two-stage experiment in which the barrel would be surrounded by a 2.54-cm layer of Astrolite explosive. The second stage would therefore consist of a constant velocity piston at 8.6 km/sec; however, the barrel collapse process would be symmetric. A conservative performance calculation of the linear augment gun gives a predicted final velocity of over 13 km/sec. Therefore the proposed experiment, if successful, will demonstrate the superiority of the symmetric collapse over the asymmetric collapse.

In conclusion, the three two-stage experiments resulted in an augmentation of about 2 km/sec over the velocity of the first stage alone. All the evidence indicates that the higher velocities anticipated were not achieved because of incomplete collapse of the barrel by the second-stage asymmetric lens, although there was certainly enough energy in the lens explosive to collapse the barrel even against the large gas pressures generated by the auxiliary pump cycle. Based on the performance of the two-stage guns and the incompletely collapsed barrels, it is postulated that the asymmetric geometry is not suitable for augmentation and that symmetric geometry may have to be used in future experiments.

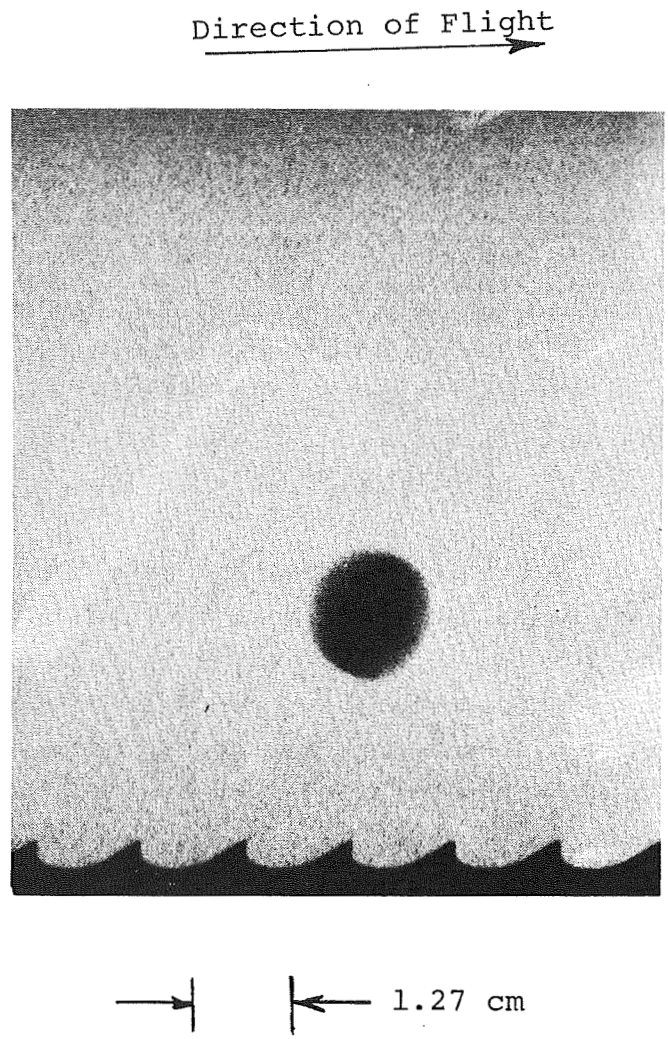

Model is 133 body diameters down-stream of the muzzle. (Range atmosphere is argon at 20 mm Hg)

FIGURE 52. RANGE RADIOGRAPH OF A 2-g, 1/2-caliber LONG PROJECTILE LAUNCHED TO 11.5 km/sec BY A TWO-STAGE GUN (Shot 397-13)

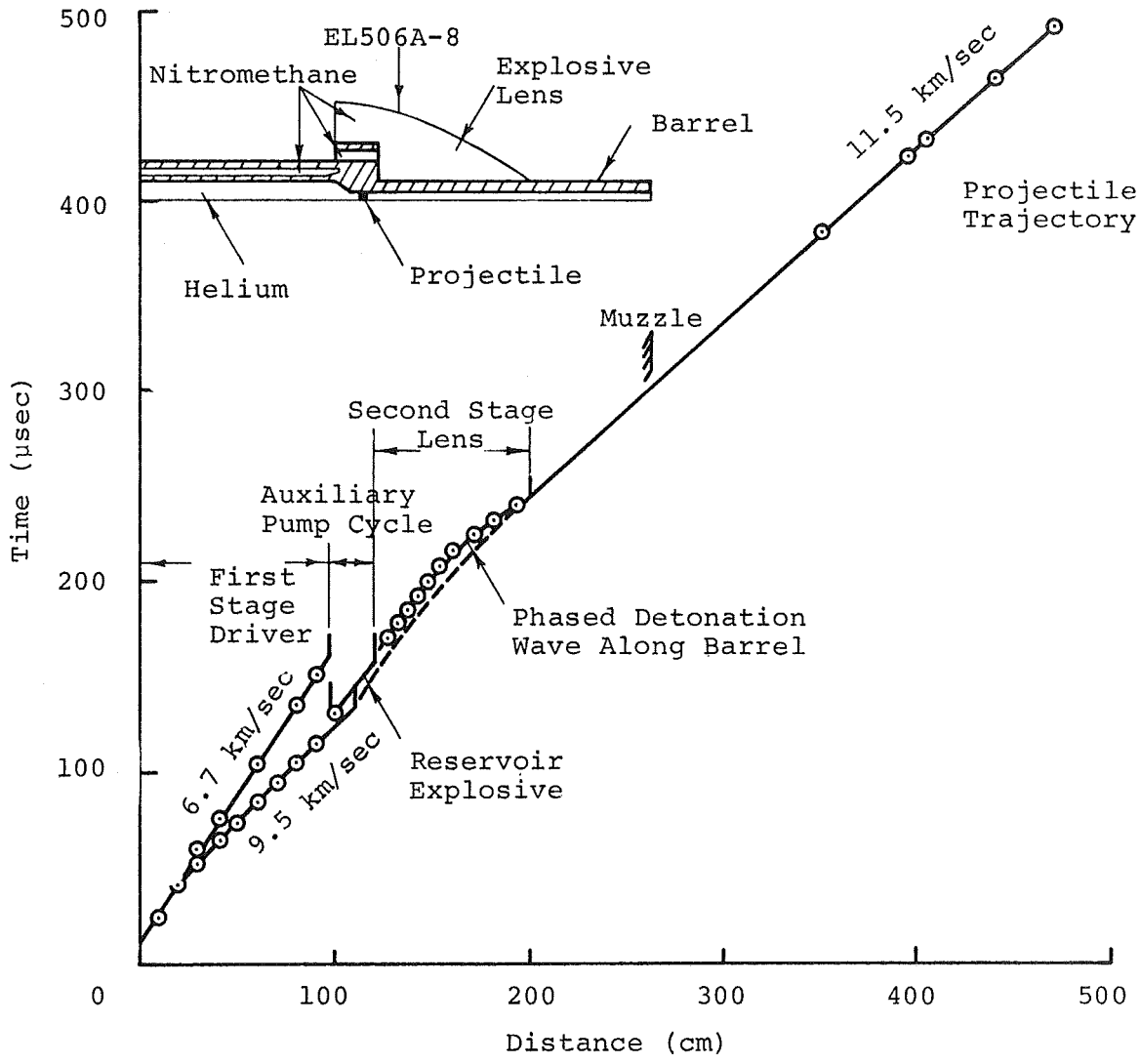

FIGURE 53. OBSERVED PERFORMANCE OF A TWO-STAGE GUN (Shot 397-13)

SECTION VI

CONCLUSIONS

During this year's program progress was made in understanding and improving the operation of explosively driven guns. A simple method of computing pressure tube expansion has been demonstrated and new insights into tube collapse and jetting have been gained. Calculations have been made that indicate phased detonation velocities as high as two to three times the explosive detonation velocity will be effective in collapsing a tube and forming a piston. Therefore, piston velocities and projectile velocities as high as 20 km/sec may be feasible.

With present explosive driver technology, it has been shown that the performance of single-stage guns is limited in part by reservoir expansion. It has also been shown that this expansion can be controlled by using explosives to collapse the reservoir. The addition of an auxiliary pump cycle to a high-pressure, single-stage gun has resulted in velocities up to 12 km/sec with 2-g projectiles. Peak pressures of 60 kbar are developed in this gun. For a limited range of projectile materials and shapes, these extremely high pressures were applied in a controlled manner and used to accelerate projectiles without loss of integrity.

Two-stage guns operating at lower peak base pressures (30 kbar) have been used to launch 2-g projectiles in good condition to 12.2 km/sec. The present performance of this gun seems to be limited in part by the asymmetric geometry of the second-stage lens. In this geometry the lens does not appear to be able to collapse the barrel completely to form the second stage piston. It is anticipated that when the barrel is collapsed in a symmetrical manner, the performance of the second stage will be improved and projectile velocities in the range of 15 to 20 km/sec should be feasible.

The capability of calculating launcher performance accurately and inexpensively has been developed. The validity of the GANG-POD computer code was demonstrated in the experiment with a single-stage launcher and then applied in the design and development of the first stage with auxiliary pump cycle, and the two-stage gun.

REFERENCES

1. E. T. Moore, Jr., "Explosive Hypervelocity Launchers," NASA CR-982, National Aeronautics and Space Administration, prepared for NASA Ames (February 1968).

2. J. D. Watson, "An Explosively Driven Gun to Launch Large Models to Reentry Velocities," PIFR-098, Physics International Company, San Leandro, California (April 1969).

3. H. F. Waldron, E. T. Moore, Jr., G. B. Steel, and C. S. Godfrey, "A Mechanism for the Conversion of the Chemical Energy of Explosives to the Kinetic and Internal Energy of a Gas," AIAA Paper No. 67-178, presented at the AIAA Fifth Aerospace Sciences Meeting, New York. New York (January 1967).

4. S. P. Gill, "Acceleration of a Metal Plate by an Oblique Detonation Wave," PITR-68-12, Physics International Company, San Leandro, California (to be published).

5. A. E. Seigel, "Theory of High Speed Guns," Agardograph 91, NATO-AGARD Fluid Dynamics Panel, North Atlantic Treaty Organization (1965).

6. I. I. Glass, "Hypervelocity Launchers. Part II. Compound Launchers--Driving Techniques," UTIAS Review No. 26, University of Toronto Institute for Aerospace Studies, Toronto, Ontario, Canada (December 1965).

7. J. D. Watson and C. S. Godfrey, "An Investigation of Projectile Integrity Using Computer Techniques," Proceedings of the Fifth Hypervelocity Techniques Symposium, Vol. II, Denver, Colorado (March 1967).

NASA-Langley, 1970 —— 11

NATIONAL AERONAUTICS AND SPACE ADMINISTRATION
WASHINGTON, D.C. 20546
OFFICIAL BUSINESS

FIRST CLASS MAIL

POSTAGE AND FEES PAID
NATIONAL AERONAUTICS AND
SPACE ADMINISTRATION

POSTMASTER: If Undeliverable (Section 158 Postal Manual) Do Not Return

"The aeronautical and space activities of the United States shall be conducted so as to contribute . . . to the expansion of human knowledge of phenomena in the atmosphere and space. The Administration shall provide for the widest practicable and appropriate dissemination of information concerning its activities and the results thereof."

—NATIONAL AERONAUTICS AND SPACE ACT OF 1958

NASA SCIENTIFIC AND TECHNICAL PUBLICATIONS

TECHNICAL REPORTS: Scientific and technical information considered important, complete, and a lasting contribution to existing knowledge.

TECHNICAL NOTES: Information less broad in scope but nevertheless of importance as a contribution to existing knowledge.

TECHNICAL MEMORANDUMS: Information receiving limited distribution because of preliminary data, security classification, or other reasons.

CONTRACTOR REPORTS: Scientific and technical information generated under a NASA contract or grant and considered an important contribution to existing knowledge.

TECHNICAL TRANSLATIONS: Information published in a foreign language considered to merit NASA distribution in English.

SPECIAL PUBLICATIONS: Information derived from or of value to NASA activities. Publications include conference proceedings, monographs, data compilations, handbooks, sourcebooks, and special bibliographies.

TECHNOLOGY UTILIZATION PUBLICATIONS: Information on technology used by NASA that may be of particular interest in commercial and other non-aerospace applications. Publications include Tech Briefs, Technology Utilization Reports and Technology Surveys.

Details on the availability of these publications may be obtained from:

SCIENTIFIC AND TECHNICAL INFORMATION DIVISION

NATIONAL AERONAUTICS AND SPACE ADMINISTRATION

Washington, D.C. 20546